Title
Effects of Laminar Fluid Shear Stress on the Function of Adult Stem Cells

Author
Diop, Rokhaya

Publication Date
2013

Peer reviewed|Thesis/dissertation

Effects of Laminar Fluid Shear Stress on the Function of Adult Stem Cells

by

Rokhaya Diop

A dissertation submitted in partial satisfaction of the

requirements for the degree of

Joint Doctor of Philosophy

with the University of California, San Francisco

in

Bioengineering

in the

Graduate Division

of the

University of California, Berkeley

Committee in charge:

Professor Song Li, Chair
Professor Mohammad R.K. Mofrad
Professor Jeffrey C. Lotz
Professor Marian C. Diamond

Fall 2013

Effects of Laminar Fluid Shear Stress on the Function of Adult Stem Cells

ABSTRACT

Effects of Laminar Fluid Shear Stress on the Function of Adult Stem Cells

by

Rokhaya Diop

Joint Doctor of Philosophy in Bioengineering

with the University of California, San Francisco

and the University of California, Berkeley

Professor Song Li, Chair

The objective of this doctoral thesis was to investigate the effects of laminar fluid shear stress on the function three types of adult stem cells: mesenchymal stem cells, neural crest stem cells and multipotent vascular stem cells. These three types of stem cells represent potential cell sources for vascular tissue engineering. Before these stem cells can be used to create tissue engineered vascular grafts, a thorough understanding of the effects of hemodynamic forces on their function is necessary. Much like cyclical stretch and normal pressure, fluid shear stress plays a major role in the microenvironment of the blood vessel wall but the effects of this mechanical force on the function of these adult stem cells is not well understood.

First, we began by investigating the effects of laminar fluid shear stress on TGF-β1/SMAD2 signaling in human mesenchymal stem cells. Human mesenchymal cells (hMSCs) are multipotent fibroblast-like cells, which are found primarily in the bone marrow. MSCs are a potential cell source for tissue engineering because of their ease of isolation and expansion, their multipotency and their low immunogenicity. We found that exposing hMSCs to fluid flow promotes transforming growth factor 1 (TGF-β1) signaling in a receptor-dependent manner. The mechanism explaining this phenomenon, however, was unclear. Based on our results, we rejected several hypotheses to explain the observed phenomenon: shear force transmission through the glycocalyx; changes in membrane fluidity; and changes in the internalization of TGF-β receptors. We were able to show that the increase in TGF-β1/Smad2 signaling when hMSC are exposed to fluid flow was not caused by shear stress but instead, by an increase in the flow rate. We were also able to show that shear stress inhibits TGF-β1/Smad2 signaling.

Second, we examined the effects of laminar fluid shear stress on the function of human neural crest stem cells. Neural crest stem cells (NCSCs) are multipotent cells that give rise to various tissues during the embryonic development of vertebrates. NCSCs were derived from induced pluripotent stem cells and, then, exposed to a laminar fluid shear stress of 10 dynes/cm^2 for various time periods. We found that laminar fluid shear stress increased NCSC proliferation. We also showed that fluid shear stress increased the activation of ERK1/2 in a time dependent manner. In addition, we observed that exposure to laminar fluid shear stress did not affect myogenic, neurogenic or osteogenic differentiation in NCSCs. We found, however, that exposure to fluid shear stress prevented adipogenic differentiation.

Third, we explored the effects of laminar fluid shear stress on the function of multipotent vascular stem cells. Multipotent vascular stem cells (MVSCs) are adult stem cells that have recently been discovered in the medial layer of blood vessels. MVSCs have been shown to give rise to a variety of cell types including: schwann cells, peripheral neurons, smooth muscle cells, adipocytes, chondrocytes and osteocytes. MVSCs were isolated from rat carotid arteries. These cells were then expanded without differentiation and exposed to a laminar fluid shear stress of 6 dynes/cm^2. We found that laminar fluid shear stress increased rat MVSC proliferation. We also showed that fluid shear stress increased the activation of ERK1/2 in a time dependent manner in MVSCs. Laminar fluid shear stress also caused a decrease in the gene expression of smooth muscle cell markers and an increase in the expression of osteoblastic differentiation genes. In addition, we observed that exposure to fluid shear stress did not affect myogenic, osteogenic and neurogenic cell differentiation in MVSCs.

The results of the aforementioned studies provide new clues in efforts to elucidate the mechanobiology of adult stem cells but further investigation into the effects of mechanical stimulation on the function of human MSCs, NCSCs and MVSCs will be necessary to provide a rational basis for the use of these cells in tissue engineering applications.

Dedicated to my mother and father,
my husband Ismaila,
my sisters Mame and Madjiguene,
my brothers Mohammed and Abdoulaye,
and to my daughter Marietou.

TABLE OF CONTENTS

List of Figures and Tables .....v-vii

Chapter 1. Introduction

1.The Human Vascular System 2-3

2. Mechanical Forces Acting on the Blood Vessel Wall 4

3. Cardiovascular Diseases and Current Therapies 5-8

3.1. Medications 5-6

3.2. Surgical Interventions 7-8

3.2.1. Balloon Angioplasty 7

3.2.1. Bypass Surgery 8

4. Vascular Tissue Engineering 9-21

4.1. Biomaterials for Vascular Tissue Engineering 9-13

4.1.1. Nondegradable Synthetic Polymers 9-10

4.1.2. Degradable Synthetic Polymers 10-11

4.1.3. Natural Polymers 11-12

4.1.4. Cell Sheets 12-13

4.1.5. Decellularized Tissue 13

4.2. Cell sources for Vascular Tissue Engineering 14-21

4.2.1. Endothelial Cells 14

4.2.2. Smooth Muscle cells 14-15

4.2.3. Fibroblasts 15

4.2.4. Endothelial Progenitor Cells 15-16

4.2.5. Embryonic Stem Cells 16-18

4.2.6. Induced Pluripotent Stem Cells 18-19

4.2.7. Mesenchymal Stem Cells 19-20

4.2.8. Neural Crest Stem Cells 20-21

4.2.9. Multipotent Vascular Stem Cells 21

Chapter 1. Introduction

5. Parallel Plate Flow Chamber System 22

References 23-30

Chapter 2.

Effects of Fluid Flow on TGF-β1 Signaling in Human Mesenchymal Stem Cells

Abstract 32

Introduction 33-38

Specific Aims 39

Materials & Methods 40-46

Results 47-49

Discussion 50-52

References 53-54

Figures 55-70

Chapter 3.

Effects of Laminar Fluid Shear Stress on Human Neural Crest Stem cell Function

Abstract 72

Introduction 73

Materials & Methods 74-77

Results 78-80

Discussion 81-82

References 83-84

Figures 85-97

Chapter 4.

Effects of Laminar Fluid Shear Stress on Multipotent Vascular Stem Cell Function

Abstract 99

Introduction 100

Chapter 4.
Effects of Laminar Fluid Shear Stress on Multipotent Vascular Stem Cell Function

Materials & Methods 101-105
Results 106-108
Discussion 109-110
References 111
Figures 112-130

Chapter 5. Conclusions and Future Directions

Conclusions 132-133
Future Directions 133-134
References 135

Appendix

Governing Equations 137
Boundary Conditions 137
Solution 138-139

List of Figures and Tables

Chapter 1. Introduction

Figure 1 3
Figure 2 4
Figure 3 7
Figure 4 8
Figure 5 22

Chapter 2.
Effects of Fluid Flow on TGF-β1 Signaling in Human Mesenchymal Stem Cells

Table 1 43
Table 2 44
Table 3 44
Table 4 45

Figure 1 55
Figure 2 56
Figure 3 57
Figure 4 58
Figure 5 59
Figure 6 60
Figure 7 61
Figure 8 62
Figure 9 63
Figure 10 64
Figure 11 65

List of Figures and Tables

Chapter 2.
Effects of Fluid Flow on TGF-β1 Signaling in Human Mesenchymal Stem Cells

Figure 12 66
Figure 13 67
Figure 14 68
Figure 15 69
Figure 16 70

Chapter 3.
Effects of Laminar Shear Stress on Human Neural Crest Stem Cell Function

Table 1 76

Figure 1 85
Figure 2 86
Figure 3 87
Figure 4 88
Figure 5 89
Figure 6 90
Figure 7 91
Figure 8 92
Figure 9 93
Figure 10 94
Figure 11 95
Figure 12 96
Figure 13 97

List of Figures and Tables

Chapter 4.
Effects of Laminar Shear Stress on Multipotent Vascular Stem Cell Function

Table 1 104

Figure 1 112
Figure 2 113
Figure 3 114
Figure 4 115
Figure 5 116
Figure 6 117
Figure 7 118
Figure 8 119
Figure 9 120
Figure 10 121
Figure 11 122
Figure 12 123
Figure 13 124
Figure 14 125
Figure 15 126
Figure 16 127
Figure 17 128
Figure 18 129
Figure 19 130

Appendix

Figure 1 136

Chapter 1

Introduction

1. The Human Vascular System

The human vascular system is an intricate system composed of the heart, the blood and blood vessels. The function of the human vascular system is to transport gases, nutrients, waste, cells, hormones and other important entities from on part of the body to another. The vascular system also helps the body maintain a constant temperature and pH. The heart plays two critical functions in the vascular system. First, it receives oxygen-poor blood from body tissues and pumps it to the lungs. Second, it receives oxygenated blood from the lungs and pumps it to the body's tissues [1].
The vascular system consists of two distinct circulatory systems: pulmonary circulation and systemic circulation. Pulmonary circulation takes deoxygenated blood from the heart to the lungs where oxygen is absorbed and carbon dioxide is removed. The blood then travels back to the heart where it is pumped into the systemic circuit. Systemic circulation carries oxygenated blood and nutrients to every cell in the body and picks up carbon dioxide and waste from body tissues [2].
Blood vessels can be divided into 3 distinct groups: arteries, capillaries and veins. Each type of blood vessel has a different function. The structure of each type of blood vessel depends on its function. Arteries carry blood away from the heart. Arteries vary in size from 2.5 cm to 0.3mm. Larger arteries (2.5 cm to 1 cm) are usually very elastic to dampen the surges of blood pressure that result from heart contractions. Mid-size arteries (1 cm to 0.3mm) have more muscular walls because their role it to regulate the supply of blood to specific organs. Arteries that are smaller than 0.3mm are called arterioles. Arterioles connect to capillaries. Capillaries are the smallest blood vessels. They range between 8 and 10 microns in diameter, which is just enough to allow single erythrocytes to pass. Capillaries are made of a single layer of endothelial cells surrounded by basal lamina. The function of capillaries is to enable the exchange of gases, nutrients and waste between the blood and body tissues [3].

In general, the walls of arteries consist of 3 layers. The innermost layer, or tunica intima, is formed by flat endothelial cells and is lined by a thin layer of connective tissue in larger arteries. The tunica intima usually has a smooth surface because it comes into contact with blood. The middle layer, or tunica media, is populated by smooth muscle cells lined in circular sheets made of elastin, laminin and collagen fibers. The alignment of smooth muscle cells is mainly circumferentital. This muscular layer enables arteries to expand or to contract in response to external cues. The outermost layer, or tunica externa (or adventitia), is made up of collagen fibers, extra-cellular matrix and fibroblast. The tunica externa protects the blood vessel and connects it to surrounding tissues. In larger blood vessels, the advential layer also contains nerves and capillaries that supply nutrients to the artery wall. Elastic membranes made up mostly of elastin lie between the 3 layers [1].

Contrary to arteries, veins carry blood from capillaries to the heart. Similarly to arteries, the walls of veins consist of 3 layers: the tunica intima, the tunica media and the tunica externa.
There are, however, several differences between arteries and veins of similar diameter size [4]:

1. The walls of veins are thinner than the walls of arteries because blood pressure is lower in veins.
2. Unlike arteries, veins contain valves to help prevent the back flow of blood.
3. The lumen of similar sized veins is larger.
4. Unlike arteries, in veins, the tunica externa is thicker than the tunica media.
5. Veins contain less elastin than arteries.
6. Veins contain more collagen than arteries.

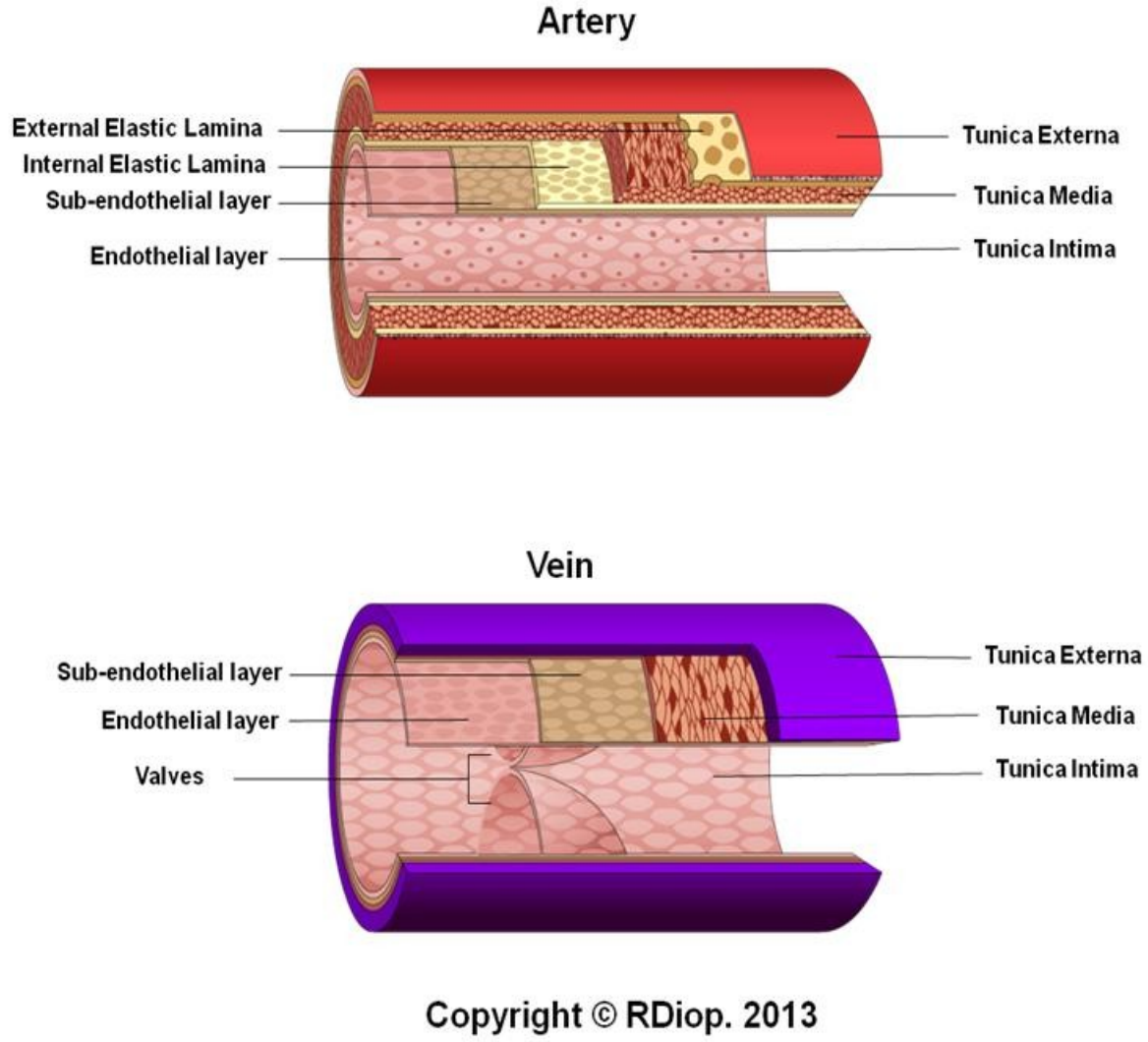

Figure 1. Anatomical comparison between the structure of an artery and a vein.

2. Mechanical Forces Acting on the Blood Vessel Wall

The blood vessel wall and vascular cells are continually subjected to mechanical forces [5, 6]. These dynamic forces include shear stress, normal pressure and cyclical mechanical stretch, which includes both axial and circumferential stresses [7].
Shear stress is created by the movement of a fluid over a fixed surface. It always acts in the direction normal to the surface. The endothelium is continually subjected to shear stress because it comes into contact with the blood. In arteries, the endothelial cells that line the lumen of blood vessels experience an average fluid shear stress ranging between 10 and 15 dynes/cm^2 [8, 9]. It is thought that endothelial cells sense a time-averaged shear stress. Endothelial cells have been reported to secrete nitric oxide, growth factors and adhesion molecules in response to shear stress. These signals cause the artery to remodel itself by changing its diameter to keep the shear stress in a constant range [10]. The vascular wall is also subjected to continuous cyclic mechanical strain due to the pulsatility of blood flow. Cyclic stretch influences smooth muscle cell phenotype via integrin and the focal adhesion signaling in both synthetic and contractile phenotypes [11]. Last, blood flow causes normal pressure or compressive perpendicular stress in the vascular wall. Collagen fibers, smooth muscle cells, and elastic fibers are the load-bearing elements of the blood vessel wall. The collagen fibers bear loads in the circumferential direction, while the elastic fibers bear loads in both longitudinally and circumferentially. Collagen fibers limit high deformations and help prevent the rupture of the vascular wall under high pressures. Elastic fibers give the tissue the ability to recoil without energy input [12].

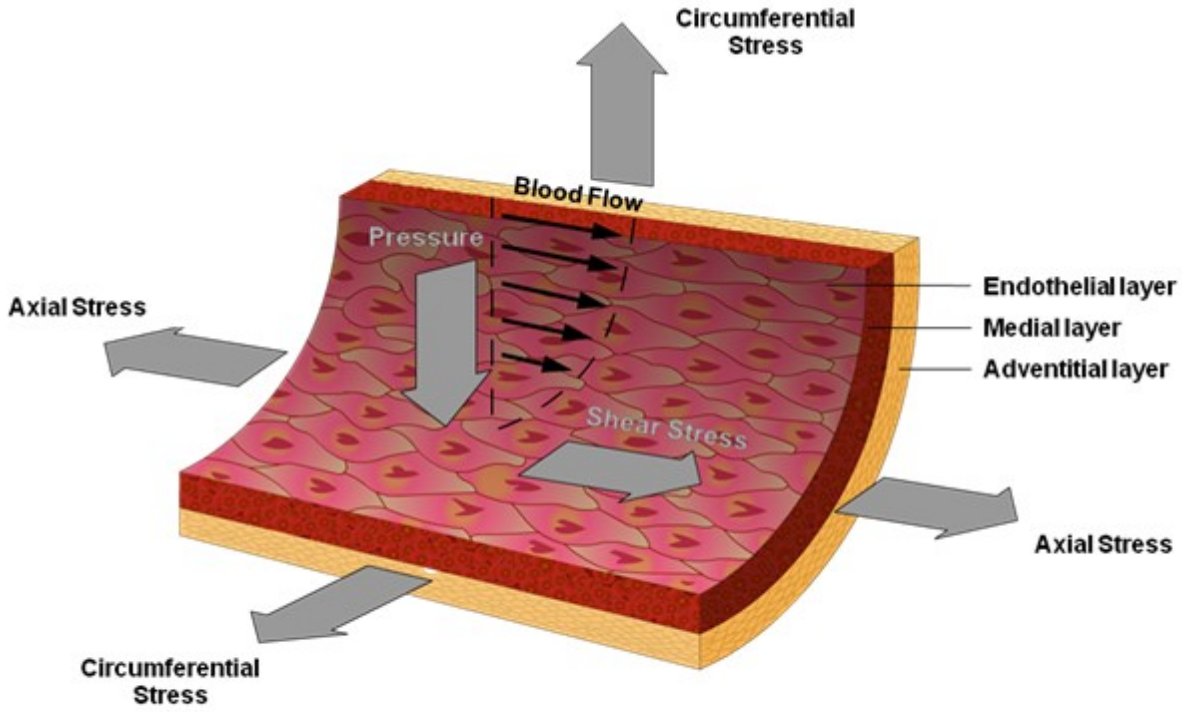

Figure 2. Mechanical Force acting on the blood vessel wall

3. Cardiovascular Diseases and Current Therapies

Cardiovascular disease refers to a number of conditions affecting the heart and blood vessels. Cardiovascular diseases constitute the biggest cause of deaths worldwide, totaling about 17.3 million deaths per year, which accounts for 31% of all deaths [13]. Major diseases that affect the heart include: cardiomyopathies (diseases of the heart muscle), congenital heart disease (generally due to birth defects), rheumatic heart disease (permanent damage to heart valves caused by rheumatic fever), cardiac arrhythmia (irregular heart beat). Other types of cardiovascular diseases affect the blood vessels. They include but are not limited to coronary artery disease, peripheral artery diseases and venous diseases.

Most cardiovascular diseases are caused by atherosclerosis. Atherosclerosis involves the accumulation of lipids and cholesterol in the wall of the blood vessel, the hardening of the blood vessel wall and the narrowing of the vessel lumen. The disease is caused by an inflammatory response to an injury to the layer of endothelial cells that line the vascular wall [14]. When endothelial cells are subjected to irritative stress, (either by biochemical factors, hypertension or mechanical stresses), they begin to express adhesion molecules that capture leukocytes on their surfaces. Changes in endothelial permeability and the composition of the extracellular matrix beneath the endothelium promote the entry and retention of cholesterol-containing low-density lipoprotein (LDL) in the blood vessel wall [15]. The early phase of atherosclerosis involves the recruitment of inflammatory cells from the circulation and their transendothelial migration [16]. Vascular intimal injury also promotes the migration and proliferation of smooth muscle cells in the intima. This leads to the formation of an atheromatous plaque below the endothelium. This plaque is composed of SMCs, collagen and elastin fibers, and lipids. Atherosclerosis ultimately leads to blockages in blood vessels, tissue eschemia, heart attacks or strokes [17].

Atherosclerosis is the underlying cause behind the majority of cardiovascular diseases but it can be prevented and treated by maintaining a healthy lifestyle (diet improvement, regular exercise, avoiding smoking and alcohol) [18]. Unfortunately for many people at risk for atherosclerosis, lifestyle changes are not sufficient to prevent or reverse the disease. In such cases, a number of treatment options are available to treat atherosclerosis.

3.1. Medications

Several drugs reduce the risk of complications from atherosclerosis by lowering cholesterol and triglyceride levels in the blood [19].

Statins lower LDL cholesterol production in the liver. Statins also increase the levels of HDL and reduce the level of triglycerides. Statins are the most effective medications for lowering LDL cholesterol and treating atherosclerosis. Other medications reduce the risk of atherosclerosis by lowering blood pressure.

Beta blockers, also known as beta-adrenergic blocking agents reduce blood pressure by blocking the effects of epinephrine. Beta blockers lower the heart rate and also help blood vessels open up to improve blood flow. Calcium-channel blockers also help reduce blood pressure.

Plant sterols can modestly reduce cholesterol levels (about 10%). Bile acid sequestrants reduce blood cholesterol levels by binding to bile acids in the intestines because cholesterol is needed to produce bile.

Fibrates such as Gemfibrozil and Fenefibrate are drugs that reduce triglyceride levels. Large doses of the vitamin Niacin can also reduce triglycerides while increasing HDL levels. Lovaza (an omega-3-acid) is a prescription drug that decreases very high levels of triglycerides. Zetia is a drug that reduces the absorption of cholesterol in the intestines. Zetia is used in combination with Statins because it is not as effective in lowering LDL levels.

The last category of medications helps treat atherosclerosis by lowering the risk of blood clots. This includes platelet inhibitors such as Aspirin, anticoagulants such as Heparin and Warfarin and thrombolytic agents. For most people at risk from atherosclerosis, the benefits of blood thinners outweigh the risk of bleeding [19].

Although it is not possible to completely reverse atherosclerosis with medication, these drugs can reduce the risk of complications dramatically. When medication is not effective, several surgical interventions are available. In the next section, we will describe some common surgical techniques used to treat diseased blood vessels.

3.2. Surgical Interventions

3.2.1 Balloon Angioplasty

A balloon angioplasty is a minimally invasive surgical intervention that can be performed to treat blood vessel stenosis (narrowing). In this procedure, fluoroscopy is used to guide a balloon-tipped catheter to the site of blockage. The balloon is then inflated to compress the plaque against the blood vessel wall. The balloon also helps expand the diameter of the blocked blood vessel. Once this is accomplished, the balloon is deflated and the catheter is removed. Angioplasty can be performed with or without vascular stenting. A stent is a tube that can be placed transluminally to prevent the newly dilated blood vessel from restenosis [1]. Two types of stents are commercially available: one is a bare stent, which consists of a wire mesh; the other is a stent graft, which is basically a covered stent. The stent can contain drugs to prevent SMC proliferation and restenosis. In 2009, according to the National Center for Health Statistics (NCHS), an estimated 596 000 patients underwent percutaneous transluminal coronary angioplasty in the United States [20].

Figure 3. Balloon Angioplasty with Wire Mesh Stent

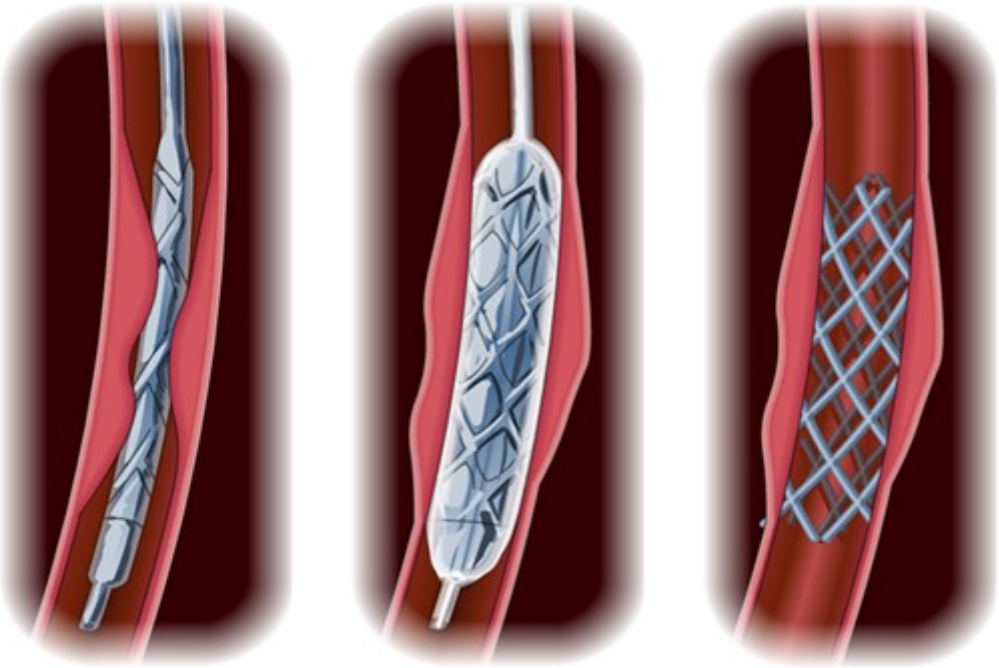

3.2. Surgical Interventions

3.2.2 Bypass Surgery

In this surgical procedure, a vascular graft, which can consist of natural tissue, synthetic or bioengineered materials, is used to bypass a narrowed or blocked blood vessel. Bypass surgery was first developed in the late 1960s [18]. In 2008, 600,000 coronary and peripheral bypass grafts were performed in the United States [21]. According to the National Center for Health Statistics (NCHS), in 2009, 242 000 patients underwent 416 000 coronary artery bypass procedures in the United States [20]

Ideally, an autologous blood vessel such as the great saphenous vein from the leg, the internal mammary artery from the chest or the radial artery from the arms is harvested to bypass the diseased blood vessel. The use of autologous veins for vascular surgery is limited by the availability of healthy blood vessels and poor long term patency [22]. Several long term studies have examined the patency of internal mammary artery and saphenous vein bypass graft after coronary artery bypass surgery. It was found that the long term post-operative patency of mammary artery grafts exceeded saphenous vein graft patency: 82% of saphenous vein grafts remained patent while 97% of mammary artery grafts remained patent within 5 years after operation [23]. Ten years after operation, repeat studies have shown that 76.3% of saphenous vein graft remained patent while 94.6% of mammary artery graft remained patent [24]. Although bypass surgery is commonly performed, the procedure is not without risk. Possible complications include stenosis due to intimal hyperplasia in new conduit, stroke and heart attack.

Figure 4. Bypass Graft

For patients who do not have autologous blood vessels suitable for graft surgery, it becomes necessary to use an allogenic (made with tissue from another individual) or a synthetic graft [25]. The drawbacks associated with synthetic and bio-inspired grafts include thrombosis, rejection, chronic inflammation and poor mechanical properties. Synthetic vascular grafts have been constructed from a wide range of biomaterials:

polyethylene terephthalate [26], expanded polytetrafluoroethylene [27], polyurethane [28], polyglycolic acid or poly-L-lactic acid [29], silk fibroin [30], among others. However, synthetic vascular grafts are associated with a high incidence of thrombosis and occlusion especially for small-diameter graft (with a diameter of 5mm or less).

4. Vascular Tissue Engineering

Vascular grafts created from autologous tissue have better long-term patency than any synthetic or bioengineered conduit currently available. Unfortunately, native tissue is not always available for vascular replacements. Vascular tissue engineering is an active area of research because better alternatives to native veins and arteries are needed. The development of biocompatible small-diameter vascular grafts that possess both the mechanical and the functional properties of native human blood vessels involves 3 important elements: a cell source, novel scaffold materials and the development of bioreactors that can mimic the dynamic environment in-vivo [31].

4.1 Biomaterials for Vascular Tissue Engineering

Biomaterials needed for vascular prostheses must have several important properties. First, they must be biocompatible meaning that they must be non-toxic, non-carcinogenic and they cannot provoke an immunogenic, inflammatory or thrombogenic response once they are implanted in the body. Second, biomaterials needed for vascular grafts must mimic the mechanical properties of the blood vessel wall: matching compliance, viscoeleasticity, fatigue resistance, durability and high tensile strengths. Third, these materials must also be easy to suture, readily available and cost-effective.

.

4.1.1. Nondegradable Synthetic Polymers

When autologous blood vessels are not available for bypass surgery, synthetic grafts are still preferred for the replacement of large arteries. Expanded polytetrafluoro-ethylene (ePTFE), polyethylene terephthalate (Dacron®) and polyurethane are commonly used to manufacture synthetic vascular grafts [32]. A comparison of Dacron and ePTFE as bypass materials for peripheral vascular surgery showed similar patency rates for the two synthetic materials [33]. It was reported that there is no significant difference between Dacron and expanded polytetrafluoroethylene (ePTFE) graft patency 5 years post-surgery (in femoropopliteal bypass grafting) (39.2% vs 38.4%)[34]. Another study compared Dacron with expanded polytetrafluoroethylene (ePTFE) in reconstructive aorto-iliac surgery. No statistically significant difference was found between the two graft materials in terms of patency rates. The 3-year patency rates were 95% for both Dacron and ePTFE. [35].

Synthetic grafts often fail due to thrombus formation. Because of their surface properties, synthetic nondegradable polymers induce platelet aggregation. It is generally accepted that a complete endothelial coverage of the luminal surface is necessary for long-term patency especially for small-diameter grafts (less than 5 mm in diameter).

Several groups have attempted to endothelialize the luminal surfaces of synthetic vascular grafts but the success of cell transplantation is limited because of difficulties in cell sourcing, attachment, and retention during pulsatile flow conditions. Hence, a variety of methods have been developed to enhance cell attachment in synthetic vascular grafts. Strategies to improve endothelialization include using protein coating, chemical or protein modification of the luminal surface of grafts (with RGD or P15 peptide for example). Other studies have been successful in reducing platelet adhesion

and in stimulating endothelial coverage by developing nitric-oxide producing polyurethanes [36].
Another important property for the design a synthetic vascular conduit is porosity. The material must be porous enough to support cell infiltration and growth but it must not allow blood leakage [37].
Last, compliance mismatch is often noted as a possible cause of failure for synthetic grafts. PTFE with a modulus of 3-6 MPa is much stiffer than arteries and veins. Dacron has a modulus of 12- 15 MPa in the circumferential direction and, of about 700kPa in the longitudinal direction. Differences in the stiffness of these synthetic materials compared to native vessels can cause changes to the laminar nature of blood flow within the vessel and may lead to thrombus formation [37].
Although synthetic non-degradable polymers are the material of choice for large blood vessel replacements, no synthetic graft has proven to be suitable in the long term. Long term data has reported failure rates between 70 and 100 percent 10 and 15 years post-implantation. In addition, these types of conduits are not suitable in the case of small-diameter blood vessels (less than 5 mm in diameter) [38].

4.1.2. Degradable Synthetic Polymers

Biodegradable synthetic materials are an alternative choice of materials for vascular graft. These materials can provide a temporary scaffold that can support cell growth in the short term. As the material degrades, the vascular graft is remodeled by the growing cells and by the extra-cellular matrix they produce. The degradation process may, however, elicit an immune response. Polymer degradation leads to a loss of ultimate strength for the vascular graft.
Materials commonly used to construct degradable scaffold include polygycolic acid (PGA), poly-L-lactic acid (PLLA) and polycaprolactone (PCL) among others. PGA degrades through enzyme-mediated hydrolysis within 6 months. The degradation of polycaprolactone (PCL) and poly-L-lactic acid (PLLA) may take several years, because these polymers are more hydrophobic [39]. By synthesizing copolymers with 2 or more polymers, material scientists can alter and fine-tune the material properties of degradable scaffolds. For example, the rate of degradation of a scaffold can be controlled by copolymerization.
As early as 1999, Niklason et al. had reported engineering a functional vascular graft from a biodegradable polymer. Vascular grafts were constructed from PGA and were seeded with smooth muscle cells and endothelia cells. The grafts were kept under pulsatile flow or static in a bioreactor for 8 weeks, the grafts were implanted in miniature swine for 4 weeks. Although, the graft that had been kept in static condition became occluded after 3 weeks, the remaining grafts stayed patent 4 weeks after implanted [40].
The first clinical application of biodegrable vascular grafts was reported in 2001 by Shin'oka et. al. A tubular vascular conduit was made from a polycaprolactone-polylactic acid (PCL-PLLA)copolymer. The scaffold was designed to degrade in 8 weeks. Smooth muscle and endothelial cells were harvested from one the patient's veins, expanded in-vitro and seeded on the tubular construct. After 10 days in culture, the vascular graft was implanted in the pulmonary artery of the patient. The tissue-engineered vascular graft remained patent 7 months after implantation[41]. In 2012, after refining their

methods, the same group had implanted vascular grafts in 25 patients (implantation of an extracardiac total cavopulmonary connection). These patients were monitored for 9 years after the implantation. They reported significant stenosis in 16% of the grafts. No evidence of infection, aneurysm or structural failure of the graft was reported [38].
Currently, biodegradable scaffolds are being fabricated by electrospinning polymer fibers. This technique makes it possible to control the diameter and the orientation of nanofibers in the scaffold. One can also control the porosity of the vascular graft, which is important for cell implantation. Recent efforts have focused on finding the ideal combination of synthetic material and biomaterial that yields the best mechanical properties and biocompatibility for use in vascular grafts. Polyurethanes, silk, collagen and elastin can be combined with PGA, PLLA, PCL or their copolymers to electrospin nanofibers for tubular vascular grafts.
Although biodegradable scaffolds have shown promising results, improvements are still needed. Technical refinements are needed to coordinate the degradation rate of biodegradable materials and the rate of tissue generation by the implanted cells. To continue, prolonged cell culture periods are still necessary to condition the vascular graft before implantation. Last, compliance mismatch limits the long-term patency of the graft.

4.1.3. Natural Polymers

Naturally-occurring polymers such as collagen, elastin and fibrin are alternatives to synthetic polymers in the fabrication of vascular grafts. Proteins which are found in the extra-cellular matrix (ECM) like collagen and elastin can be used to create vascular conduits which offer multiple advantages. First, there is a low risk of inflammatory response. Second, ECM proteins provide a scaffold that can support cell migration and proliferation. Third, the composition of ECM proteins dictates the mechanical properties of the tissue. Finally, ECM proteins are biologically active and may regulate the phenotype of cells like smooth muscle cells.
Weinberg and Bell were the first to demonstrate that collagen-based gels could be used to generate tissue-engineered blood vessels. They successfully seeded bovine smooth muscle cells (SMCs) and fibroblasts in two layers of collagen gel supported by a Dacron mesh. The lumen of the construct was subsequently coated with bovine endothelial cells. Although, this tissue-engineered vascular substitute failed due to poor mechanical strength, this experiment showed the feasibility of a tissue-engineered vascular graft [26].
To improve the mechanical properties of collagen-based constructs, several studies have explored the effects of fiber and cell alignment as well as crosslinking of fibers [42, 43]. When cells are entrapped in a polymer gel, they exert forces on the polymer fibers which cause the gel to contract. This contraction changes the orientation of the fibers and of the cells. Several groups have used a non-adhesive mandrel as a method to support the gel during the contraction phase. This technique yields fibers and cells that are circumferentially aligned [44]. To increase mechanical strength, collagen fibers can be crosslinked using enzymes such as lysyloxidase and transglutaminases. Although glutaraldehyde is a much more effective crosslinking agent, it was found to be cytotoxic [21]. Stegmen et. al. applied mechanical stimulation by cyclically stretching their gel-based vascular constructs to improve mechanical strength [45]. The improved

mechanical properties of vascular constructs subjected to mechanical conditioning were corroborated by Seliktar et. al [46]. Despite many efforts to improve the mechanical properties of collagen-based constructs, this type of conduits are limited by poor mechanical strength [44].
Unlike collagen, fibrin is not an ECM protein. Instead, fibrin is isolated from blood plasma. Fibrin is polymerized from fibrinogen through its cleavage by the enzyme thrombin. Fibrin is a fibrous protein involved in blood clotting and wound healing. When fibrin polymerizes, it forms a biodegradable mesh that is an ideal temporary scaffold for cells. Cells that are seeded in fibrin gel deposit more collagen and elastin than cells grown in collagen gels. Furthermore, vascular constructs made from fibrin gels are usually stronger than those made from collagen.[47]
To improve the elasticity of tissue-engineered blood vessels, researchers are incorporating elastin in vascular constructs [48]. In human blood vessels, layers of elastic membranes consisting mainly of elastin fibers lie between the intimal, medial and adventitial layers and give the wall elasticity. Elastin is also known to regulate smooth muscle cell activity [49]. Different techniques have been applied to incorporate elastin in tissue engineered vascular graft: direct elastogenesis by culturing smooth muscle cells [43, 50], freeze- drying [51], or electrospining [52].
Although natural polymers offer great potential for tissue-engineered blood vessels, the success of this approach requires more research into developing scaffold that can mimic the three-dimensional structure of ECM fibers, improving the efficiency of cell adhesion and proliferation within the scaffold.

4.1.4. Cell sheets

An innovative approach devised by L'heureux et al. was to use cell sheets to create tissue-engineered blood vessels. Human smooth muscle cells were cultured on tissue culture plates to form a cohesive sheet. A sheet of human fibroblast was produced in the same manner. The sheet of smooth muscle cells was then removed from the plate and rolled around a mandrel to form the medial layer of the tissue-engineered vessel. The sheet of fibroblast was then rolled around the medial layer to form the adventitial layer. After 8 weeks of additional culture, the mandrel was removed and the lumen was coated with human endothelial cells. The resultant tissue-engineered blood vessel (TEBV) had a functional endothelium and good mechanical strength but it lacked elasticity. Another drawback is the long culture time needed prior to implantation (> 13 weeks) [53].
Results of a clinical trial based on cell sheet technology were published in 2009. This publication reported that 25 patients had undergone an arterio-venous shunt using tissue-engineered grafts made from the patients' own cells. The mechanical properties of the TEBVs were compared to those of human internal mammary artery and saphenous vein segments. Results from mechanical testing showed high burst strength, resistance to fatigue loading, good suturability and clinically relevant compliance up to 21 months after implantation [54].
Currently, the company Cytograft, which was founded by Dr. L'Heureux and Dr.McAllister, makes use of cell sheet technology to create vascular grafts made from the patient's skin fibroblast cells. Trademarked under the name Lifeline Technology, the

company tissue-engineered blood vessel replacement for arterio-venous shunts has reached phase 3 clinical trials [55].

4.1.5 Decellularized Tissue

Decellularized tubular tissues can potentially be used as scaffolds for tissue engineered vascular conduits because they retain some of the structure of the native ECM. The process of decellularization removes the cellular components of the tissue by a combination of chemical and mechanical treatments: enzymatic digestion, treatment with chemical detergents, vigorous mechanical agitation and sonication. Because the tissue loses its mechanical strength after this process, it is necessary to crosslink the fibers of the remaining matrix. The efficiency of decellularization is dependent on the tissue type but it is unlikely that any combination of method can remove all cellular components from the tissue. The process of decellularization also alters the native structure of the ECM [56]. Decellularized tissue can come from allogenic or zenogenic sources. Xenogenic tissue, however, is not often used because of the increased risks of inflammation, immune rejection and viral infection [57].
Decellularized blood vessels such as carotid arteries, umbilical arteries and veins have been used as vascular grafts with limited success [57-59]. One challenge is to retain patency in the conduit. Recellularization with endothelial cells before implantation has been shown to increase the patency of the vascular conduit in animal models [60, 61].
Some studies have attempted to use of decellularized tissue from sources other than vascular tissue. Lantz et. al used small intestine submucosa as small-diameter autologous arterial grafts for the carotid and femoral arteries in 18 dogs. They reported that 75% of grafts remained patent during the 48-week study and there was evidence of aneurysm in 11% of grafts [62].
Alternatively, Narita et. al used decellarized ureters as small-diameter autologous arterial grafts for dogs. The decellularized tissues were seeded with canine endothelial cells and myofibroblasts prior to implantantation. They reported that the grafts remained patent at least 6 months after implantation [63].

In summary, there has been notable progress over the last two decades in the development of materials for tissue engineered blood vessels. Different approaches have been taken to develop a suitable scaffold materials, especially for small-diameter vascular grafts, but to date native arteries and veins remain the gold standard.

4. Vascular Tissue Engineering

4.2. Cell Sources for Vascular Tissue Engineering

Early efforts in the field of tissue engineered blood vessels utilized vascular cells (vascular smooth muscle cells, endothelial cells, and fibroblasts) to recreate structures similar to native human blood vessels [26, 40, 43]. The success of this approach was limited in part by the low proliferative capacity of human vascular cells. The isolation and characterization of progenitor cells and stem cells opened new possibilities for tissue-engineered vascular graft.
The advantage of stem cells lies in their ability to replicate indefinitely and to differentiate into multiple cell types. Progenitor cells can be easily isolated, however, they can only differentiate into a specific cell type because they are more specialized than stem cells

4.2.1 Endothelial Cells

The endothelium is a continuous monolayer that provides a thrombo-resistant barrier in the blood vessel wall. The endothelium also regulates transport between the blood and the tissue. In addition, the endothelium plays an important role in the regulation of cell function such as smooth muscle cell migration and proliferation as well as leukocyte activation.
Endothelial cells (ECs) are not only regulated by chemical signals such as hormones, cytokines, and neurotransmitters but also by mechanical stimulation (shear stress and mechanical strain generated by blood flow) [64]. In arteries, endothelial cells that line the lumen of blood vessels experience an average fluid shear stress caused by blood flow ranging between 10 and 15 dynes/cm^2 [8, 9].
As noted previously, the presence of a confluent endothelial layer is necessary in order to avoid thrombosis and intimal hyperplasia an implanted vascular graft.
There are two methods to endothelialize a vascular graft. One method is to seed the graft with endothelial cells in-vitro and then implant the graft. Luminal endotheliazation in humans requires a large number of ECs. Unfortunately, ECs have limited capacity for regeneration. ECs can no longer divide after 70 cell cycles [65]. In addition, culture time requires 2 to 4 weeks. Cell seeding ex-vivo is therefore not an ideal solution. The alternative method is to design surface properties on the luminal side of the graft that can induce in-situ endothelialization.

4.2.2 Smooth Muscle Cells

Vascular smooth muscle cells (SMCs) are thought to arise from the multiple embryologic origins: the mesoderm, the neural crest and, the proepicardium [66-68]. It has been shown that vascular smooth muscle cells can acquire different phenotypes within different locations in the blood vessel wall [69, 70]. It is not clear, however, that the developmental origin of the SMCs can explain their phenotypic heterogeneity.

In the medial layer of the blood vessel, SMCs experience a very low shear stress of about 1 dynes/cm^2 due to interstitial fluid flow [71]. SMCs also experience cyclic mechanical strain due to the pulsatility of blood flow [72]. SMCs allow the blood vessel to maintain vascular tone and function in response to various physiological cues. In addition, SMCs synthesize elastin, different types of collagens and proteoglycans [73]. Smooth muscle cells can adopt two different phenotypes: a contractile state in healthy vessels, and a synthetic state under pathological conditions. It has been shown that SMCs lose their contractile phenotype in culture. Smooth muscle cells in the synthetic state proliferate at a faster rate and produce more ECM proteins than in the contractile state [74]. It is known that smooth muscle cells can alter their phenotype in response to cell-to-cell interactions, interactions with the ECM and hormonal activity [75]. Vascular SMCs have been used to engineer small-diameter vascular grafts but a non-invasive method of harvesting these cells from patients is not possible.

4.2.3 Fibroblasts

Human fibroblasts are an attractive cell source for vascular graft engineering because they can be easily extracted from skin biopsies and can be expanded rapidly in culture [31, 53]. Fibroblasts populate the outermost layer of the blood vessel wall [76]. Fibroblasts synthesize extracellular cellular matrix components (collagen and elastin) as well as proteoglycans.
During wound healing or under pathological conditions, fibroblasts can become myofibroblasts. They begin to express smooth-muscle cell markers and acquire a contractile phenotype [77]. Fibroblast have been utilized since the first published attempt at creating a tissue engineered blood vessel by Bell and Weinberg in 1986 [26]. The latest example of an application of human skin fibroblasts is in cell sheet engineering. The technology is currently being commercialized by Cytograph, inc [55].

4.2.4 Endothelial Progenitor Cells

Endothelial progenitor cells (EPCs) represent a promising source of endothelial cells for synthetic vascular grafts and tissue-engineered blood vessels because they can be easily isolated, and possess a high potential for proliferation [78]. Endothelial progenitor cells can be found in the bone marrow, peripheral blood or cord blood. EPCs originate from the bone marrow and can differentiate into mature endothelial cells. Upon stimulation, EPCs are released in the blood circulation and migrate to vascular regions with injured endothelia [79]. The controversy about endothelial progenitor cells lies in the fact that there exist multiple phenotypic definitions for EPCs. In cell culture, there are 2 phenotypes of EPCs: “early EPCs” and “late EPCs”. In addition to cell culture, there exist different methods to identify EPCs by locating markers for stemness as well as endothelial cell markers namely: VEGF-2, VE-Cadherin and von Willebrand factor [64].

The drawback in using EPCs is their low yield: in normal adults, the concentration of EPCs in peripheral blood is very low (2–3 cells/mm^3). The concentration of EPCs in cord blood, however, is 3.5 times higher [80].
A great deal of research has been dedicated to improving endothelialization in vascular conduits. In early studies, endothelial cells were used to minimize the risk of thrombosis [40, 81-87]. In recent years, however, more attention has being given to endothelial progenitor cells (EPCs) because of their ease of isolation. Several studies have indicated that endothelial progenitor cells can be utilized to create a function endothelial layer for vascular conduits.
In several animal studies, EPCs have been successfully used to endothelialize vascular grafts ex-vivo prior to implantation [80, 88, 89]. Human EPC seeding on various scaffold materials has also been extensively studied ex-vivo [90-92].
In 2001, endothelial progenitor cells isolated from sheep peripheral blood were shown to provide a non-thrombogenic luminal surface when implanted in decellularized porcine iliac arteries. The EPC-seeded grafts remained patent up to 130 days. Vascular grafts seeded with EPCs remained patent 115 days longer than grafts without EPCs. In addition, grafts exhibited NO-mediated vascular relaxation comparable to native ovine carotid artery [80]. The ability of EPCs to form a non-thrombogenic surface after implantation into vascular grafts was also observed with small diameter grafts made with microporous segmented polyurethane film coated with gelatin [90].
More recently, Allen et al. used endothelial progenitor cells (EPCs) to create an endothelial cell layer on modified expanded poly-tetrafluoroethylene (ePTFE) vascular grafts. They first differentiated human EPCs into endothelial-like cells in-vitro. These cells were positive for endothelial cell markers (VE-cadherin, Flk-1 and PECAM-1); they assumed an endothelial cobblestone morphology and produced endothelial nitric oxide synthase (eNOS). When seeded onto the ePTFE vascular grafts, the human endothelial-like cells could produce anti-thrombogenic factors that inhibit platelet adhesion and blood clot formation in-vitro [93]. The same year, these conclusions were independently confirmed by Ranjan et. al [27]. These results suggest that this methodology could be applied in-vivo.
In order to improve the performance of vascular grafts, research is now focused on developing strategies to increase the mobilization and homing of EPCs to the inner surface vascular conduits. These strategies include the use of oligosaccharides[94], peptides[95], antibodies [96], and more recently, oligonucleotides aptamers to attract EPCs to the vascular graft surface in an effort to prevent thrombosis.

4.2.5 Embryonic Stem Cells

Embryonic stem cells (ESCs) are isolated from the inner cell mass of the blastocyst. ESCs are characterized by their unlimited proliferative potential and their ability to differentiate into all cell types of the body [97]. Embryonic stem cells offer an excellent cell source for tissue regeneration and cell therapy. However, the use of embryonic stem cells for tissue engineering applications depends on our ability to control stem cell proliferation and direct stem cell differentiation [98].

There exist differences between human and mouse embryonic stem cells. While human embryonic stem cells (hESCs) offer greater clinical applications, the mouse model provides significant insight into human stem cell differentiation and early human development [99]. Murine embryonic stem (mESC) cells proliferate more rapidly than human ESCs in culture. The cell population doubling time is between 12 and 15 hours for mice whereas the doubling time for hESCs is between 30 and 35 hours [100]. Regardless of the species, all ESCs can maintain their pluripotency or can differentiate into any cell type depending on the culture conditions. Pluripotency makes embryonic stem cells an attractive option for tissue engineering applications and cell therapy for human diseases.

In vitro, ESCs are cultivated on a feeder layer of embryonic fibroblasts to maintain an undifferentiated phenotype. The feeder cells come from primary embryonic fibroblasts and produce leukemia inhibitory factor (LIF). The addition of leukemia inhibitory factor to the culture medium can also prevent the differentiation of ESCs thus eliminating the need for feeder cells [101]. Several feeder-free culture systems have been developed and are now commercially available. Pluripotent ESCs are characterized by a high expression of endogenous alkaline phosphatase and telomerase. While human ESCs express the surface marker stage-specific cell embryonic antigen (SSEA)-3/4, mouse ESCs express the stage-specific embryonic antigen SSEA-1. The maintenance of pluripotency in ESCs requires the expression of transcription factors such as Oct-3/4, Nanog, and Rex-1 [102]. Embryonic stem cell differentiation begins whenever transcription factor Oct-4 is absent [100]. In the absence of a feeder layer or LIF, ESCs start to differentiate.

When ESCs are cultured in suspension, they form embryoid bodies and replicate the early stages of embryonic development. These embryoid bodies contain differentiated cells from all 3 germ layers: the endoderm, ectoderm, and mesoderm [103]. Growth factors, cell-to-cell interactions and differential access to nutrients all play a role during the differentiation process [104]. Murine ESCs can form both simple and cystic embryoid bodies. Human ESCs can only form cystic embryoid bodies.

Growth factors and chemical compounds are commonly used to direct the differentiation of ESCs. The addition of VEGF to the Flk1-positive cultures promotes endothelial differentiation, whereas mural cells are induced by platelet-derived growth factor (PDGF-BB) [105]. Pancreatic endocrine insulin-expressing cells were derived from undifferentiated ESCs by sequential addition of retinoic acid and sodium butyrate. Meanwhile, sequential addition of retinoic acid and betacellulin (BTC) or activin A yielded neuronal and glial-like cell types in the presence of AA or BTC [104]. Another approach to direct differentiation is by genetic modification, which includes both the suppression and the over-expression of genes. However, this approach involves the use of viral vectors, which are unsafe for clinical applications [100].

During the process of differentiation, soluble factors, mechanical forces, and the extracellular matrix (ECM) together contribute to stem cell fate. To predictably direct embryonic stem cell differentiation, a better understanding of the effects of each factor is necessary.

There have been few studies aimed at creating vascular grafts from embryonic stem cells. However, some studies have shown that embryonic stems cells offer great potential for vascular graft engineering. A study by Huang et al. (2005) examined the

vascular differentiation of a mixture of mouse ESCs containing about 30% Flk1+ positive cells seeded in a microporous polyurethane tube. The compliance of the graft was similar to the compliance of the human artery. The graft was subjected to a low pulsatile flow mimicking the wall shear stress and circumferential strain present in the human venous system. The study reported that cells on the luminal surface reorient in the direction of flow. While the cells at the surface became positive for PECAM-1, the cells in the deeper layer became positive for smooth muscle actin. Results from this study introduced the possibility of engineering a vascular graft containing multiple vascular cell types using embryonic stem cells [28]. The main obstacle in the use of embryonic stem cells lies in removing residual undifferentiated cells from the engineered vascular grafts. Residual stem cells inevitably lead to teratoma formation in the host. Another problem lies in the ability to guide the differentiation of embryonic stem cells toward the desired cell type with efficiency and reliability. If these difficulties can be over, the embryonic stem cells may become a more attractive option for vascular graft engineering.

4.2.6 Induced Pluripotent Stem Cells

Induced pluripotent stem cells (iPSCs) are pluripotent stem cells that are generated from somatic cells through the expression of a set four reprogramming factors: OCT4, SOX2, KLF4, and c-MYC [106], or OCT4, SOX2, NANOG, and LIN28 [107]. iPSCs are pluripotent like ESCs but, unlike ESCs, they do not raise ethical issues associated with the destruction of embryos. iPSCs also eliminate the concerns about immune rejection, which are also associated with ESCs.

iPSCs were initially generated using retroviruses to deliver the four reprogramming factors to somatic cells. There are, however, inherent risks associated with viral delivery methods: the random integration of foreign DNA into the cell and mutagenesis.

Researchers have sought to use safer methods of delivery to eliminate these risks. iPSCs have been generated through non-viral methods such as electroporation with non-integrating episomal vectors[108] or mini-circle DNA [109] transfection of plasmid DNA[110] , synthetic mRNAs [111] or microRNAs [112]. Nonetheless, more research is needed to increase reprogramming efficiency and to overcome technical challenges associated with these methods.

To continue, several small molecules have been found to reduce the number of reprogramming factors and enhance reprogramming efficiency.

For example, both vitamin C and valproic acid (VPA) have been shown for improve reprogramming efficiency [113, 114]. Chromatin modifying proteins, like Jhdm1a/1b, in combination with OCT4 can reprogram mouse somatic cells [115]. Mouse cells can also be reprogrammed using only OCT4 by activating Sonic Hedgehog.

In addition, it was recently discovered that microRNAs can reprogram both human and mouse somatic cells without the use of transcription factors[116].

The development of iPSCs technology offers numerous potential applications.

First, iPSCs can readily be used to provide human cells for toxicology studies to develop better drugs. Second, iPSCs can facilitate the study of various diseases by allowing researchers to model these diseases in-vitro. Third, iPSCs can be used to

generate patient-specific cells that can, in turn, be used to engineer tissues or whole organs.

4.2.7 Mesenchymal Stem Cells

Mesenchymal stem cells (MSCs) are multipotent stem cells that can be isolated from various adult tissues. Although bone marrow is the most abundant source of MSCs, these cells are also found in muscle, fat, dermis, peripheral and cord blood. MSCs have been shown to differentiate into adipocytes, chondrocytes, osteoblasts and vascular smooth muscle cells [117]. The differentiation of MSCs can be directed by different growth factor combinations. Supplementing the basal culture medium with dexamethasone, ascorbate and β-glycerophosphate induces differentiation into osteoblasts. Supplementing with TGF-β3, dexamethasone and ascorbate induces chondrogenic differentiation while dexamethasone and hydrocortisone will induce myogenic differentiation [118]. Adipogenic induction requires the addition of h-insulin, dexamethasone, indomethacin and IBMX [119]. To continue, the addition of vascular endothelial growth factor (VEGF) is sufficient to induce differentiation toward an endothelial phenotype [120].
Human MSCs derived from bone marrow can be expanded without losing their multipotency [117]. Although no single cell surface marker for MSCs exists, they are in general positive for STRO-1 (a stromal cell surface antigen), CD105 (endoglin, receptor for transforming growth factor-β, TGF-β, and integrins), CD29 (integrinβ1), CD44 (receptor for hyaluronic acid and matrix proteins) and CD166 (a cell adhesion molecule), and negative for CD14 (monocyte surface antigen), CD34 (HSC surface antigen), and CD45 (leukocyte surface antigen) [6].
MSCs do not express the major histocompatibility complex II (MHC II) antigens that are responsible for immune rejection. MSCs are therefore a good cell source for allogeneic cell transplantation [121].
Several research groups have attempted to engineer vascular conduits using mesenchymal stem cells (MSCs). In an in-vivo study, Hashi et. al seeded MSCs in small-diameter vascular grafts made from electrospun poly-L-lactic acid nanofibers. They showed that the presence of MSCs results in the formation of an organized layer of endothelial cells (ECs) and smooth muscle cells (SMCs), similar to native arteries. The presence of MSCs also improved the long-term patency of the vascular grafts. The study attributes this clear improvement to the antithrombogenic properties of MSCs [122]. A year later, Mirza et. al. confirmed some of the findings mentioned above. In their study, undifferentiated mesenchymal stem cells were seeded in polyurethane grafts, which were subsequently implanted in rats. Their results showed full graft endotheliazation and only partial differentiation of MSCs into smooth muscle after 2 weeks in-vivo [123]. Differences in the two conclusions may be attributed to the duration of these two studies.
In an in-vitro study, Gong and Niklason reported that they had successfully engineered small diameter vascular grafts from hMSCs seeded in polyglycolic acid (PGA) mesh scaffolds. Using a biomimicing system, they exposed vascular constructs to 5% cyclic strain for up to 8 weeks. They noted that the morphology and histology of the

engineered vessel wall was similar to that of native vessels. However, they indicated that more work is necessary to improve the mechanical properties and the endothelialization of the engineered vessels [124].
Cho et. al differentiated bone marrow derived MSCs into endothelial-like and smooth muscle-like cells in-vitro. The partially differentiated cells were then seeded onto decellularized canine arteries, which were implanted into dogs. They reported that their vascular grafts remained patent up to 8 weeks [125]. Zhao et. al. later used the same method with autologous ovine MSCs seeded on decellularized carotic arteries. Their study showed that the implanted grafts remained patent up to 5 months. They also showed the presence of an endothelium and smooth muscle cells in the grafts at 5 months [126].
As noted earlier the bone marrow is not the only source for MSCs. Human adipose-derived MSCs were partially differentiated and seeded onto PGA to engineer small diameter blood vessels in-vitro. After 8 weeks of mechanical stimulation in a bioreactor, the differentiated MSCs expressed a smooth muscle cell phenotype with the characteristic markers: smooth muscle alpha actin (α-SMA), calponin, and smooth muscle myosin heavy chain (SM-MHC) [127]. More recently, another group showed independently that human adipose-derived MSCs could be partially differentiated in-vitro before being seeded onto decellularized veins. After incubation in a bioreactor, the differentiated cells exhibited a contractile phenotype as well as smooth muscle cell markers [128]. In a more recent study, Harris et. al. demonstrated that adipose-derived mesenchymal stem cells (ASCs) are a potential cell source for vascular grafts. ASCs seeded into vascular grafts differentiated towards a smooth-muscle phenotype as shown by the up-regulation of calponin, caldesmon, and myosin heavy chain [129].
Although more work needs to be done, the studies mentioned above demonstrate that mesenchymal stem cells are a promising cell source for vascular graft engineering.

4.2.8 Neural Crest Stem Cells

The neural crest refers to a population of cells located between the neural tube and the dorsal ectoderm during the embryonic development of vertebrates [130, 131]. Neural crest stem cells (NCSCs) are multipotent cells that undergo epithelial to mesenchymal transition and migrate extensively to give rise to a variety of tissues: cranial and facial bone, cartilage, nerve tissue, smooth muscle, connective tissue and even melanocytes [132].
NCSCs have been studied extensively in rodent and avian models. They have been isolated from embryonic and adult rodent tissues: bone marrow [133], skin [134], cornea [135] ,heart tissue[136], hair follicle [137] and gut [138]. Markers for NCSCs include: p75, human natural killer protein 1 (HNK1), Nestin, Activating Protein 2 (AP2) and vimentin [139-141]. Recently, NCSCs have been derived from mouse and human ESCs and iPSCs [142, 143]. Since it is not possible to conduct in-vivo studies on human NCSCs, this approach yields new possibilities for research in the study of human development and regenerative medicine.

NCSCs derived from ESCs and iPSCs have been shown to differentiate into peripheral neurons, Schwann cells, chondrocytes, osteoblasts, adipocytes and smooth muscle cells [141, 144]. NCSCs could provide a potential cell source for tissue engineering because they give rise to smooth muscle tissue during development [130]. Human NCSCs have also been shown to differentiate into smooth muscle cells in-vitro [144]. In order to use these stem cells for tissue engineering applications, however, a better understanding of the effects of biomechanical factors on NCSC differentiation and proliferation is still needed. In this thesis, we will study how laminar fluid shear stress affects the differentiation and proliferation of human NCSCs.

4.2.9 Multipotent Vascular Stem Cells

In disease states such as atherosclerosis, intimal hyperplasia and restenosis, smooth muscle cells migrate from the medial layer of the blood vessels to the intima. They proliferate and contribute to intimal thickening. It has long been thought that the de-differentiation of mature and contractile smooth muscle cells into proliferative and synthetic smooth muscle cells was involved in these pathological conditions [145, 146]. Contrarily to this generally accepted theory, some have argued that a distinct population of smooth muscle cells within the vessel wall is involved in this phenomenon [147, 148] . This paradigm has again been called into question by a recent study by Tang et al [149]. The study identified a novel population of adult stem cells within the medial layer of the blood vessel. These cells named “multipotent vascular stem cells” (MVSCs) are positive for Sox10, Sox17, neural crest cell markers, general MSC makers but negative for EC markers. MVSCs express low levels of SMA but do not express SM-MHC or Calponin1. In addition, MVSCs have the potential to differentiate into peripheral neurons, Schwann cells, adipocytes, chondrocytes, osteocytes and mature smooth muscle cells. Furthermore, it was reported that MVSCs are not derived from SMCs. The study also showed that, in vivo, MVSCs become proliferative and contribute significantly to vascular remodeling in response to injury [149]. MVSCS may be an excellent cell source for vascular tissue engineering but in order to utilize these stem cells, a better understanding of the effects of biomechanical factors on MVSC differentiation and proliferation is necessary. In this thesis, we will focus on the effects of laminar fluid shear stress on MVSC function.

5. Parallel Plate Flow Chamber System

In this dissertation, a parallel plate flow chamber system was used to study the effects of fluid flow on three different adult stem cell types: MSCs, NCSCs, and MVSCs. This system is widely used to isolate the effects of laminar fluid flow and fluid shear stress under defined conditions. The parallel plate flow chamber was first designed in 1973 by Hochmuth et al in their study of red blood cells [150]. Briefly, a glass slide is seeded with cells and mounted on a rectangular flow channel by sandwiching a silicone gasket between the glass slide and a polycarbonate flow chamber base. A fluid circulates through the flow chamber system with the help of a peristaltic pump. The parallel plate flow system depicted in figure 5 was set up in a humidified cell culture incubator for all experiments.

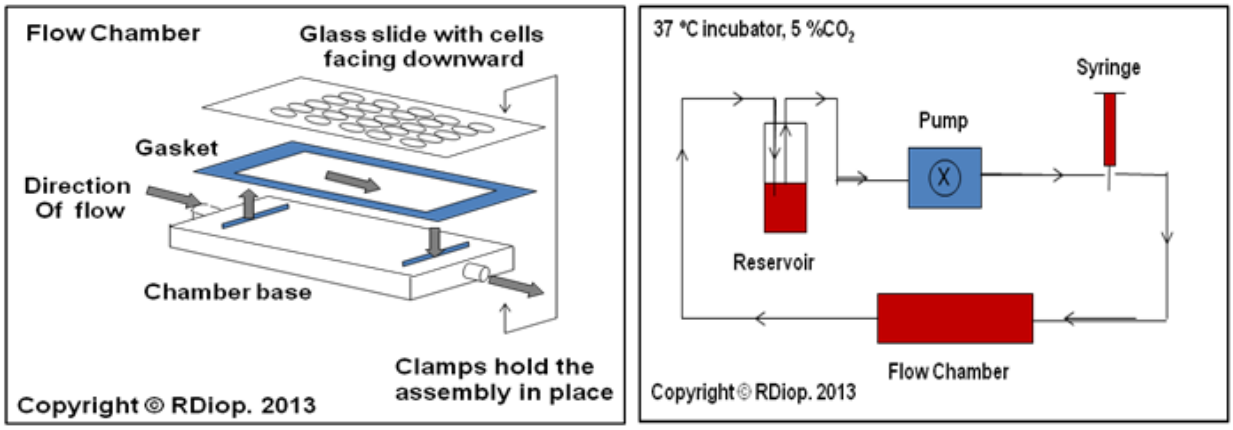

Figure 5. Diagrams of the parallel plate flow chamber system. The flow chamber is created by mounting a glass slide seeded with cells on a rectangular polycarbonate chamber base. A silicone gasket is inserted between the glass slide and the chamber base to allow fluid to circulate. Clamps are used to hold the assembly in place. A peristaltic pump is used to circulate fluid through the system. A syringe is used to dampen the vibrations caused by the pump.

A derivation of the equation relating the shear stress experienced by the cells inside the flow chamber to the volumetric flow rate of the pump for this experimental system can be found in the appendix.

References

1. Marieb, E. and J. Mallatt, *Human Anatomy*. 3rd ed. 2001, San Francisco: Benjamin Cummings.
2. Bjorklund, R., *Circulatory system*. 2009, New York: Michelloe Bisson.
3. Gray, H., et al., *Gray's Anatomy*. 40th ed. 2008: Churchill, Livingstone. Elsevier.
4. Saladin, K.S., *Human Anatomy*. 3rd ed. 2011, New York, NY: McGraw Hill.
5. Lehoux, S. and A. Tedgui, *Cellular mechanics and gene expression in blood vessels.* J Biomech, 2003. **36**(5): p. 631-43.
6. Park, J.S., et al., *Mechanobiology of mesenchymal stem cells and their use in cardiovascular repair.* Front Biosci, 2007. **12**: p. 5098-116.
7. Berardi, D.E. and J.M. Tarbell, *Stretch and Shear Interactions Affect Intercellular Junction Protein Expression and Turnover in Endothelial Cells.* Cell Mol Bioeng, 2009. **2**(3): p. 320-331.
8. Weinberg, P.D. and C. Ross Ethier, *Twenty-fold difference in hemodynamic wall shear stress between murine and human aortas.* J Biomech, 2007. **40**(7): p. 1594-8.
9. Fung, Y.C. and S.Q. Liu, *Elementary mechanics of the endothelium of blood vessels.* J Biomech Eng, 1993. **115**(1): p. 1-12.
10. Traub, O. and B.C. Berk, *Laminar shear stress: mechanisms by which endothelial cells transduce an atheroprotective force.* Arterioscler Thromb Vasc Biol, 1998. **18**(5): p. 677-85.
11. Halka, A.T., et al., *The effects of stretch on vascular smooth muscle cell phenotype in vitro.* Cardiovasc Pathol, 2008. **17**(2): p. 98-102.
12. Silver, F.H., I. Horvath, and D.J. Foran, *Viscoelasticity of the vessel wall: the role of collagen and elastic fibers.* Crit Rev Biomed Eng, 2001. **29**(3): p. 279-301.
13. Organization, T.W.H., *Global Atlas on Cardiovascular Disease Prevention and Control*, S. Mendis, Editor 2011: Geneva, Switzerland.
14. Libby, P., P.M. Ridker, and A. Maseri, *Inflammation and atherosclerosis.* Circulation, 2002. **105**(9): p. 1135-43.
15. Libby, P., P.M. Ridker, and G.K. Hansson, *Progress and challenges in translating the biology of atherosclerosis.* Nature, 2011. **473**(7347): p. 317-25.
16. Blankenberg, S., S. Barbaux, and L. Tiret, *Adhesion molecules and atherosclerosis.* Atherosclerosis, 2003. **170**(2): p. 191-203.
17. Libby, P., *Inflammation in atherosclerosis.* Arterioscler Thromb Vasc Biol, 2012. **32**(9): p. 2045-51.
18. Slijkhuis, W., W. Mali, and Y. Appelman, *A historical perspective towards a non-invasive treatment for patients with atherosclerosis.* Neth Heart J, 2009. **17**(4): p. 140-4.
19. WebMD. Available from: http://www.webmd.com/cholesterol-management/medications-to-treat-atherosclerosis.
20. Roger, V.L., et al., *Heart disease and stroke statistics--2012 update: a report from the American Heart Association.* Circulation, 2012. **125**(1): p. e2-e220.
21. Ravi, S. and E.L. Chaikof, *Biomaterials for vascular tissue engineering.* Regen Med, 2010. **5**(1): p. 107-20.

22. Galambos, B., et al., *Successful human vascular reconstructions with long-term refrigerated venous homografts.* Eur Surg Res, 2009. **43**(3): p. 256-61.
23. Lytle, B.W., et al., *Long-term (5 to 12 years) serial studies of internal mammary artery and saphenous vein coronary bypass grafts.* J Thorac Cardiovasc Surg, 1985. **89**(2): p. 248-58.
24. Zeff, R.H., et al., *Internal mammary artery versus saphenous vein graft to the left anterior descending coronary artery: prospective randomized study with 10-year follow-up.* Ann Thorac Surg, 1988. **45**(5): p. 533-6.
25. Vara, D.S., et al., *Cardiovascular tissue engineering: state of the art.* Pathol Biol (Paris), 2005. **53**(10): p. 599-612.
26. Weinberg, C.B. and E. Bell, *A blood vessel model constructed from collagen and cultured vascular cells.* Science, 1986. **231**(4736): p. 397-400.
27. Ranjan, A.K., et al., *Human blood vessel-derived endothelial progenitors for endothelialization of small diameter vascular prosthesis.* PLoS ONE, 2009. **4**(11): p. e7718.
28. Huang, H., et al., *Differentiation from embryonic stem cells to vascular wall cells under in vitro pulsatile flow loading.* J Artif Organs, 2005. **8**(2): p. 110-8.
29. Roh, J.D., et al., *Small-diameter biodegradable scaffolds for functional vascular tissue engineering in the mouse model.* Biomaterials, 2008. **29**(10): p. 1454-63.
30. Enomoto, S., et al., *Long-term patency of small-diameter vascular graft made from fibroin, a silk-based biodegradable material.* J Vasc Surg. **51**(1): p. 155-64.
31. L'Heureux, N., et al., *Human tissue-engineered blood vessels for adult arterial revascularization.* Nat Med, 2006. **12**(3): p. 361-5.
32. de Mel, A., et al., *Biofunctionalization of biomaterials for accelerated in situ endothelialization: a review.* Biomacromolecules, 2008. **9**(11): p. 2969-79.
33. Roll, S., et al., *Dacron vs. PTFE as bypass materials in peripheral vascular surgery--systematic review and meta-analysis.* BMC Surg, 2008. **8**: p. 22.
34. Takagi, H., et al., *A contemporary meta-analysis of Dacron versus polytetrafluoroethylene grafts for femoropopliteal bypass grafting.* J Vasc Surg, 2010. **52**(1): p. 232-6.
35. Polterauer, P., et al., *Dacron versus polytetrafluoroethylene for Y-aortic bifurcation grafts: a six-year prospective, randomized trial.* Surgery, 1992. **111**(6): p. 626-33.
36. Reynolds, M.M., et al., *Nitric oxide releasing polyurethanes with covalently linked diazeniumdiolated secondary amines.* Biomacromolecules, 2006. **7**(3): p. 987-94.
37. Venkatraman, S., F. Boey, and L.L. Lao, *Implanted cardiovascular polymers: Natural, synthetic and bio-inspired.* Progress in Polymer Science, 2008. **33**(9): p. 853-874.
38. Shinoka, T. and C. Breuer, *Tissue-engineered blood vessels in pediatric cardiac surgery.* Yale J Biol Med, 2008. **81**(4): p. 161-6.
39. Htay, A.S., S.H. Teoh, and D.W. Hutmacher, *Development of perforated microthin poly(epsilon-caprolactone) films as matrices for membrane tissue engineering.* J Biomater Sci Polym Ed, 2004. **15**(5): p. 683-700.
40. Niklason, L.E., et al., *Functional arteries grown in vitro.* Science, 1999. **284**(5413): p. 489-93.

41. Shin'oka, T., Y. Imai, and Y. Ikada, *Transplantation of a tissue-engineered pulmonary artery.* N Engl J Med, 2001. **344**(7): p. 532-3.
42. Tranquillo, R.T., et al., *Magnetically orientated tissue-equivalent tubes: application to a circumferentially orientated media-equivalent.* Biomaterials, 1996. **17**(3): p. 349-57.
43. L'Heureux, N., et al., *In vitro construction of a human blood vessel from cultured vascular cells: a morphologic study.* J Vasc Surg, 1993. **17**(3): p. 499-509.
44. Nerem, R.M. and D. Seliktar, *Vascular tissue engineering.* Annu Rev Biomed Eng, 2001. **3**: p. 225-43.
45. Stegemann, J.P. and R.M. Nerem, *Phenotype modulation in vascular tissue engineering using biochemical and mechanical stimulation.* Ann Biomed Eng, 2003. **31**(4): p. 391-402.
46. Seliktar, D., et al., *Dynamic mechanical conditioning of collagen-gel blood vessel constructs induces remodeling in vitro.* Ann Biomed Eng, 2000. **28**(4): p. 351-62.
47. Long, J.L. and R.T. Tranquillo, *Elastic fiber production in cardiovascular tissue-equivalents.* Matrix Biol, 2003. **22**(4): p. 339-50.
48. Berglund, J.D., R.M. Nerem, and A. Sambanis, *Incorporation of intact elastin scaffolds in tissue-engineered collagen-based vascular grafts.* Tissue Eng, 2004. **10**(9-10): p. 1526-35.
49. Patel, A., et al., *Elastin biosynthesis: The missing link in tissue-engineered blood vessels.* Cardiovasc Res, 2006. **71**(1): p. 40-9.
50. Ross, J.J. and R.T. Tranquillo, *ECM gene expression correlates with in vitro tissue growth and development in fibrin gel remodeled by neonatal smooth muscle cells.* Matrix Biol, 2003. **22**(6): p. 477-90.
51. Buttafoco, L., et al., *First steps towards tissue engineering of small-diameter blood vessels: preparation of flat scaffolds of collagen and elastin by means of freeze drying.* J Biomed Mater Res B Appl Biomater, 2006. **77**(2): p. 357-68.
52. Boland, E.D., et al., *Electrospinning collagen and elastin: preliminary vascular tissue engineering.* Front Biosci, 2004. **9**: p. 1422-32.
53. L'Heureux, N., et al., *A completely biological tissue-engineered human blood vessel.* FASEB J, 1998. **12**(1): p. 47-56.
54. Konig, G., et al., *Mechanical properties of completely autologous human tissue engineered blood vessels compared to human saphenous vein and mammary artery.* Biomaterials, 2009. **30**(8): p. 1542-50.
55. Cytograph, I. *TISSUE ENGINEERED BLOOD VESSEL*. 2012; Available from: http://www.cytograft.com.
56. Gilbert, T.W., T.L. Sellaro, and S.F. Badylak, *Decellularization of tissues and organs.* Biomaterials, 2006. **27**(19): p. 3675-83.
57. Dahl, S.L., et al., *Decellularized native and engineered arterial scaffolds for transplantation.* Cell Transplant, 2003. **12**(6): p. 659-66.
58. Gui, L., et al., *Development of decellularized human umbilical arteries as small-diameter vascular grafts.* Tissue Eng Part A, 2009. **15**(9): p. 2665-76.
59. Daniel, J., K. Abe, and P.S. McFetridge, *Development of the human umbilical vein scaffold for cardiovascular tissue engineering applications.* ASAIO J, 2005. **51**(3): p. 252-61.

60. Borschel, G.H., et al., *Tissue engineering of recellularized small-diameter vascular grafts.* Tissue Eng, 2005. **11**(5-6): p. 778-86.
61. Yang, D., et al., *Tissue-engineered blood vessel graft produced by self-derived cells and allogenic acellular matrix: a functional performance and histologic study.* Ann Plast Surg, 2009. **62**(3): p. 297-303.
62. Lantz, G.C., et al., *Small intestinal submucosa as a small-diameter arterial graft in the dog.* J Invest Surg, 1990. **3**(3): p. 217-27.
63. Narita, Y., et al., *Decellularized ureter for tissue-engineered small-caliber vascular graft.* J Artif Organs, 2008. **11**(2): p. 91-9.
64. Obi, S., et al., *Fluid shear stress induces arterial differentiation of endothelial progenitor cells.* J Appl Physiol, 2009. **106**(1): p. 203-11.
65. Naito, Y., et al., *Vascular tissue engineering: towards the next generation vascular grafts.* Adv Drug Deliv Rev, 2011. **63**(4-5): p. 312-23.
66. Wasteson, P., et al., *Developmental origin of smooth muscle cells in the descending aorta in mice.* Development, 2008. **135**(10): p. 1823-32.
67. Dettman, R.W., et al., *Common epicardial origin of coronary vascular smooth muscle, perivascular fibroblasts, and intermyocardial fibroblasts in the avian heart.* Dev Biol, 1998. **193**(2): p. 169-81.
68. Bergwerff, M., et al., *Neural crest cell contribution to the developing circulatory system: implications for vascular morphology?* Circ Res, 1998. **82**(2): p. 221-31.
69. Bochaton-Piallat, M.L., et al., *Phenotypic heterogeneity of rat arterial smooth muscle cell clones. Implications for the development of experimental intimal thickening.* Arterioscler Thromb Vasc Biol, 1996. **16**(6): p. 815-20.
70. Frid, M.G., E.P. Moiseeva, and K.R. Stenmark, *Multiple phenotypically distinct smooth muscle cell populations exist in the adult and developing bovine pulmonary arterial media in vivo.* Circ Res, 1994. **75**(4): p. 669-81.
71. Wang, D.M. and J.M. Tarbell, *Modeling interstitial flow in an artery wall allows estimation of wall shear stress on smooth muscle cells.* J Biomech Eng, 1995. **117**(3): p. 358-63.
72. Yang, Z., G. Noll, and T.F. Luscher, *Calcium antagonists differently inhibit proliferation of human coronary smooth muscle cells in response to pulsatile stretch and platelet-derived growth factor.* Circulation, 1993. **88**(3): p. 832-6.
73. Vijayagopal, P. and P.V. Menon, *Varied low density lipoprotein binding property of proteoglycans synthesized by vascular smooth muscle cells cultured on extracellular matrix.* Atherosclerosis, 2005. **178**(1): p. 75-82.
74. Beamish, J.A., et al., *Molecular regulation of contractile smooth muscle cell phenotype: implications for vascular tissue engineering.* Tissue Eng Part B Rev, 2010. **16**(5): p. 467-91.
75. Manabe, I. and R. Nagai, *Regulation of smooth muscle phenotype.* Curr Atheroscler Rep, 2003. **5**(3): p. 214-22.
76. Niklason, L.E., *Techview: medical technology. Replacement arteries made to order.* Science, 1999. **286**(5444): p. 1493-4.
77. Gibson, G.E., et al., *A reproducible procedure for primary culture and subsequent maintenance of multiple lines of human skin fibroblasts.* Age, 1998. **21**(1): p. 7-14.

78. Brown, M.A., et al., *Characterization of umbilical cord blood-derived late outgrowth endothelial progenitor cells exposed to laminar shear stress.* Tissue Eng Part A, 2009. **15**(11): p. 3575-87.
79. Allen, J., et al., *Toward Engineering a Human Neoendothelium with Circulating Progenitor Cells.* Stem Cells, 2009.
80. Kaushal, S., et al., *Functional small-diameter neovessels created using endothelial progenitor cells expanded ex vivo.* Nat Med, 2001. **7**(9): p. 1035-40.
81. Jarrell, B.E., et al., *Use of an endothelial monolayer on a vascular graft prior to implantation. Temporal dynamics and compatibility with the operating room.* Ann Surg, 1986. **203**(6): p. 671-8.
82. Clowes, A.W., T.R. Kirkman, and M.A. Reidy, *Mechanisms of arterial graft healing. Rapid transmural capillary ingrowth provides a source of intimal endothelium and smooth muscle in porous PTFE prostheses.* Am J Pathol, 1986. **123**(2): p. 220-30.
83. Pasic, M., et al., *Endothelial cell seeding improves patency of synthetic vascular grafts: manual versus automatized method.* Eur J Cardiothorac Surg, 1996. **10**(5): p. 372-9.
84. Lamm, P., et al., *Autologous endothelialized vein allograft: a solution in the search for small-caliber grafts in coronary artery bypass graft operations.* Circulation, 2001. **104**(12 Suppl 1): p. I108-14.
85. Zilla, P., et al., *Clinical in vitro endothelialization of femoropopliteal bypass grafts: an actuarial follow-up over three years.* J Vasc Surg, 1994. **19**(3): p. 540-8.
86. Zilla, P., et al., *Use of fibrin glue as a substrate for in vitro endothelialization of PTFE vascular grafts.* Surgery, 1989. **105**(4): p. 515-22.
87. Isenberg, B.C., C. Williams, and R.T. Tranquillo, *Endothelialization and flow conditioning of fibrin-based media-equivalents.* Ann Biomed Eng, 2006. **34**(6): p. 971-85.
88. He, H., et al., *Canine endothelial progenitor cell-lined hybrid vascular graft with nonthrombogenic potential.* J Thorac Cardiovasc Surg, 2003. **126**(2): p. 455-64.
89. Aper, T., et al., *Autologous blood vessels engineered from peripheral blood sample.* Eur J Vasc Endovasc Surg, 2007. **33**(1): p. 33-9.
90. Shirota, T., et al., *Human endothelial progenitor cell-seeded hybrid graft: proliferative and antithrombogenic potentials in vitro and fabrication processing.* Tissue Eng, 2003. **9**(1): p. 127-36.
91. Matsuda, T., *Recent progress of vascular graft engineering in Japan.* Artif Organs, 2004. **28**(1): p. 64-71.
92. Allen, J.B., et al., *Toward engineering a human neoendothelium with circulating progenitor cells.* Stem Cells, 2010. **28**(2): p. 318-28.
93. Allen, J.B., et al., *Toward engineering a human neoendothelium with circulating progenitor cells.* Stem Cells. **28**(2): p. 318-28.
94. Suuronen, E.J., et al., *Tissue-engineered injectable collagen-based matrices for improved cell delivery and vascularization of ischemic tissue using CD133+ progenitors expanded from the peripheral blood.* Circulation, 2006. **114**(1 Suppl): p. I138-44.

95. Taite, L.J., et al., *Nitric oxide-releasing polyurethane-PEG copolymer containing the YIGSR peptide promotes endothelialization with decreased platelet adhesion.* J Biomed Mater Res B Appl Biomater, 2008. **84**(1): p. 108-16.
96. Rossi, M.L., et al., *The first report of late stent thrombosis leading to acute myocardial infarction in patient receiving the new endothelial progenitor cell capture stent.* Int J Cardiol, 2009.
97. Yu, J. and J.A. Thomson, *Pluripotent stem cell lines.* Genes Dev, 2008. **22**(15): p. 1987-97.
98. Godier, A.F., et al., *Engineered microenvironments for human stem cells.* Birth Defects Res C Embryo Today, 2008. **84**(4): p. 335-47.
99. Nichols, J. and Q.L. Ying, *Derivation and propagation of embryonic stem cells in serum- and feeder-free culture.* Methods Mol Biol, 2006. **329**: p. 91-8.
100. Grivennikov, I.A., *Embryonic stem cells and the problem of directed differentiation.* Biochemistry (Mosc), 2008. **73**(13): p. 1438-52.
101. Zandstra, P.W., et al., *Leukemia inhibitory factor (LIF) concentration modulates embryonic stem cell self-renewal and differentiation independently of proliferation.* Biotechnol Bioeng, 2000. **69**(6): p. 607-17.
102. Cormier, J.T., et al., *Expansion of undifferentiated murine embryonic stem cells as aggregates in suspension culture bioreactors.* Tissue Eng, 2006. **12**(11): p. 3233-45.
103. Doss, M.X., A. Sachinidis, and J. Hescheler, *Human ES cell derived cardiomyocytes for cell replacement therapy: a current update.* Chin J Physiol, 2008. **51**(4): p. 226-9.
104. McKiernan, E., et al., *Directed differentiation of mouse embryonic stem cells into pancreatic-like or neuronal- and glial-like phenotypes.* Tissue Eng, 2007. **13**(10): p. 2419-30.
105. Yamashita, J., et al., *Flk1-positive cells derived from embryonic stem cells serve as vascular progenitors.* Nature, 2000. **408**(6808): p. 92-6.
106. Takahashi, K., et al., *Induction of pluripotent stem cells from adult human fibroblasts by defined factors.* Cell, 2007. **131**(5): p. 861-72.
107. Yu, J., et al., *Induced pluripotent stem cell lines derived from human somatic cells.* Science, 2007. **318**(5858): p. 1917-20.
108. Yu, J., et al., *Human induced pluripotent stem cells free of vector and transgene sequences.* Science, 2009. **324**(5928): p. 797-801.
109. Jia, F., et al., *A nonviral minicircle vector for deriving human iPS cells.* Nat Methods, 2010. **7**(3): p. 197-9.
110. Si-Tayeb, K., et al., *Generation of human induced pluripotent stem cells by simple transient transfection of plasmid DNA encoding reprogramming factors.* BMC Dev Biol, 2010. **10**: p. 81.
111. Warren, L., et al., *Highly efficient reprogramming to pluripotency and directed differentiation of human cells with synthetic modified mRNA.* Cell Stem Cell, 2010. **7**(5): p. 618-30.
112. Miyoshi, N., et al., *Reprogramming of mouse and human cells to pluripotency using mature microRNAs.* Cell Stem Cell, 2011. **8**(6): p. 633-8.
113. Esteban, M.A., et al., *Vitamin C enhances the generation of mouse and human induced pluripotent stem cells.* Cell Stem Cell, 2010. **6**(1): p. 71-9.

114. Huangfu, D., et al., *Induction of pluripotent stem cells from primary human fibroblasts with only Oct4 and Sox2.* Nat Biotechnol, 2008. **26**(11): p. 1269-75.
115. Wang, T., et al., *The histone demethylases Jhdm1a/1b enhance somatic cell reprogramming in a vitamin-C-dependent manner.* Cell Stem Cell, 2011. **9**(6): p. 575-87.
116. Anokye-Danso, F., et al., *Highly efficient miRNA-mediated reprogramming of mouse and human somatic cells to pluripotency.* Cell Stem Cell, 2011. **8**(4): p. 376-88.
117. Watabe, T. and K. Miyazono, *Roles of TGF-beta family signaling in stem cell renewal and differentiation.* Cell Res, 2009. **19**(1): p. 103-15.
118. Gang, E.J., et al., *Skeletal myogenic differentiation of mesenchymal stem cells isolated from human umbilical cord blood.* Stem Cells, 2004. **22**(4): p. 617-24.
119. Baksh, D., L. Song, and R.S. Tuan, *Adult mesenchymal stem cells: characterization, differentiation, and application in cell and gene therapy.* J Cell Mol Med, 2004. **8**(3): p. 301-16.
120. Oswald, J., et al., *Mesenchymal stem cells can be differentiated into endothelial cells in vitro.* Stem Cells, 2004. **22**(3): p. 377-84.
121. Le Blanc, K., et al., *HLA expression and immunologic properties of differentiated and undifferentiated mesenchymal stem cells.* Exp Hematol, 2003. **31**(10): p. 890-6.
122. Hashi, C.K., et al., *Antithrombogenic property of bone marrow mesenchymal stem cells in nanofibrous vascular grafts.* Proc Natl Acad Sci U S A, 2007. **104**(29): p. 11915-20.
123. Mirza, A., et al., *Undifferentiated mesenchymal stem cells seeded on a vascular prosthesis contribute to the restoration of a physiologic vascular wall.* J Vasc Surg, 2008. **47**(6): p. 1313-21.
124. Gong, Z. and L.E. Niklason, *Small-diameter human vessel wall engineered from bone marrow-derived mesenchymal stem cells (hMSCs).* FASEB J, 2008. **22**(6): p. 1635-48.
125. Cho, S.W., et al., *Small-diameter blood vessels engineered with bone marrow-derived cells.* Ann Surg, 2005. **241**(3): p. 506-15.
126. Zhao, Y., et al., *The development of a tissue-engineered artery using decellularized scaffold and autologous ovine mesenchymal stem cells.* Biomaterials, 2010. **31**(2): p. 296-307.
127. Wang, C., et al., *A small diameter elastic blood vessel wall prepared under pulsatile conditions from polyglycolic acid mesh and smooth muscle cells differentiated from adipose-derived stem cells.* Biomaterials, 2010. **31**(4): p. 621-30.
128. Harris, L.J., et al., *Differentiation of adult stem cells into smooth muscle for vascular tissue engineering.* J Surg Res, 2011. **168**(2): p. 306-14.
129. Harris, L.J., et al., *Differentiation of Adult Stem Cells into Smooth Muscle for Vascular Tissue Engineering.* J Surg Res, 2009.
130. Dupin, E., et al., *Neural crest progenitors and stem cells.* C R Biol, 2007. **330**(6-7): p. 521-9.
131. Bronner-Fraser, M., *Origins and developmental potential of the neural crest.* Exp Cell Res, 1995. **218**(2): p. 405-17.

132. Crane, J.F. and P.A. Trainor, *Neural crest stem and progenitor cells.* Annu Rev Cell Dev Biol, 2006. **22**: p. 267-86.
133. Woodbury, D., et al., *Adult rat and human bone marrow stromal cells differentiate into neurons.* J Neurosci Res, 2000. **61**(4): p. 364-70.
134. Wong, C.E., et al., *Neural crest-derived cells with stem cell features can be traced back to multiple lineages in the adult skin.* J Cell Biol, 2006. **175**(6): p. 1005-15.
135. Yoshida, S., et al., *Isolation of multipotent neural crest-derived stem cells from the adult mouse cornea.* Stem Cells, 2006. **24**(12): p. 2714-22.
136. Tomita, Y., et al., *Cardiac neural crest cells contribute to the dormant multipotent stem cell in the mammalian heart.* J Cell Biol, 2005. **170**(7): p. 1135-46.
137. Sieber-Blum, M., et al., *Pluripotent neural crest stem cells in the adult hair follicle.* Dev Dyn, 2004. **231**(2): p. 258-69.
138. Kruger, G.M., et al., *Neural crest stem cells persist in the adult gut but undergo changes in self-renewal, neuronal subtype potential, and factor responsiveness.* Neuron, 2002. **35**(4): p. 657-69.
139. Morrison, S.J., et al., *Prospective identification, isolation by flow cytometry, and in vivo self-renewal of multipotent mammalian neural crest stem cells.* Cell, 1999. **96**(5): p. 737-49.
140. Stemple, D.L. and D.J. Anderson, *Isolation of a stem cell for neurons and glia from the mammalian neural crest.* Cell, 1992. **71**(6): p. 973-85.
141. Wang, A., et al., *Induced pluripotent stem cells for neural tissue engineering.* Biomaterials, 2011. **32**(22): p. 5023-32.
142. Lee, G., et al., *Isolation and directed differentiation of neural crest stem cells derived from human embryonic stem cells.* Nat Biotechnol, 2007. **25**(12): p. 1468-75.
143. Lee, G., et al., *Derivation of neural crest cells from human pluripotent stem cells.* Nat Protoc, 2010. **5**(4): p. 688-701.
144. Wang, A., et al., *Derivation of smooth muscle cells with neural crest origin from human induced pluripotent stem cells.* Cells Tissues Organs, 2012. **195**(1-2): p. 5-14.
145. Ross, R., *Atherosclerosis--an inflammatory disease.* N Engl J Med, 1999. **340**(2): p. 115-26.
146. Thyberg, J., *Phenotypic modulation of smooth muscle cells during formation of neointimal thickenings following vascular injury.* Histol Histopathol, 1998. **13**(3): p. 871-91.
147. Murry, C.E., et al., *Monoclonality of smooth muscle cells in human atherosclerosis.* Am J Pathol, 1997. **151**(3): p. 697-705.
148. Pearson, T.A., et al., *Clonal markers in the study of the origin and growth of human atherosclerotic lesions.* Circ Res, 1978. **43**(1): p. 10-8.
149. Tang, Z., et al., *Differentiation of multipotent vascular stem cells contributes to vascular diseases.* Nat Commun, 2012. **3**: p. 875.
150. Hochmuth, R.M., N. Mohandas, and P.L. Blackshear, Jr., *Measurement of the elastic modulus for red cell membrane using a fluid mechanical technique.* Biophys J, 1973. **13**(8): p. 747-62.

Chapter 2

Effects of Fluid Flow on TGF-β1 Signaling in Human Mesenchymal Stem Cells.

Abstract

Human mesenchymal stem cells (hMSCs) are multipotent fibroblast-like cells, which are found primarily in the bone marrow. hMSCs are a potential cell source for vascular graft engineering because of their ease of isolation and expansion, their multipotency and their low immunogenicity.

We discovered that exposing hMSCs to fluid flow promotes transforming growth factor 1 (TGF-β1) signaling in a receptor-dependent manner. The mechanism explaining this phenomenon, however, is unclear. In this study, we examined several hypotheses, which could provide a suitable explanation.

First, we looked at the effects of degrading the glycocalyx on the induction TGF-β1/SMAD2 signaling by fluid flow. We found that degrading the glycocalyx had only negligible effects.

Second, we investigated if changing the fluidity of the cell membrane affected the way in which fluid flow promotes TGF-β1/SMAD2 signaling. We concluded that fluid flow did not promote TGF-β1/SMAD2 signaling by changing the fluidity of the cell membrane.

Third, we disrupted the internalization of TGF-β1 receptors through clathrin-dependent and caveolae-dependent pathways before applying fluid flow. We then observed the effects of these disruptions on TGF-β1 signaling through SMAD2 phosphorylation. We found that disrupting the internalization of TGF-β1 receptors had little effect on the increase in TGF-β1/SMAD2 signaling due to fluid flow.

Finally, we uncoupled the effects of fluid shear stress on TGF-β1 signaling from those of the flow rate. By changing the dimension of the gasket in the flow chamber, we were able to vary the shear stress while holding the volumetric flow rate constant (and vice versa). We observed the effects of each individual factor on TGF-β1/SMAD2 signaling separately. We found that shear stress actually inhibits TGF-β1/SMAD2 signaling in hMSCs. We also concluded that the increase in TGF-β1/SMAD2 signaling when hMSC are exposed to fluid flow is caused by an increase in the flow rate (or the motion of the TGF-β1 ligands) and not by fluid shear stress.

Keywords— human mesenchymal stem cells, laminar fluid shear stress, TGF-β1, SMAD2 signaling, mechanotransduction, flow rate, clathrin, caveolin 1.

Introduction

Human Mesenchymal Stem Cells

Human mesenchymal stem cells (hMSCs) are multipotent stem cells that can be isolated from various adult tissues. Although the bone marrow is the most abundant source of hMSCs, these cells are also found in muscle, fat, dermis, peripheral and cord blood. MSCs have been shown to differentiate into adipocytes, cardiomyocytes, chondrocytes, osteoblasts and smooth muscle cells [1]. MSCs are a potential cell source for tissue engineering because of their ease of isolation and expansion, their multipotency and their low immunogenicity [2].

In order to utilize MSCs in tissue engineering applications, however, we must be able to control their proliferation and direct their differentiation. The differentiation of MSCs can be directed by different growth factor combinations. Supplementing the basal culture medium with dexamethasone, ascorbate and β-glycerophosphate induces differentiation into osteoblasts. Supplementing with TGF-β3, dexamethasone and ascorbate induces chondrogenic differentiation while dexamethasone and hydrocortisone will induce myogenic differentiation [3]. Adipogenic induction requires the addition of h-insulin, dexamethasone, indomethacin and IBMX [4].

Human MSCs derived from bone marrow can be expanded more than a billion-fold in culture without losing their stem cell capacity [1]. Although no single cell surface marker for MSCs exists, they are in general positive for STRO-1 (a stromal cell surface antigen), CD105 (endoglin, receptor for transforming growth factor-β, TGF-β, and integrins), CD29 (integrinβ1), CD44 (receptor for hyaluronic acid and matrix proteins) and CD166 (a cell adhesion molecule), and negative for CD14 (monocyte surface antigen), CD34 (HSC surface antigen), and CD45 (leukocyte surface antigen) [5].

MSCs do not express the major histocompatibility complex II (MHC II) antigens that are responsible for immune rejection. MSCs are therefore an excellent candidate cell source for allogeneic cell transplantation [6]. MSCs offer a great potential for tissue engineering applications. However, the molecular mechanisms governing proliferation and differentiation of MSCs and the effects of mechanical stimulation on MSC function are not fully understood.

The TGF-β Signaling Pathway

The transforming growth factor-beta (TGF-β) family of cytokines, includes nearly 30 different proteins in mammals. TGF-β, bone morphogenic proteins (BMPs), nodal, activin and inhibin are prominent examples. There exists three isoforms of TGF-β designated TGF-β1, TGF-β2, and TGF-β3, which are encoded by distinct genes and are expressed in a tissue specific manner. TGF-β signaling plays a crucial role in embryonic development and cellular processes such as proliferation, differentiation, migration and apoptosis [7].

TGF-β activates signaling through two cell surface receptors: type I (RI), type II (RII). Type I and type II receptors are serine/threonine kinases that form a heteromeric complex. In response to ligand binding, the type II receptors form a complex with the type I receptors allowing the phosphorylation and activation of the type I receptor kinases. In mammals, there are 7 types of the RI receptors and 5 types of RII receptors. Each type of receptor will bind specific members of the TGF-β family cytokines [8].

The SMAD proteins are the only known TGF-β signal transducers. There exists 8 types SMAD protein which are classified into three groups: receptor-activated SMADs (R-SMADs), which include SMAD 1,2,3,5 and 8; the common partner SMAD (SMAD4), and the inhibitory SMADs (I-SMADs), which are SMAD6 and SMAD7. Receptor SMADs are further divided into 2 subgroups. SMAD2and SMAD3 are activated by RI receptors specific to TGF-β, nodal and activin. SMAD 1,5 and 8, however, are activated by BMP specific RI receptors [9].

Receptor SMADs become activated when the Ser-Ser-X-Ser motif at their C-terminal is phosphorylated by type I receptors. When they are not activated, R-SMADs are anchored as dimers to the plasma membrane through SARA (SMAD Anchor for Receptor Activation) and other molecules. SARA is necessary for SMAD 2phosphorylation by the TGF- β1 receptor. Activated R-SMADs interact with the common partner SMAD, SMAD4, and translocate to the nucleus where the SMAD complex interacts with various DNA binding proteins to regulate gene expression [10].

Inhibitory SMADs can inhibit TGF-β1 signaling through multiple mechanisms. They can associate with activated type I receptor to prevent the activation of R-SMADs. They can also interact with activated R-SMADs and interferes with the formation of a complex with SMAD4. To continue, SMAD 6 and 7 can function in the nucleus to recruit HDAC to repress transcription. Another way in which SMAD7 inhibits TGF-b signaling is by associating with ubiquitin ligases Smurf 1 and Smurf 2. These molecules induce the ubiquitination and degradation of type I receptors. SMAD7 inhibits both TGF-β, activin and BMP signaling. SMAD6 preferentially inhibits BMP signaling [11].

Findings over the past few years have suggested that TGF-β signaling is not linear and isolated. TGF-β signaling interact with other signaling pathways, including the MAP kinase pathway, Mitogen-activated protein (MAP) kinase, phosphatidylinositol-3 kinase/Akt, Wnt, Hedgehog and Notch pathways [10].

Endocytotic Regulation of TGF- β Signaling

Two major endocytotic pathways are known to regulate the uptake of TGF-β cell surface receptors: the clathrin-dependent pathway and the lipid-raft/caveolar pathway. Studies suggest that TGF-β receptors are constantly turned over and that their downregulation is enhanced by ligand treatment [12].

a) Clathrin-Mediated Endocytosis

Clathrin-mediated endocytosis is utilized by many cell surface receptors such as G protein-coupled receptors, tyrosine kinase receptors and non-kinase receptors [11].
Clathrin-dependent endocytosis requires the recruitment of soluble clathrin from the cytoplasm to the plasma membrane. Clathrin proteins assemble into a polygonal lattice at the plasma membrane to form coated pits. Clathrin assembly is mediated by the clathrin adaptor protein AP-2 which binds to the dileucine-based motif in TGF-β receptor RII [13]. Clathrin-coated pits then pinch off from the membrane with the aid of dynamin to form clathrin-coated vesicles. Clathrin-coated vesicles are uncoated after endocytosis and then fuse with the early endosome. The early endosome is highly enriched in phosphatidylinositol-3-phosphate (PtdIns3P) and has PtdIns3P-binding 'Fab1,YOTB,Vac1, EEA1' (FYVE)-domain proteins, which can control the activity and destination of other proteins in the compartment [14].
It is known that the SMAD2 anchoring protein SARA is bound to receptors at the plasma membrane and that SARA is highly enriched in the early endosome. SARA localization to the early endosome is dependent on its FYVE domain, which binds PtdIns3P.
The enrichment of SARA in the early endosome might suggest that clathrin-dependent endocytosis brings the receptor in closer proximity to the SARA-bound SMAD2. However, because SARA is also bound to receptors at the plasma membrane, receptors need not move into the early endosome to access SMAD2-bound SARA. Clathrin-dependent internalization may promote TGF-β signaling by taking receptors away from lipid rafts and caveolae, which inhibit TGF-β signaling directly through caveolin-1 and SMAD7 binding [13].
It remains unclear how essential clathrin-dependent endocytosis is in TGF-β signaling.

Endocytotic Regulation of TGF- β Signaling (continued)

b) Lipid Raft/Caveolin-Mediated Endocytosis

Lipid rafts are cholesterol and sphingolipid-rich microdomains in the plasma membrane. Their size, lifetime and composition are not well characterized. In addition, the mechanism for lipid raft internalization remains unclear. However, lipid rafts have been implicated in various processes such as lipid sorting, protein trafficking and signal transduction [14].

The most commonly reported lipid rafts are Caveolin-1 enriched plasma membrane compartments known as caveolae (for “little caves”). Caveolae are flask-shaped invaginations on the surface of many mammalian cells. They are around 60 to 80 nm in diameter and can constitute up to a third of the plasma membrane area of the cells. There are three mammalian caveolin proteins. While Caveolin-3 is muscle specific, Caveolin-1 and 2 are found in non-muscle cells. Only neurons and leukocytes lack caveolae. Unlike Caveolin-2, Caveolin-1 appears to be necessary for caveolae formation. Caveolin-1 forms oligomers and binds cholesterol and fatty acids [15]. Caveolin-1 has been shown to inhibit TGF-β signaling by direct association with TGF-β receptor1. Caveolin-1 binding interferes with SMAD2 phosphorylation and subsequent signaling events [16].

Studies have shown that lipid rafts/caveolae negatively modulate TGF-β signaling by promoting TGF-β receptor turnover. SMAD7-Smurf2 complexes target activated TGF-β receptors to lipid rafts/caveolae. Lipid raft/caveolin-1-dependent internalization of TGF-β receptors promotes receptor degradation and signaling termination. In the absence of caveolin-1, SMADs can still associate with TGF-β receptors in lipid rafts. SMAD7–Smurf2-dependent receptor turnover can still occur. Therefore, although caveolin-1 facilitates receptor turnover, raft-dependent degradation can occur in the absence of caveolin [13].

One aim of this study is to determine if fluid shear stress can induce changes in the regulation of the receptor internalization.

Shear Stress-Induced Mechanotransduction

Shear stress is created by the movement a fluid over a solid surface. It is known that cells can sense fluid shear stress however it remains unclear how cells sense and convert this mechanical force into biochemical signals [17]. Several mechanisms have been proposed however there is no consensus on any one model. The main theories include: tensegrity, integrin-mediated mechanotransduction, membrane-mediated mechanotransduction (membrane fluidity), direct change of conformation of mechano-sensitive cell surface proteins, force transmission through the glycocalyx [18].
In endothelial cells, shear stress has been found to activate multiple signaling pathways: focal adhesion kinase (FAK), mitogen-activated protein kinase (MAPK), phosphoinositide-3 kinase (PI3-K), Akt and Rho family GTPases, and increases integrin clustering and integrin-ligand binding [5]. Little is known, however, about shear-stress activation of signaling pathways in mesenchymal stem cells.
One of the objectives of this study is to explain how shear stress can activate the TGF-β1 pathway. Preliminary data has shown that signal transduction is dependent on the activation of TGF-β receptor R1 and on the presence of the TGF-β1 ligand. It remains unclear how shear stress can promote the association between the ligand and its receptor.
Because we know that shear stress must act at the receptor level, we will limit our examination to the apical surface of the cell. We can put aside the role of integrin-mediated mechanotransduction and tensegrity. We will focus on the role of membrane-mediate mechanotransduction and the glycocalyx as possible explanations.

a) <u>Membrane-mediate mechanotransduction</u>

When a force is applied on the lipid bilayer, two things can happen. First, the change of lateral forces in the lipid bilayer can cause a change in the conformation of a transmembrane protein, leading to its activation. Second, because the membrane contains different kinds of lipids, forces at the cell membrane, either from outside or from inside, can cause significant changes in local curvature. In turn, local changes in membrane curvature can reorganize the membrane chemically because lipids that are more stable in curved membranes diffuse in while lipids that are more stable in flat membranes diffuse out. Inositol phospholipids are the main determinants of the actin cytoskeleton and are especially unstable in flat membranes. Inositol phospholipids are among the membrane constituents that might form local clusters as a result of exposure to shear stress [19]. The inherent difficulty is to differentiate the effects of forces directly exerted on transmembrane proteins and the effects of changes in lipid diffusivity and distribution.
Studies have reported that fluid shear stress increases membrane fluidity [20, 21]. We hypothesize that the increase in membrane fluidity will increase the lateral diffusivity of TGF-β receptors which, in turn, will result in the formation of the heteromeric complexes that initiate TGF-β signaling in the cell.

Shear Stress-Induced Mechanotransduction (continued)

b) Role of the Glycocalyx in Mechanotransduction

The glycocalyx is a network of proteoglycans with glycosaminoglycan side chains and glycoproteins bearing acidic oligosaccharides and sialic acids. The glycosaminoglycans (GAGs) associated with the glycocalyx include heparan sulfate (HS), chondroitin sulfate (CS), and hyaluronic acid (HA). The composition of the glycocalyx explains its net negative charge. The thickness of the glycocalyx is estimated to be 0.5 to 4.5μm depending on the measurement technique. Enzymes, growth factors and cytokines, amino acids, cations and water, all associate with the glycocalyx. Cells actively regulate the content and the properties of their glycocalyx by a continuous metabolic turnover that allows them to adapt to changes in the local environment [22].

The glycocalyx might play a role in decentralized or centralized mechanisms of mechanotransduction. Decentralized mechanisms of mechanotransduction involve mechanosensing at the glycocalyx and transduction at sites away from the surface. Transmembrane proteins such as syndecans, which contain both HS and CS have an established association with the cytoskeleton and, through this interaction, can decentralize the signal by distributing it to multiple sites within the cell [23].

In centralized mechanisms, however, both sensing and transduction occur within the glycocalyx. For example, membrane-bound glypicans that contain HS but not CS are localized to caveolae, which are believed to serve as sites for this type of signal transduction [23].

Weinbaum and Tarbell propose a hypothesis for mechanotransduction based on their studies of the glycocalyx. When the glycocalyx is intact, it senses fluid shear stress through its GAG chains, like the leaves of a tree sense the force of wind. This force is transmitted to the cell through the core proteins of the proteoglycans on the cell surface. The force is then distributed throughout the cell by the cytoskeleton. Therefore, mechanotransduction can take place at many locations in the cell, including the apical membrane, intercellular junctions, basal adhesion plaques, and the cytoskeleton itself [24].

When the glycocalyx is degraded by enzymes or disease, the cell senses shear stress directly at the apical plasma membrane. In this case, the distribution of force to the apical surface of the cell is altered. However, the force experienced by the basal adhesion plaques to balance the applied force on the surface will not be different whether the glycocalyx is intact or degraded. Therefore, at the basal lamina, the cell experience the same force whether there is a glycocalyx on at the surface or not [24].

Specific Aims

1) To examine if shear force transmission through the glycocalyx plays a role in TGF-β1 receptor signaling.
    a. degrade heparin sulfate proteoglycans by enzymatic digestion before applying shear stress;
    b. determine the effects on SMAD2 phosphorylation as a measure of TGF-β1 signaling by western blot analysis.

2) To investigate if fluid shear stress promotes TGF-β1 receptor signaling by changing the fluidity of the cell membrane.
    a. treat hMSCs with benzyl alcohol (BA) to increase membrane fluidity;
    b. treat hMSCs with water soluble cholesterol to reduce membrane fluidity;
    c. determine the effects on SMAD2 phosphorylation by western blot analysis.

3) To determine if fluid shear stress affects the internalization of TGF-β1 receptors through clathrin-dependent and lipid raft/caveolae dependent pathways:
    a. knockdown Clathrin (heavy chain) protein expression with Si-RNA and observe the effects on Clathrin distribution and SMAD2 phosphorylation by immuno-fluorescence microscopy;
    b. disrupt Caveolae and lipid raft formation using Fillipin III, observe the effects on caveolin-1 by immuno-fluorescence microscopy, and determine the effects on SMAD2 phosphorylation by western blot analysis.

4) To uncouple the effects of fluid shear stress from those of the flow rate on TGF-β1 signaling:
    a. vary the fluid shear stress while holding the volumetric flow rate constant and determine the effects on SMAD2 phosphorylation by western blot analysis;
    b. vary the flow rate while holding fluid shear stress constant and determine the effects on SMAD2 phosphorylation by western blot analysis.

Materials and Methods

Reagents

Transforming growth factor, TGF-β1 (100-21C, PeproTech Inc., Rocky Hill New Jersey) was utilized in all experiments. TGF-β type 1 receptor inhibitor, SB431542 (S4317, Sigma, St. Louis, Mo.) was used to block TGF-β1signalling. Heparinase III (H8891, Sigma, St. Louis, Mo.) was added to degrade heparin sulfate proteoglycans. Benzyl Alcohol (305197, Sigma, St. Louis, Mo.) was used to increase cell membrane fluidity. Water soluble cholesterol (C4951, Sigma, St. Louis, Mo.) was supplemented to reduce cell membrane fluidity. Cholesterol binding reagent, Filippin III, (70440, Cayman Chemical, Ann Arbor, MI.) was used to disrupt caveolae and lipid raft structures in hMSCs. Cells were transfected with Clathrin SiRNA (Dharmacon Inc., Lafayette, Co.) in knockdown experiments.

Antibodies against SMAD2 and Phospho-SMAD2 (3122 and 3108 respectively, Cell Signaling Technology, Danvers, MA); antibodies against SMAD2/3 and Phospho-SMAD2/3 (sc-6033 and sc-11769 respectively, Santa Cruz Biotechnology, CA); Clathrin heavy chain antibody (sc-6579, Santa Cruz Biotechnology, CA) and Caveolin1 antibody (sc-894, Santa Cruz Biotechnology, CA) were used for western blotting and immunostaining analysis.

Cell Culture

Human mesenchymal stem cells (hMSCs) were acquired from Cambrex (East Rutherford, NJ) and cultured for expansion without differentiation in MSC basal growth medium (Cambrex) with 10% mesenchymal cell growth serum, 1% penicillin/ streptomycin, and 2% L-glutamine at 37°C and 5% CO_2.
These hMSCs were positive for cell surface markers CD105, CD166, CD29, and CD44, and negative for CD34, CD14, and CD45 (data not shown).

Cell Seeding Prior to Shear Stress Experiments

Autoclaved glass slides (Erie Scientific, Portsmouth, NH) were exposed to ultraviolet (UV) light for 1 hour for sterilization. Slides were then coated with 2% gelatin (Sigma Aldrich, St. Louis, MO) and placed under UV light for 1 hour at room temperature to allow for protein adsorption before being washed with phosphate buffered saline (PBS, pH 7.4). Cells were seeded onto the gelatin-coated slides at approximately 50% confluency. The cells were allowed to grow to 80% confluency before shear stress experiments.

Fluid Shear Stress Experiments

Laminar fluid shear stress was applied to hMSCs using a parallel-plate flow chamber. Human MSCs were cultured to confluency on glass slides coated with 2% gelatin. After serum deprivation for 3 hours, hMSCs were mounted on the flow channel. Glass slides seeded with hMSCs were mounted on a rectangular flow channel by sandwiching a silicone gasket between the glass slide and a polycarbonate flow chamber base. hMSCs were subjected to a laminar shear stresses of 6 dynes/cm^2 for 30 minutes (unless otherwise specified). The circulating media contained Dulbecco's modified

Eagle's medium (DMEM) with no fetal bovine serum (FBS) and supplemented with 1% penicillin-streptomycin (Invitrogen Co., Carlsbad, CA). Culture medium was circulated throughout the system using a peristaltic pump. All shear stress experiments included static controls. hMSCs static controls were cultured on slides that were kept in the same incubator.

The circulating media was supplemented with transforming growth factor 1, TGF-β1 (PeproTech Inc., Rocky Hill New Jersey). The controls contained no TGF-β1 in the media. The flow system was set up in a humidified cell culture incubator (37 ºC, 5 %CO_2).

<u>Experimental Set-Up for Fluid Flow Experiments</u>.

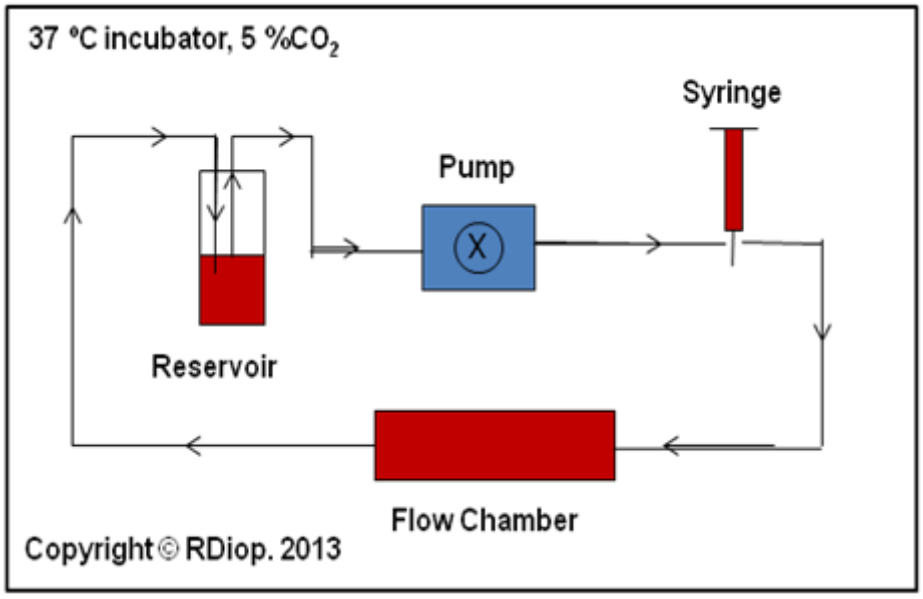

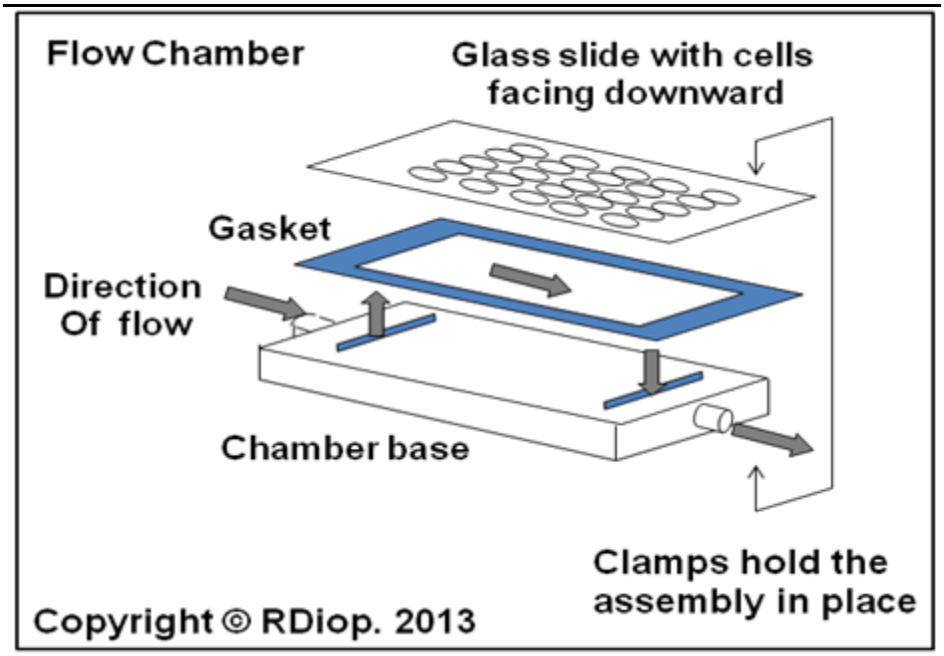

Materials and Methods

Glycocalyx Experiments

Before shear stress experiments, human mesenchymal stem cells (hMSCs) were pre-treated with heparinase III (at 4U/ml, Sigma, St. Louis, Mo) for 3 hours to degrade heparin sulfate (HS) in the glycocalyx. hMSCs were then subjected to 30 minutes of shear stress at 6 dynes/cm^2 in serum free media (both with and without TGF-$\beta 1$) or kept under static condition as controls. After shear stress experiments, SMAD2 phosphorylation in each sample was examined by immunoblotting analysis and quantified with Image J software (NIH.)

Membrane Fluidity Experiments

hMSCs were treated with 45 mM benzyl alcohol (BA-305197, Sigma, St. Louis, Mo.) for 2 hours to increase membrane fluidity. In concurrent experiments, hMSCs were treated with 100 μM water soluble cholesterol (C4951, Sigma, St. Louis, Mo.) for 3 hours to reduce membrane fluidity. To determine the optimal concentration and duration of treatment, dosage trials and a time-course were conducted for both reagents.
In all experiments, some hMSC samples were left untreated as controls. After treatment, hMSCs were exposed to shear stress at 6 dynes/cm^2 for 30 minutes in serum free media with or without TGF-$\beta 1$. Some samples were kept as static controls.
After shear stress experiments, SMAD2 phosphorylation in each sample was detected by immunoblotting analysis and quantified with Image J software (NIH.)

Lipid Raft/Caveolae Experiments

Before shear stress experiments, human mesenchymal stem cells (hMSCs) were pre-treated with Filippin III, (at 1.5 U/ml Cayman Chemical, Ann Arbor, MI.) for 15 minutes to disrupt caveolae and lipid rafts in hMSCs. hMSCs were then subjected to 30 minutes of shear stress at 6 dynes/cm^2 in serum free media (both with and without TGF-$\beta 1$) or kept under static condition as controls. After shear stress experiments, SMAD2 phosphorylation in each sample was examined by immunoblotting analysis and quantified with Image J software (NIH.)

Clathrin Knockdown Experiments

Small interfering RNA duplex oligonucleotides for clathrin heavy chain were purchased from Dharmacon, Inc. (Lafayette, CO). Cells were transfected at 50-60% confluency following the protocol provided by the manufacturer. The final concentration of siRNA was 100nM. Fresh DMEM w/ 10 % FBS was added 6 hours after transfection. Cells were seeded 24 hours after transfection. Shear stress experiments were conducted 48 hours after transfection. Following the shear stress experiments, hMSCs were fixed with 4% of paraformaldehyde. Static controls were also fixed after 30 minutes of incubation. Cells were double stained for clathrin and p-SMAD2/3.

Materials and Methods

Uncoupling the Effects of Fluid Shear Stress and Flow Rate on TGF-β1 Signaling

One method to uncouple shear stress and flow rate is to change the geometry of the flow channel where cells come in contact with the fluid by changing the dimensions of the gasket.

In a parallel-plate flow system, shear stress is directly proportional to the flow rate based on the following equation:

$$\tau = \mu \left(\frac{6}{wh^2} \right) Q$$

where,

Q is the volumetric flow rate across the chamber (in ml/sec)

τ is the shear stress (in dynes/cm^2),

μ is the viscosity of the medium (0.00755 dynes * seconds/cm^2 at 37°C),

W is the inner width of the gasket (in cm)

h is the gasket height (in cm).

Since fluid shear stress is inversely proportional to the height^2 (h^2) and width (w) of the gasket, the flow rate can be held constant while fluid shear stress increases if both h and w are reduced accordingly. Similarly, shear stress can be held constant while the flow rate decreases if h and w are reduced accordingly.

In the first set of experiments, the flow rate was held constant while the shear stress varied.

Table 1. Summary of Experiments – Constant flow rate (Q) = 0.2cm^3 per second

Experiment	Length (in cm)	w (in cm)	h (in microns)	Estimated max. shear (dynes/cm^2)
1	6.4	7.2	250	2
2	6.4	3.6	250	4
3	6.4	2.4	250	6
4	6.4	1.2	250	12
5	6.4	0.8	250	18
6	6.4	2.4	125	24
7	6.4	1.2	125	48

Note that experiments 1 through 7 were each repeated at least 3 times.

Materials and Methods

Uncoupling the Effects of Fluid Shear Stress and Flow Rate on TGF-β1 Signaling

Table 2 . Summary of Samples for Constant Flow Rate Experiments

Samples	A	B	C	D	E	F	G	H
Flow	-	+	-	+	-	+	-	+
TGF-β1 (0.01ng/ml)	-	-	+	+	-	-	+	+
Shear Stress (dynes/cm2)	0	6	0	6	0	X	0	X
Flow rate (in ml/min)	0	12	0	12	0	12	0	12

In the second set of experiments, shear stress was held constant as the flow rate varied.

Table 3. Summary of Experiments – Constant shear stress = 12 dynes/cm^2

Experiment	Length (in cm)	w (in cm)	h (in microns)	Estimated Flow Rate (cm^3/min)
8	6.4	4.8	250	48
9	6.4	3.6	250	36
10	6.4	2.4	250	24
11	6.4	1.2	125	3
12	6.4	0.6	125	1.5

Note that experiments 8 through 12 were each repeated at least 3 times.

Materials and Methods

Uncoupling the Effects of Fluid Shear Stress and Flow Rate on TGF-β1 Signaling

Table 4 . Summary of Samples for Constant Shear Stress Experiments

Samples	I	J	K	L	M	N	O	P
Flow	-	+	-	+	-	+	-	+
TGF-β1 (0.01ng/ml)	-	-	+	+	-	-	+	+
Shear Stress (dynes/cm^2)	0	12	0	12	0	12	0	12
Flow rate (in ml/min)	0	24	0	24	0	V	0	V

In all experiments, hMSCs were seeded on glass plates as described previously. The media contained no fetal bovine serum. Experimental samples were exposed to shear stress for 30 minutes. Control samples were kept in the same incubator under static conditions. After shear stress experiments, SMAD2 phosphorylation in each sample was detected by immunoblotting analysis and quantified with Image J software (NIH.)

Materials and Methods

Immunofluorescent Staining and Confocal Microscopy

Human MSCs were fixed with 4% paraformaldehyde in PBS for 15 min, permeabilized with 0.5% Triton X-100 in PBS for 10 min, and blocked with 1% BSA for 30 min. The samples were incubated overnight at 4^{o} C with primary antibodies; followed by a 1hr incubation with Rhodamine conjugated IgG secondary antibody or FITC-conjugated IgG secondary antibody (Jackson ImmunoResearch, West Grove, PA). For nuclear staining, samples were incubated in PBS with DAPI for 5 min (Invitrogen Corp., Carlsbad CA). We used a Nikon spectral confocal microscope to capture multiple *Z*-sections for each sample (0.2 to 0.4 μm thick sections over a range of 20 μm). These sections were subsequently integrated to create maximum intensity projections of each sample using Nikon Imaging Software, Elements.

Protein isolation and Immunoblotting

Cells were lysed with 150 μL of RIPA buffer (25 mM Tris (pH 7.4), 0.5 M NaCl, 1% TritonX-100, 0.1% SDS, 1 mM PMSF, 10 lg/mL leupeptin, and 1 mM Na3VO4). The protein samples were then centrifuged to isolate the supernatant. The protein concentration in all samples was quantified using DC Protein Assay (Biorad, Hercules, CA). Protein samples were prepared in SDS sample buffer (2% SDS, 10% (v/v) glycerol, 60 mM Tris, and 0.05% (v/v) mercaptoethanol) and boiled for 5 min prior loading onto 10% SDS-PAGE gels. After electrophoresis, the separated proteins were transferred onto a nitrocellulose membrane (Biorad, Hercules, CA). The membrane was blocked with Tris-buffered saline containing 3% non-fat powdered milk for 1 h and then incubated with the primary antibody in Tris-buffered saline-Tween overnightat 4 °C. The blots were subsequently washed in Tris-buffered saline-Tween and then incubated with an appropriate horseradish peroxidase-conjugated secondary antibody in Tris-buffered saline-Tween. Proteins were visualized using enhanced chemiluminescence (Biorad, Hercules, CA). Image analysis was performed with the ImageJ software package (NIH).

Statistical Analysis

For each group, the mean and standard deviation (SD) were calculated. Experiments were repeated at least 3 times for statistical analysis. Statistical significance compared to static control was determined using analysis of variance (ANOVA) followed by a Student t-test.

Results

Effects of fluid flow on TGF-β1/SMAD2 signaling.

To determine the effects of fluid flow on TGF-β1/SMAD2 signaling, we used immunoblotting analysis. In these experiments, human mesenchymal stem cells (MSCs) were subjected to a shear stress of 6 dynes/cm^2 for various periods of time with 0.1ng/ml TGF -β1 in the circulating media. Figure 1 shows that SMAD2 phosphorylation starts in the first 5 minutes due to the presence of TGF-β1 in the media. SMAD2 phosphorylation is sustained for at least 60 minutes. The effect of fluid flow on TGF-β1/SMAD2 signaling becomes noticeable after 30 minutes of exposure. Figure 2 shows an average increase of 76% in SMAD2 phosphorylation due to fluid flow (flow rate, Q, was set at 0.2 cm^3 per second.)
In addition, we find that the increase in TGF-β1/SMAD2 signaling due to fluid flow is receptor dependent (figure 3A and 3B.) Adding an inhibitor of TGF-β type I receptor (SB431542) to the circulating media blocks TGF-β1/SMAD2 signaling and eliminates the increase in SMAD2 phosphorylation, which was previously observed.

Effects of glycocalyx degradation on the increase in TGF-β1/SMAD2 signaling due to fluid flow.

To determine if glycocalyx degradation has an effect on the increase in TGF-β1/SMAD2 signaling induced by fluid flow, human MSCs were treated with F. *heparinum* heparinase III to degrade heparin sulfate (HS) prior to flow experiments. Immunoblotting analysis was then used to measure the levels of SMAD2 phosphorylation. Figure 4 demonstrates that degrading the glycocalyx reduces the amount of SMAD2 phosphorylation overall (>50%). Figure 4 shows, however, that disrupting the glycocalyx does not attenuate the increase in TGF-β1/SMAD2 signaling due to fluid flow. In samples treated with Heparinase III, we observe an average increase of 70% in SMAD2 phosphorylation due to fluid flow.

Effects of Membrane fluidity on the increase in TGF-β1/SMAD2 signaling due to fluid flow.

To determine the effects of membrane fluidity on the increase in TGF-β1/SMAD2 signaling induced by fluid flow, human MSCs were treated with water soluble cholesterol (Chl) to reduce membrane fluidity, or, with benzyl alcohol (BA) to increase membrane fluidity prior to flow experiments.
In experiments where we reduced membrane fluidity, we first determined the optimal dosage and time for the treatment by performing a series of trials. Figure 5 summarizes the results. We found that, in the presence of TGF-β1, Cholesterol enhanced SMAD2 phosphorylation in a dose and time-dependent manner. The optimal dose and time for the treatment were determined to be: 100 μM cholesterol for 3 hours. Figure 6 summarizes the results of flow experiments with water soluble cholesterol. The figure shows that we continue to observe an increase in TGF-β1/SMAD2 signaling due to fluid

flow. The average increase in SMAD2 phosphorylation due to fluid flow was 78% for samples treated with cholesterol.
To continue, in experiments where we increased membrane fluidity, we also conducted a series of trials to determine the optimal dosage and time for the treatment (data not shown). The optimal dose and time for the treatment were determined to be: 45 mM benzyl alcohol for 2 hours. Figure 7 summarize the results of the flow experiments with benzyl alcohol treatment. We observed that increasing membrane fluidity promotes the endogenous production of TGF-β1. All samples expressed some level of SMAD2 phosphorylation. We also found that the levels of SMAD2 phosphorylation were higher in samples exposed to fluid flow compared to static controls.

Effects of TGF-β1 receptor internalization on the increase in TGF-β1/SMAD2 signaling due to fluid flow.

First, we examined the lipid raft/caveolar pathway. We disrupted caveolae structures and lipid rafts in human MSCs by treating samples with Filippin III, a potent cholesterol binding reagent. Figure 8 shows that exposing hMSCs to Filipin III prior to flow experiments decreased the expression of caveolin-1. Figure 9 demonstrates that disrupting caveolae with Filippin III does not attenuate the increase in TGF-β1/SMAD2 signaling due to fluid flow. The average increase in SMAD2 phosphorylation due to fluid flow was 90% for samples treated with Filipin III compared to 70% in non-treated samples.
Second, we looked at the clathrin-dependent pathway. We observed the effects of fluid flow on clathrin heavy chain protein expression. We found no significant variation over a 30 minute time period (figure 10). In addition, we transfected human MSCs with small interfering RNA to knock down clathrin heavy chain expression. Immunocytochemical analysis (figure 11) shows that, when we knocked down clathrin heavy chain, we observed a significant reduction in p-SMAD2/3 expression both in static and flow samples. Furthermore, we no longer observe an increase in TGF-β1/SMAD2 signaling caused by fluid flow.

Uncoupling the effects of fluid shear stress from those of the flow rate on TGF-β1/ SMAD2 signaling.

In the parallel-plate flow chamber system used in this study, fluid shear stress is inversely proportional to the height^2 (h^2) and to the width (w) of the gasket. The flow rate can be held constant while fluid shear stress increases if both h and w are reduced accordingly. Similarly, shear stress can be held constant while the flow rate decreases if h and w are reduced accordingly.
In the first series of experiments (summarized in tables 1, 2 and figure 12), we held the flow rate constant at 12ml/min, while we increased fluid shear stress from 2 to 48 dynes/cm^2. Figure 12 shows that SMAD2 phosphorylation follows a biphasic curve. SMAD2 phosphorylation is higher at low levels of fluid shear stress (<6 dynes/cm^2).

SMAD2 phosphorylation decreases sharply between 6 and 12 dynes/cm^2. Beyond 12 dynes/cm^2, levels of SMAD2 phosphorylation remain relatively low and constant.
In the second series of experiments (summarized in tables 3,4 and figure 13), we held the shear stress at 12 dynes/cm^2 while we increased the flow rate from 1.5ml/min to 48ml/min. We found that, from 0 to 24ml/min, SMAD2 phosphorylation increased as the flow rate increased. SMAD2 phosphorylation plateaus after the flow rate reaches 24ml/min.

Inhibitory effects of fluid shear stress on TGF-β1/SMAD2 signaling in human MSCs.

We used immunoblotting analysis to examine TGF-β1/SMAD2 signaling when TGF- β1 was added to the media *after* exposure to a fluid shear stress of 6 dynes/cm^2 for 30 minutes. Figure 14 shows that SMAD2 phosphorylation was lowered by 25% in the shear samples compared to the static control.

Effects of fluid flow on Caveolin-1 Expression in hMSCs.

In these experiments, human MSCs were subjected a shear stress of 6 dynes/cm^2 or kept as static controls for 30 minutes in the presence and the absence of TGF-β1. Immunoblotting analysis shows that fluid shear stress caused a 3 fold increase in Caveolin-1 expression regardless of the presence TGF-β1 (figure 15.)
Figure 16 shows that the increase in calveolin-1 induced by fluid flow was not affected by treatments with heparinase and cholesterol. The figure suggests, however, that treating human MSCs with Filipin III before applying shear stress attenuates this effect.

Discussion

In this study, we found that, in human mesenchymal stem cells, fluid flow promotes TGF-β1/SMAD2 signaling in a receptor dependent manner. The effects of fluid flow on TGF-β1/SMAD2 signaling become noticeable after 30 minutes of exposure (shear stress, τ = 6 dynes/cm^2). Furthermore, the increase in TGF-β1/SMAD2 signaling is maintained even after prolonged exposure to fluid flow (> 1hour).
The role of laminar fluid shear stress is unclear in this context. This study attempted to determine if shear stress plays a role in promoting TGF-β1/SMAD2 signaling in hMSCs and to find a mechanism that explains this phenomenon.

We first examined the glycocalyx. The glycocalyx is a network of proteoglycans with glycosaminoglycan side chains and glycoproteins bearing acidic oligosaccharides and sialic acids. The glycosaminoglycans (GAGs) associated with the glycocalyx include heparan sulfate (HS), heparin, chondroitin sulfate (CS), dermatan sulfate (DS), keratan sulfate (KS) and hyaluronic acid (HA). The composition of the glycocalyx explains its net negative charge [24]. Few in-vitro studies have examined the role of the glycocalyx in mechanotransduction. Florian et al. were the first to demonstrate that glycosaminoglycans play a role in mechanotransduction in endothelial cells [25]. Later,Thi et al reported in their study of endothelial cells that the glycocalyx could mediate the reorganization of the actin cytoskeleton [26]. To continue, Pahakis et al. showed that specific glycosaminoglycans are necessary for nitric oxide production in endothelial cells [27]. In this study, we followed a protocol similar to the one used in Pahakis et al. to selectively degrade the glycocalyx in order to determine if mechanotransduction plays a role in the activation of TGF-β1/SMAD2 signaling. If fluid shear stress acts through the glycocalyx to activate TGF-β1 receptors, removing components of the glycocalyx would block or reduce TGF-β1 signaling. Under static conditions, we observed a significant reduction in TGF-β1/SMAD2 signaling after the treatment. We found, however, that disrupting the glycocalyx does not attenuate the increase in TGF-β1/SMAD2 signaling due to fluid flow. We conclude, therefore, that the glycocalyx may play a role in TGF-β1/SMAD2 signaling but mechanotransduction within the glycocalyx cannot explain the increase in TGF-β1/SMAD2 signaling caused by fluid flow.

Second, we investigated if membrane fluidity affects the activation of TGF-β1 receptors. When shear stress is applied, the change in the lateral forces in the lipid bilayer can cause a change in the conformation of a transmembrane protein, leading to its activation. Applied forces at the cell membrane can also cause significant changes in local curvature, which in turn result in the local reorganization of lipid composition [19]. The movement of phospholipids can also affect the lateral diffusion of transmembrane proteins such as TGF-β receptors. Studies have reported that fluid shear stress increases membrane fluidity [20, 21]. Benzyl alcohol (BA) is a widely used membrane fluidizer that does not denature proteins. The precise mechanism for BA-induced membrane perturbation, however, remains unclear [28, 29]. Cholesterol, on the other

hand, has been shown to reduce membrane fluidity [29, 30]. These two chemical agents were used to change membrane fluidity.
We hypothesized that an increase in membrane fluidity would increase the lateral diffusivity of TGF-β receptors, which, in turn, would promote the formation of the heteromeric complexes that initiate TGF-β signaling. Decreasing membrane fluidity, however, would reduce the movements of TGF-β receptors, which would in turn reduce TGF-β signaling. Our results showed that increasing membrane fluidity induced endogenous TGF-β1/SMAD2 signaling. Our results also showed that decreasing membrane fluidity enhanced TGF-β1/SMAD2 signaling. We concluded, therefore, that a change in membrane fluidity was not an explanation for the increase in TGF-β1/SMAD2 signaling due to fluid flow.

Third, we looked at the effects of TGF-β1 receptor internalization on the increase in TGF-β1/SMAD2 signaling caused by fluid flow. Two major endocytic pathways are known to regulate the uptake of TGF-β cell surface receptors: the clathrin-mediated pathway and the lipid-raft/caveolar pathway.
In the clathrin-dependent pathway, TGF-β receptors are shuffled into early endosome antigen 1-positive (EEA1) vesicles that promote TGF-β signaling through SMAD signaling. In the lipid raft/caveolar pathway, however, the TGF-β receptors are driven into vesicles containing the SMAD7–Smurf2 complex. This complex mediates a ubiquitin-dependent degradation of TGF-β receptors [12].
We hypothesized that, in the presence TGF-β1 ligand, fluid shear stress would promote the internalization of TGF-β receptors through the clathrin dependent pathway and/or inhibit internalization through lipids rafts and caveolae. The net result would be an up-regulation of TGF-β signaling. We found that the downregulation of clathrin heavy chain expression leads to a significant decrease in SMAD2 phosphorylation, which suggests that clathrin plays a significant in TGF-β1/SMAD2 signaling. However, we observed no change in clathrin expression when fluid flow was applied. Also, we found that exposure to fluid flow caused an increase in caveolin-1 expression. In addition, disrupting caveolae/lipid raft structures caused a reduction in TGF-β1/SMAD2 signaling but failed to eliminate increase in TGF-β1/SMAD2 signaling caused by fluid flow. These observations lead us to conclude that changes in TGF-β receptor internalization cannot explain why TGF-β1/SMAD2 signaling increases when hMSCs are exposed to fluid flow.

Last, we uncoupled the effects of fluid shear stress on TGF-β1/SMAD2 signaling from the effects of the flow rate. Our results showed that shear stress inhibits TGF-β1/SMAD2 signaling in hMSCs while higher flow rates enhanced TGF-β1/SMAD2 signaling. Since fluid shear stress and fluid motion act simultaneously in the cell microenvironment, the net effect on TGF-β1/SMAD2 signaling is a combination of both inhibition and induction. We concluded that the increase in TGF-β1/SMAD2 signaling when hMSC are exposed to fluid flow is caused by the increased motion of the TGF-β1 ligands. The enhancing effects of flow rates mask the inhibitory effects of fluid shear stress.

Furthermore, we observed that fluid flow promotes caveolin-1 expression in hMSCs. Whether this effect is caused by shear stress is still left to be determined. If this is the case, it might provide a clue for why shear stress inhibits TGF-β1/SMAD2 signaling in hMSCs since the caveolar pathway leads to the degradation of TGF-β receptors and an attenuation of TGF-β1/SMAD2 signaling.

The implication of these findings are important because a previous study reported that the effects of laminar shear stress (at 6 dynes/cm^2) on hMSC gene expression mirrored the changes caused by the addition of TGF-β1 (5ng/ml) (unpublished). The study found through DNA microarray analysis that the expression of over 200 genes was similarly regulated by both treatments. This study also reported that fluid flow could activate the TGF-β1 pathway. According to these results, laminar shear stress could potentially induce human mesenchymal stem cells to differentiate toward a vascular smooth-muscle phenotype because previous studies had demonstrated that TGF-β1 is an inducer of myogenic differentiation [31-33]. Based on the results of the current study, we can postulate that the conclusions of the aforementioned study were incorrect. We must take into consideration the fact that, throughout the study, the circulating media was always supplemented with fetal bovine serum which contains the cytokine, TGF-β1. It is possible that fluid flow increased the motion of the TGF-β1 cytokine toward its receptors on the cell surface thereby explaining why the effects of fluid flow mirrored those caused by the addition of TGF-β1 to static cultures.

In conclusion, the findings of the current study put into question previous conclusions made about the role of shear stress in other studies. Because fluid motion and shear stress act in concert, we find that one must investigate the effects of each factor separately before drawing conclusions about the net effects of both factors on cellular function.

References

1. Watabe, T. and K. Miyazono, *Roles of TGF-beta family signaling in stem cell renewal and differentiation.* Cell Res, 2009. **19**(1): p. 103-15.
2. Hedrick, M.H. and E.J. Daniels, *The use of adult stem cells in regenerative medicine.* Clin Plast Surg, 2003. **30**(4): p. 499-505.
3. Gang, E.J., et al., *Skeletal myogenic differentiation of mesenchymal stem cells isolated from human umbilical cord blood.* Stem Cells, 2004. **22**(4): p. 617-24.
4. Baksh, D., L. Song, and R.S. Tuan, *Adult mesenchymal stem cells: characterization, differentiation, and application in cell and gene therapy.* J Cell Mol Med, 2004. **8**(3): p. 301-16.
5. Park, J.S., et al., *Mechanobiology of mesenchymal stem cells and their use in cardiovascular repair.* Front Biosci, 2007. **12**: p. 5098-116.
6. Le Blanc, K., et al., *HLA expression and immunologic properties of differentiated and undifferentiated mesenchymal stem cells.* Exp Hematol, 2003. **31**(10): p. 890-6.
7. Miyazawa, K., et al., *Two major Smad pathways in TGF-beta superfamily signalling.* Genes Cells, 2002. **7**(12): p. 1191-204.
8. Wrighton, K.H., X. Lin, and X.H. Feng, *Phospho-control of TGF-beta superfamily signaling.* Cell Res, 2009. **19**(1): p. 8-20.
9. Javelaud, D. and A. Mauviel, *Crosstalk mechanisms between the mitogen-activated protein kinase pathways and Smad signaling downstream of TGF-beta: implications for carcinogenesis.* Oncogene, 2005. **24**(37): p. 5742-50.
10. Guo, X. and X.F. Wang, *Signaling cross-talk between TGF-beta/BMP and other pathways.* Cell Res, 2009. **19**(1): p. 71-88.
11. Chen, Y.G., *Endocytic regulation of TGF-beta signaling.* Cell Res, 2009. **19**(1): p. 58-70.
12. Felberbaum-Corti, M., F.G. Van Der Goot, and J. Gruenberg, *Sliding doors: clathrin-coated pits or caveolae?* Nat Cell Biol, 2003. **5**(5): p. 382-4.
13. Di Guglielmo, G.M., et al., *Distinct endocytic pathways regulate TGF-beta receptor signalling and turnover.* Nat Cell Biol, 2003. **5**(5): p. 410-21.
14. Le Roy, C. and J.L. Wrana, *Clathrin- and non-clathrin-mediated endocytic regulation of cell signalling.* Nat Rev Mol Cell Biol, 2005. **6**(2): p. 112-26.
15. Doherty, G.J. and H.T. McMahon, *Mechanisms of Endocytosis.* Annu Rev Biochem, 2009.
16. Razani, B., et al., *Caveolin-1 regulates transforming growth factor (TGF)-beta/SMAD signaling through an interaction with the TGF-beta type I receptor.* J Biol Chem, 2001. **276**(9): p. 6727-38.
17. Wang, J.H. and B.P. Thampatty, *Mechanobiology of adult and stem cells.* Int Rev Cell Mol Biol, 2008. **271**: p. 301-46.
18. Stolberg, S. and K.E. McCloskey, *Can shear stress direct stem cell fate?* Biotechnol Prog, 2009. **25**(1): p. 10-9.
19. Janmey, P.A. and D.A. Weitz, *Dealing with mechanics: mechanisms of force transduction in cells.* Trends Biochem Sci, 2004. **29**(7): p. 364-70.

20. Butler, P.J., et al., *Shear stress induces a time- and position-dependent increase in endothelial cell membrane fluidity.* Am J Physiol Cell Physiol, 2001. **280**(4): p. C962-9.
21. Haidekker, M.A., N. L'Heureux, and J.A. Frangos, *Fluid shear stress increases membrane fluidity in endothelial cells: a study with DCVJ fluorescence.* Am J Physiol Heart Circ Physiol, 2000. **278**(4): p. H1401-6.
22. Tarbell, J.M., S. Weinbaum, and R.D. Kamm, *Cellular fluid mechanics and mechanotransduction.* Ann Biomed Eng, 2005. **33**(12): p. 1719-23.
23. Tarbell, J.M. and M.Y. Pahakis, *Mechanotransduction and the glycocalyx.* J Intern Med, 2006. **259**(4): p. 339-50.
24. Tarbell, J.M. and E.E. Ebong, *The endothelial glycocalyx: a mechano-sensor and -transducer.* Sci Signal, 2008. **1**(40): p. pt8.
25. Florian, J.A., et al., *Heparan sulfate proteoglycan is a mechanosensor on endothelial cells.* Circ Res, 2003. **93**(10): p. e136-42.
26. Thi, M.M., et al., *The role of the glycocalyx in reorganization of the actin cytoskeleton under fluid shear stress: a "bumper-car" model.* Proc Natl Acad Sci U S A, 2004. **101**(47): p. 16483-8.
27. Pahakis, M.Y., et al., *The role of endothelial glycocalyx components in mechanotransduction of fluid shear stress.* Biochem Biophys Res Commun, 2007. **355**(1): p. 228-33.
28. Nagy, E., et al., *Hyperfluidization-coupled membrane microdomain reorganization is linked to activation of the heat shock response in a murine melanoma cell line.* Proc Natl Acad Sci U S A, 2007. **104**(19): p. 7945-50.
29. Butler, P.J., et al., *Rate sensitivity of shear-induced changes in the lateral diffusion of endothelial cell membrane lipids: a role for membrane perturbation in shear-induced MAPK activation.* FASEB J, 2002. **16**(2): p. 216-8.
30. Cooper, R.A., *Influence of increased membrane cholesterol on membrane fluidity and cell function in human red blood cells.* J Supramol Struct, 1978. **8**(4): p. 413-30.
31. Galmiche, M.C., et al., *Stromal cells from human long-term marrow cultures are mesenchymal cells that differentiate following a vascular smooth muscle differentiation pathway.* Blood, 1993. **82**(1): p. 66-76.
32. Kinner, B., J.M. Zaleskas, and M. Spector, *Regulation of smooth muscle actin expression and contraction in adult human mesenchymal stem cells.* Exp Cell Res, 2002. **278**(1): p. 72-83.
33. Wang, D.J., et al., *Proteomic profiling of bone marrow mesenchymal stem cells upon TGF-beta stimulation.* The Journal of Biological Chemistry, 2004. **(In press)**.

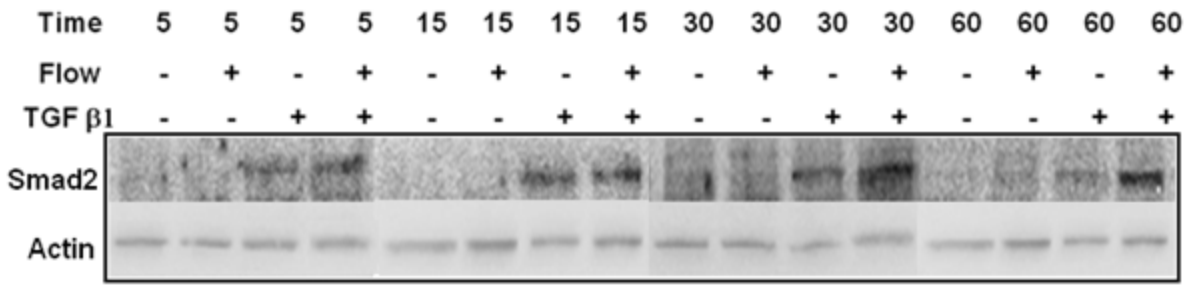

Figure 1. Effects of Fluid Flow on TGF-β1/SMAD2 Signaling in Human MSCs.

Smad2 phosphorylation begins within the first 5 minutes due to the presence of TGF-β1 in the media. The effect of fluid flow becomes noticeable after 30 minutes of exposure. MSCs were seeded on 2% gelatin coated glass slides and either subjected to a shear stress of 6 dynes/cm^2 or kept as static controls. The concentration of TGF-β1 added to the circulation medium was 0.1ng/ml. Total actin protein levels are shown to demonstrate equal loading between samples.

A.

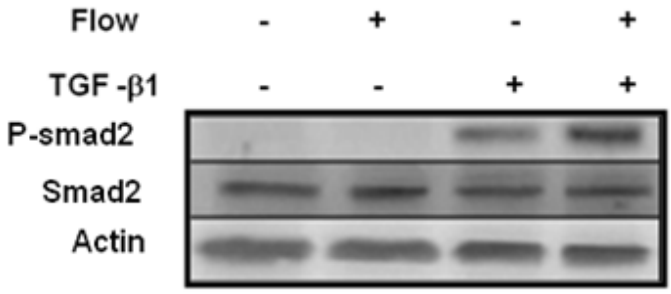

B.

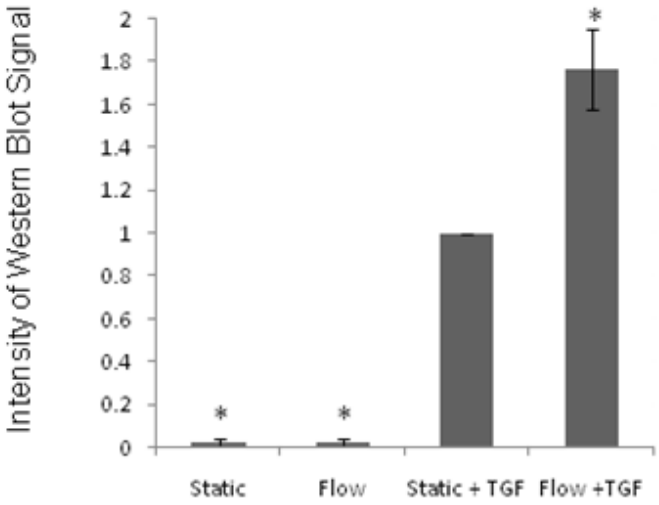

Figure 2. Increase in TGF-β1/SMAD2 Signaling due to Fluid Flow.

Human MSCs were seeded on 2% gelatin coated glass slides. MSCs were then subjected to a shear stress of 6 dynes/cm^2 or kept as static controls for 30 minutes. The concentration of TGF β1 was 0.1 ng/ml. A) Western Blot; B) Bar graph summarizing the quantification of immunoblotting results. Bars represent mean ± SD. Statistical significance compared to the static sample w/ TGF-β1 was determined using analysis of variance followed by student t-test. * indicates $P \leq 0.05$ (N=10)

A.

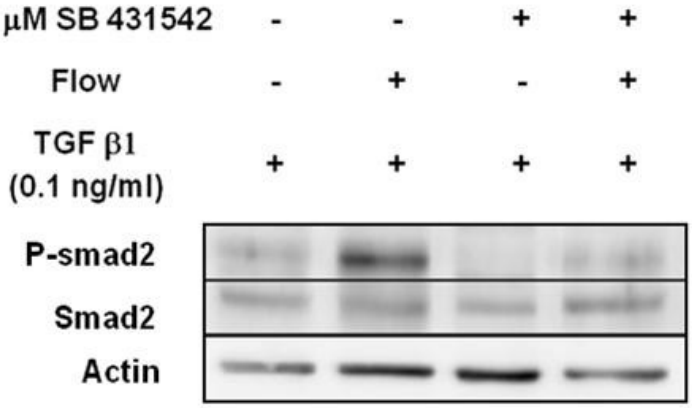

B.

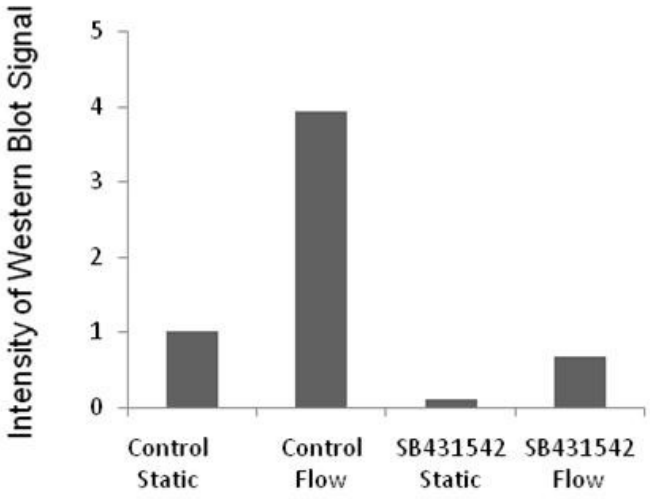

Figure 3. Receptor-dependence of the increase in TGF-β1/SMAD2 Signaling due to Fluid Flow.

Human MSCs were seeded on 2% gelatin coated glass slides and either subjected to a shear stress of 6 dynes/cm^2 or kept as static controls for 30 minutes. Sample MSCs were treated with 10 μM SB431542, a TGF-β type I receptor inhibitor. Controls were not treated with the inhibitor.

A) Western Blot; B) Bar graph summarizing the quantification of immunoblotting results.

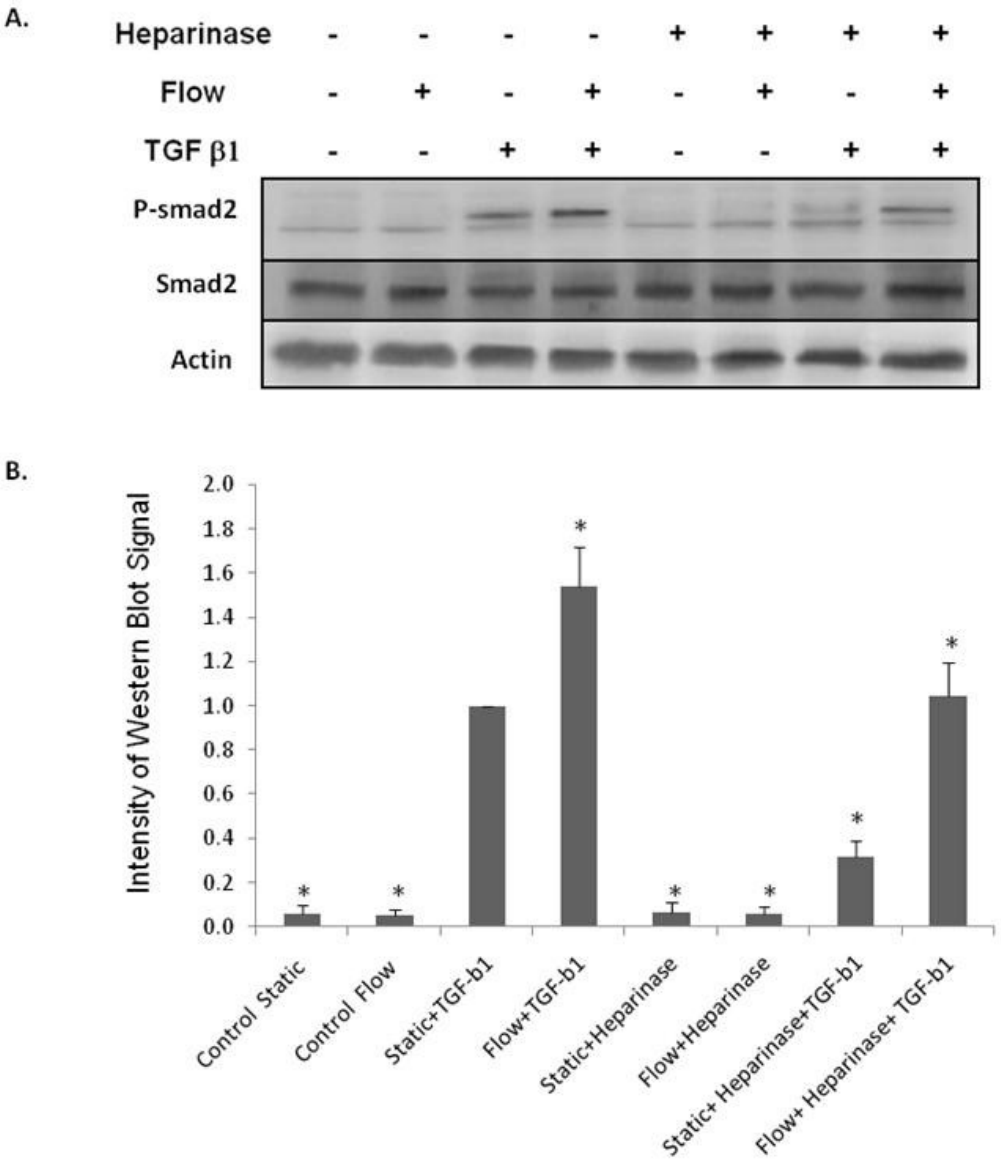

Figure 4. Effects of glycocalyx degradation on the Activation of TGF-β1/SMAD2 Signaling in human MSCs.

MSCs were seeded on 2% gelatin coated glass slides. MSCs were then subjected to a shear stress of 6 dynes/cm^2 or kept as static controls for 30 min. Prior to the shear experiments, sample MSCs were pre-treated with Heparinase III (4U/ml) for 3 hours. The concentration of TGF-β1 was 0.5ng/ml in all experiments.

A) Western Blot; B) Bar graph summarizing the quantification of immunoblotting results. Bars represent mean ± SD.

Statistical significance compared to the static sample w/ TGF-β1 was determined using analysis of variance followed by student t-test.

* indicates $P \leq 0.05$ (N=6)

A.

Cholesterol (in μM)	0	0	50	50	100	100	200	200
Flow	-	-	-	-	-	-	-	-
TGF-β1 (0.5ng/ml)	-	+	-	+	-	+	-	+

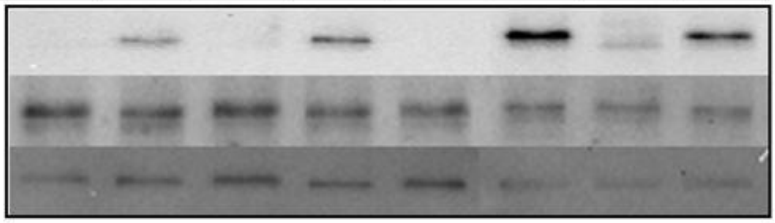

B.

Time (minutes)	60	60	120	120	180	180	240	240
Cholesterol (100 μM)	-	+	-	+	-	+	-	+
Flow	-	-	-	-	-	-	-	-
TGF-β1 (0.5ng/ml)	+	+	+	+	+	+	+	+

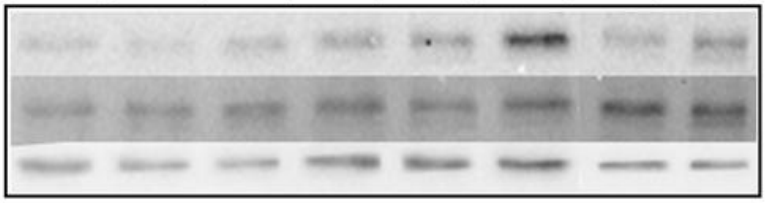

Fig 5. Time and Dosage Dependence of Cholesterol Treatment on TGF-β1/ SMAD2 Signaling in Human MSCs.
A) In the presence of TGF-β1, Cholesterol enhances SMAD2 phosphorylation in a dose-dependent manner for human MSCs. The duration of these experiments was 3 hours.
B) Time-dependence of the effects of Cholesterol on SMAD2 phosphorylation. MSCs were treated with 0.5 ng/ml TGF-β1 during the final 30 minutes and 100 μM cholesterol for the times indicated above.

A.

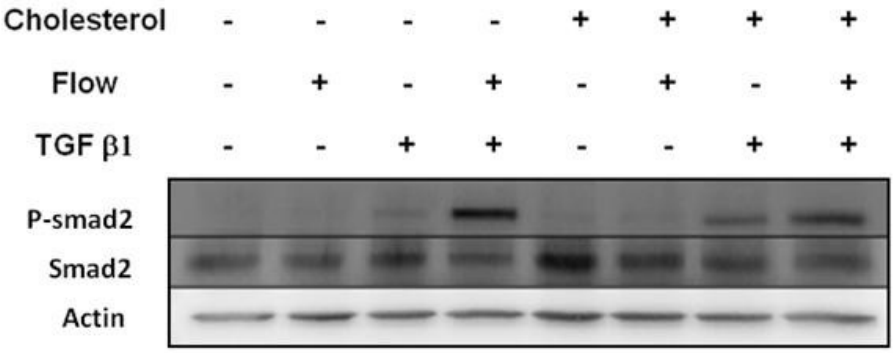

B.

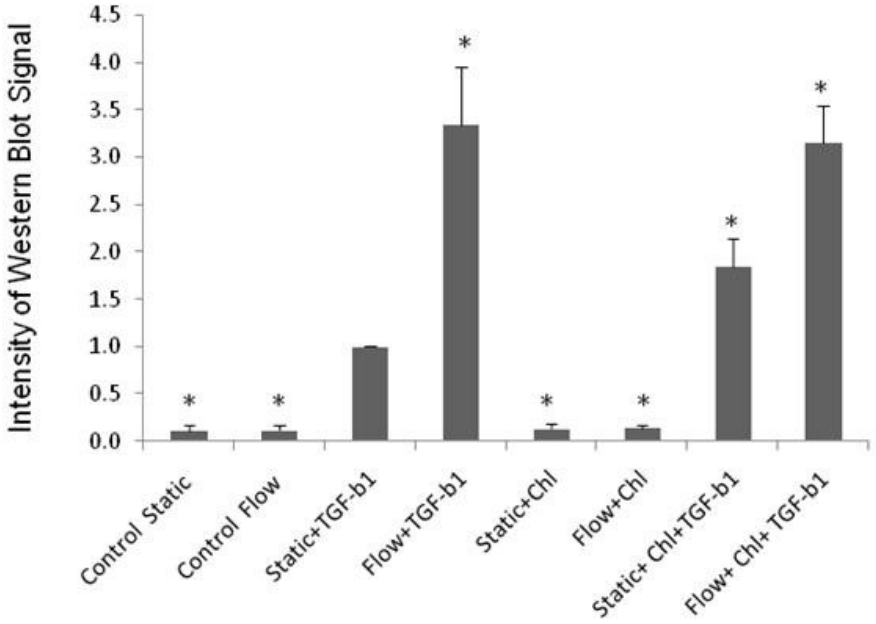

Fig 6. Effects of Decreasing Membrane Fluidity on the Activation of TGF-β1/ SMAD2 Signaling in human MSCs.
MSCs were seeded on 2% gelatin coated glass slides. MSCs were then subjected to a shear stress of 6 dynes/cm^2 or kept as static controls for 30 min. Prior to the shear experiments, sample MSCs were pre-treated with Cholesterol (Chl, 100 μM) for 3 hours. The concentration of TGF-β1 was 0.5ng/ml in all experiments.
A) Western Blot B) Bar graph summarizing the quantification of immunoblotting results. Bars represent mean ± SD.
Statistical significance compared to the static sample w/ TGF-β1 was determined using analysis of variance followed by student t-test.
* indicates $P \leq 0.05$ (N=3).

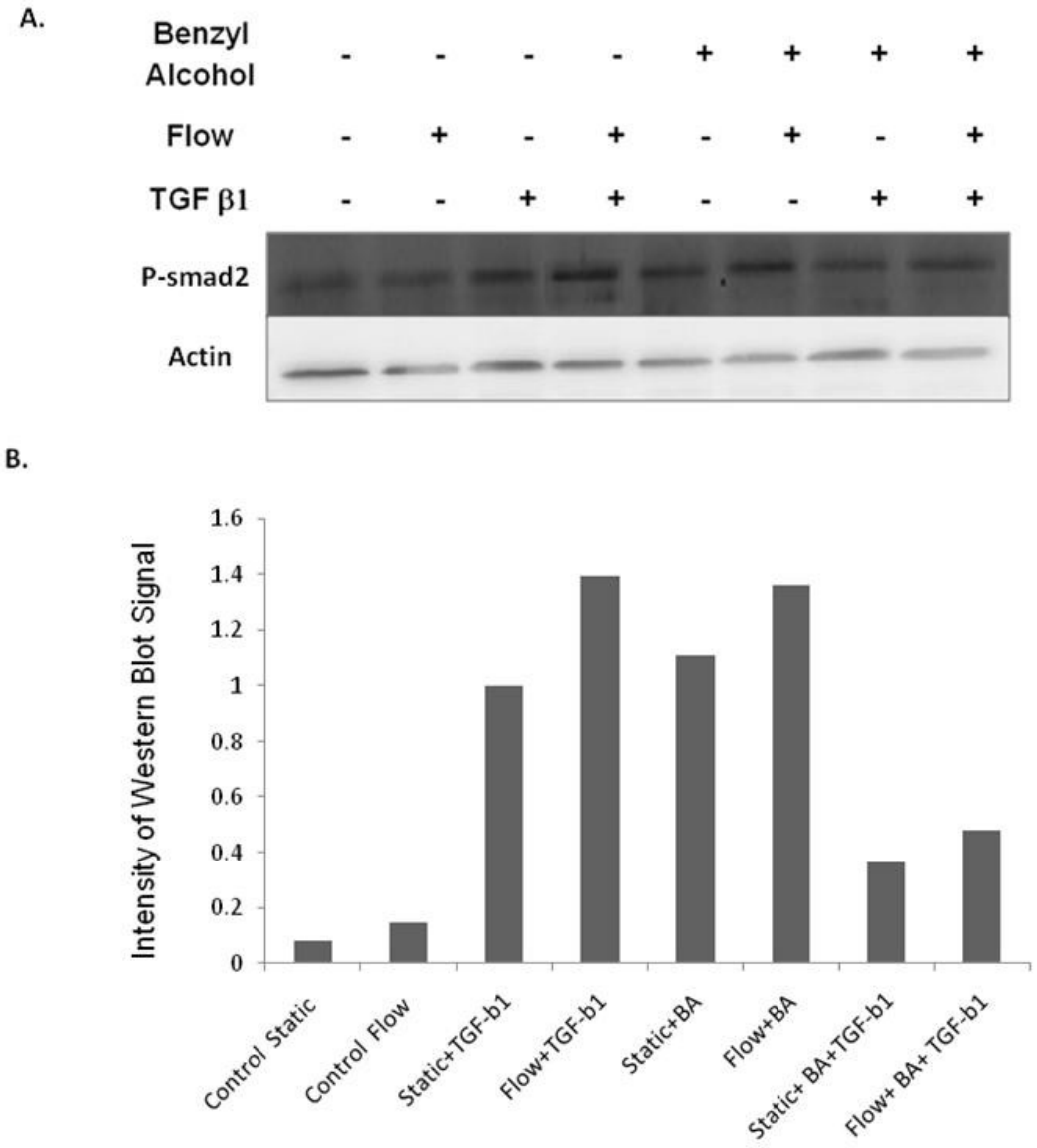

Fig 7. Effects of Increasing Membrane Fluidity on the Activation of TGF-β1/ SMAD2 Signaling in human MSCs. MSCs were seeded on 2% gelatin coated glass slides. MSCs were then subjected to a shear stress of 6 dynes/cm² or kept as static controls for 30 min. Prior to the shear experiments, MSCs were pre-treated with Benzyl Alcohol (BA, 45 mM) for 2 hours. The concentration of TGF-β1 was 0.5ng/ml. A) Western Blot B) Bar graph summarizing the quantification of immunoblotting results.

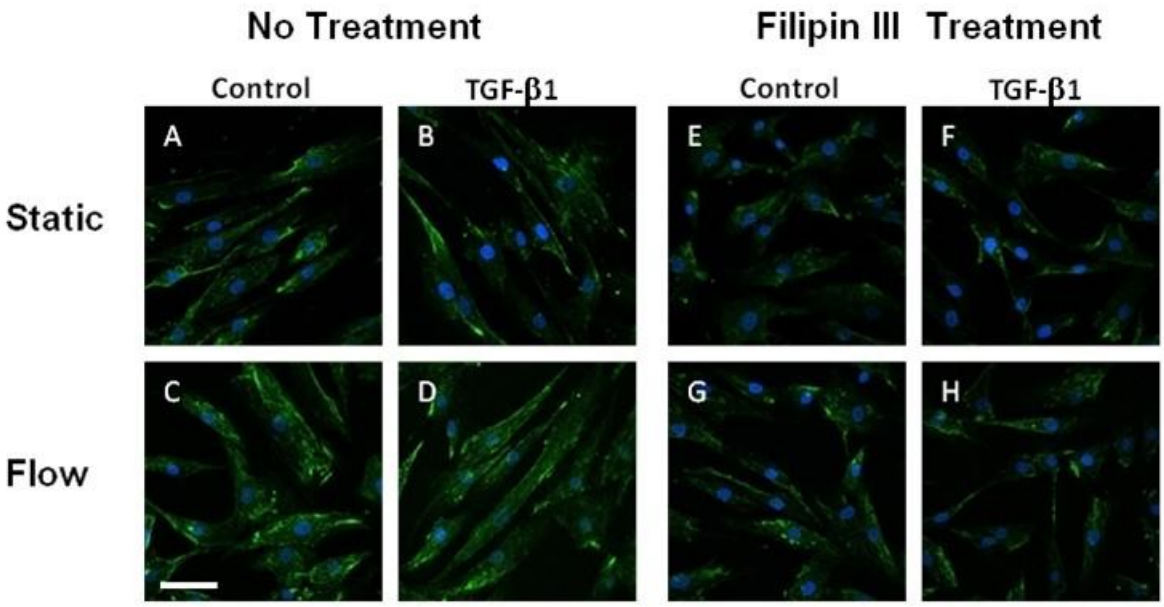

Figure 8. Effects of Filipin III treatment on Caveolin-1 expression in human MSCs.

MSCs were seeded on 2% gelatin coated glass slides. MSCs were then subjected to a shear stress of 6 dynes/cm^2 or kept as static controls for 30 minutes.

Prior to experiments, MSCs were pre-treated with Filipin III (1.5U/ml) for 15 min. The concentration of TGF-β1 was 0.5ng/ml. Scale bar = 80 μm.Caveolin-1 in green and DAPI in blue

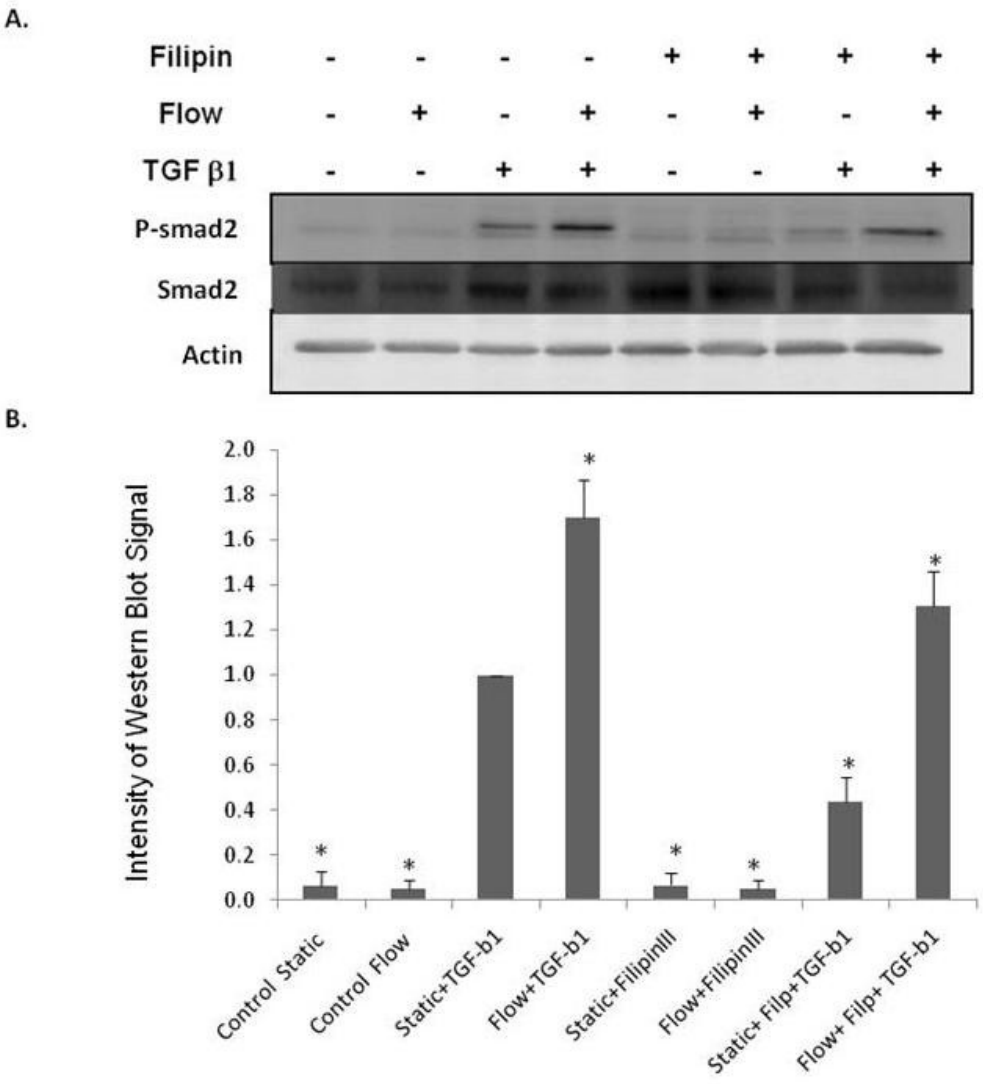

Fig 9. Effects of Caveolae/Lipid Raft Disruption on the Activation of TGF-β1/ SMAD2 Signaling in human MSCs.
MSCs were seeded on 2% gelatin coated glass slides. MSCs were then subjected to a shear stress of 6 dynes/cm^2 or kept as static controls for 30 min. Prior to the shear experiments, sample MSCs were pre-treated with Filipin III (1.5U/ml) for 15 min. The concentration of TGF-β1 was 0.5ng/ml in all experiments.
A) Western Blot B) Bar graph summarizing the quantification of immunoblotting results. Bars represent mean ± SD.
Statistical significance compared to the static sample w/ TGF-β1 was determined using analysis of variance followed by student t-test. * indicates $P \leq 0.05$ (N=4)

A.

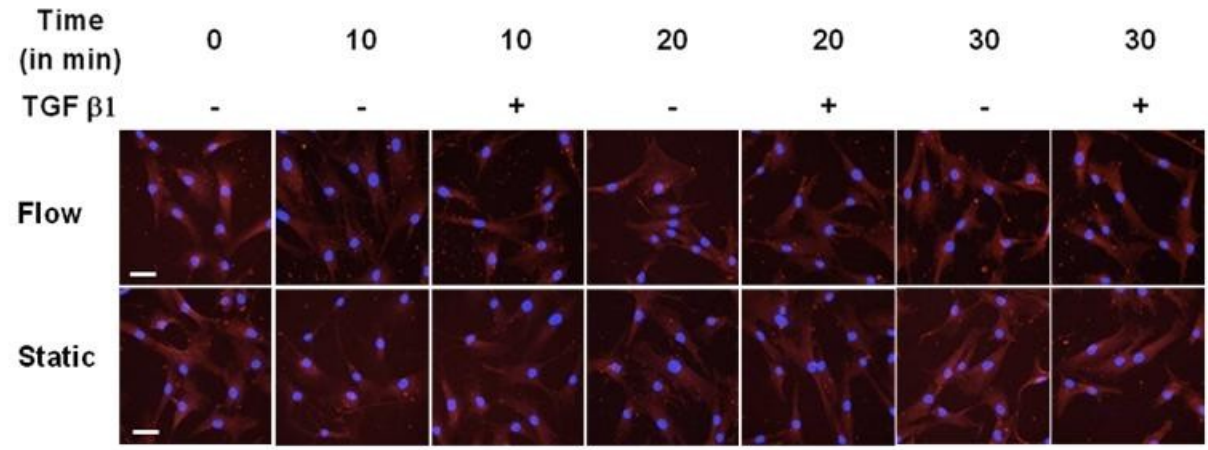

B.

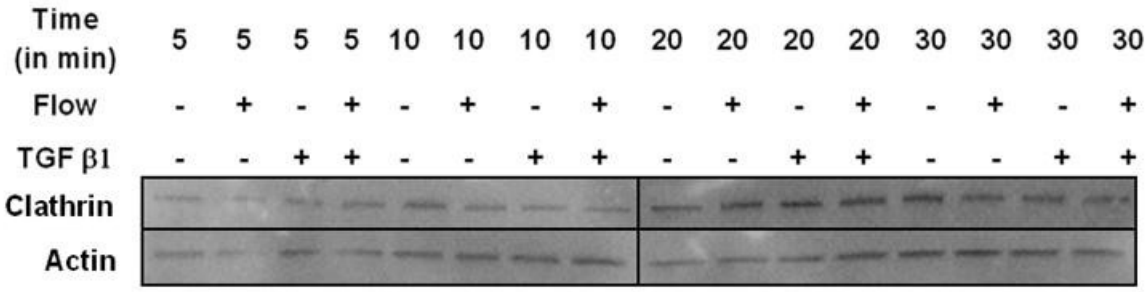

Figure 10. Effects of fluid flow on clathrin heavy chain protein expression in human MSCs.

MSCs were seeded on 2% gelatin coated glass slides. MSCs were then subjected to a shear stress of 6 dynes/cm^2 or kept as static controls for the times indicated above. The concentration of TGF-β1 was 0.1ng/ml.
A) Immunocytochemical Analysis ; B) Western Blot Results.
Scale bar = 40 μm.

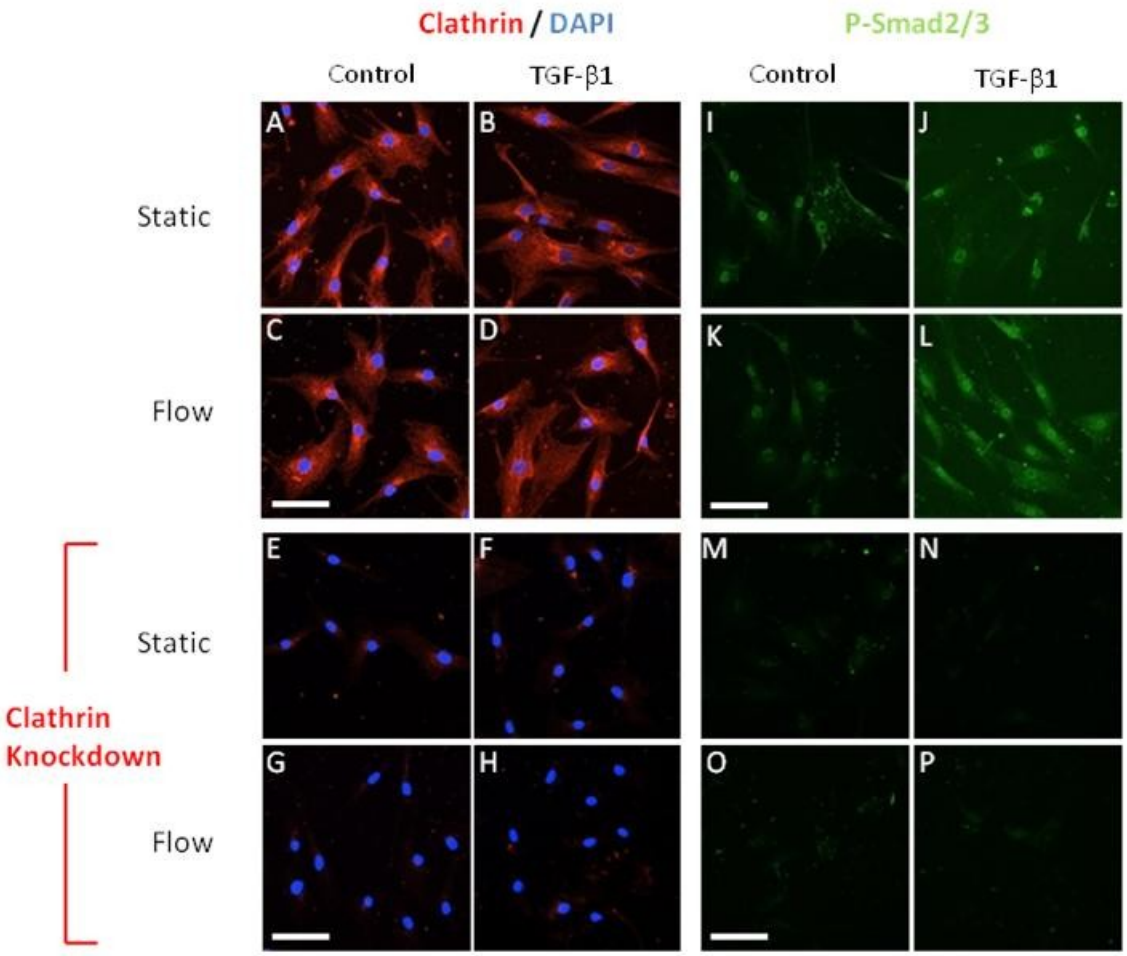

Figure 11. Effects of clathrin heavy chain knockdown on the activation of TGF-β1/ SMAD2 signaling in human MSCs.

Immunocytochemical analysis of clathrin heavy chain and P-smad2/3. Clathrin heavy chain mRNA expression was knocked down using SiRNA. MSCs were seeded on 2% gelatin coated glass slides. MSCs were then subjected to a shear stress of 6 dynes/cm^2 or kept as static controls for 30 minutes. The concentration of TGF-β1 was 0.1ng/ml. Scale bar = 80 μm. Clathrin in red, P-smad2/3 in green and DAPI in blue.

A.

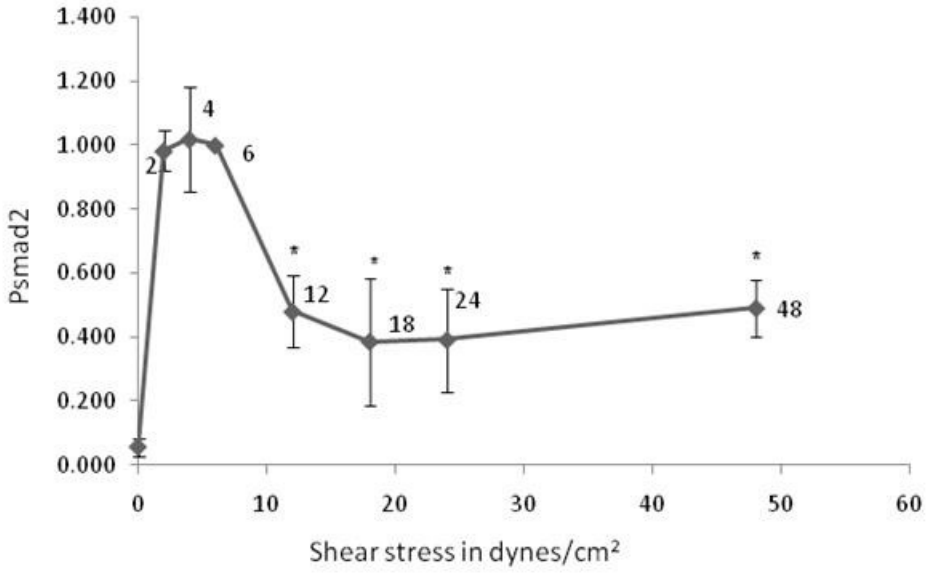

B.

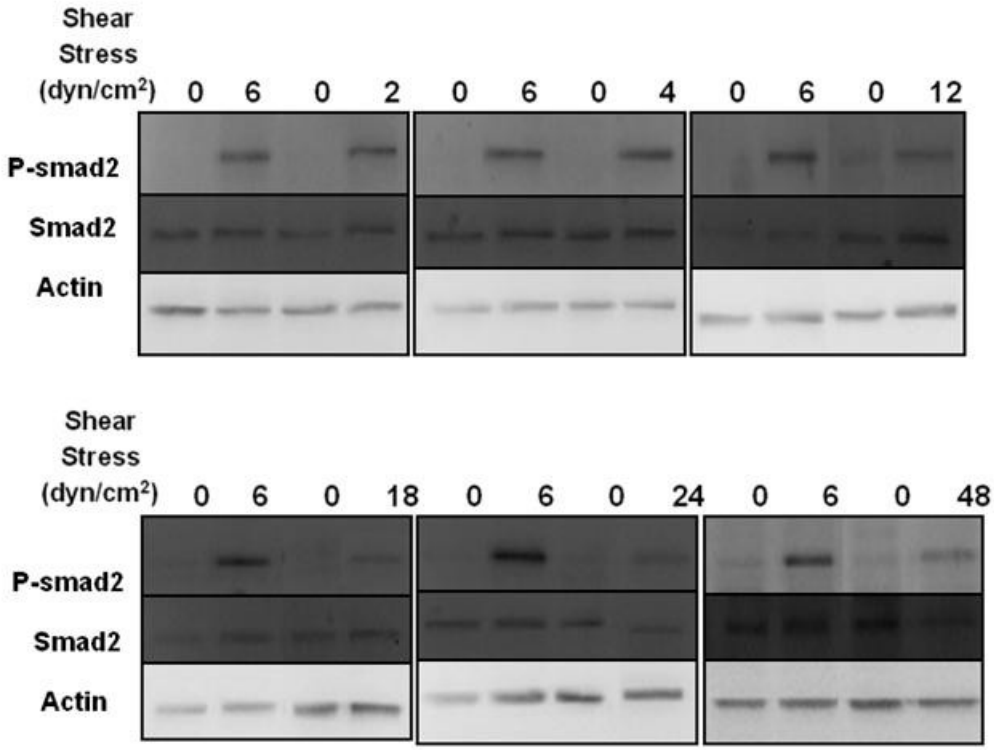

Figure 12. Effects of fluid shear stress on Smad2 phosphorylation.
MSCs were seeded on 2% gelatin coated glass slides and subjected to a flow rate of 12ml/min or kept as static controls for 30 min.
The concentration of TGF-β1 was 0.01ng/ml for all experiments.
A) Smad2 phosphorylation was quantified after western blot analysis. B) Western blot Bars represent mean ± SD. Statistical significance was determined using analysis of variance followed by student t-test. * indicates $P \leq 0.05$ (N=4)

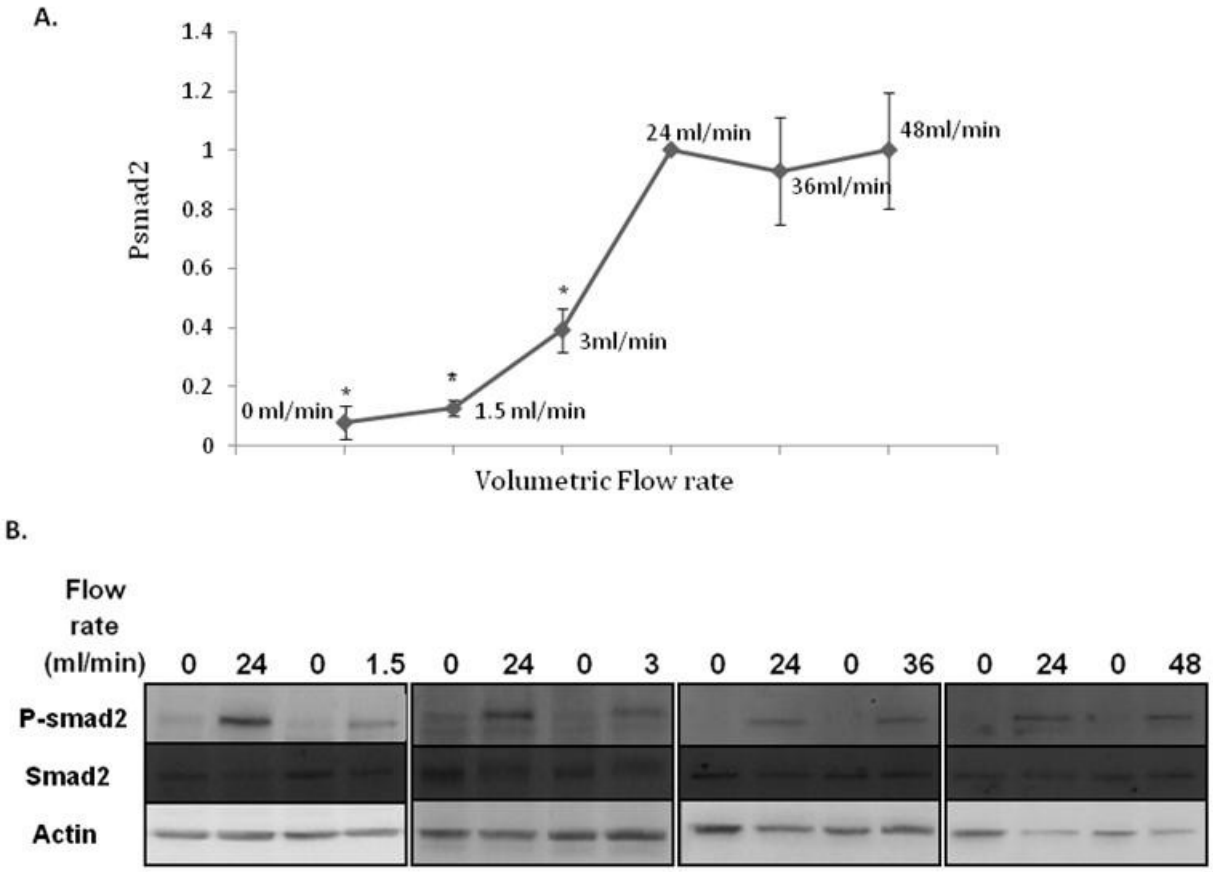

Figure 13. Effects of the Flow rate on Smad2 phosphorylation in MSC.

Human MSCs were seeded on 2% gelatin coated glass slides and subjected to a shear stress of 12 dynes/cm^2 or kept as static controls for 30 min. The concentration of TGF- β1 was 0.01ng/ml for all experiments.

A) Smad2 phosphorylation was quantified after western blot analysis. B) Western blot. Bars represent mean ± SD. Statistical significance was determined using analysis of variance followed by student t-test. * indicates $P \leq 0.05$ (N=4)

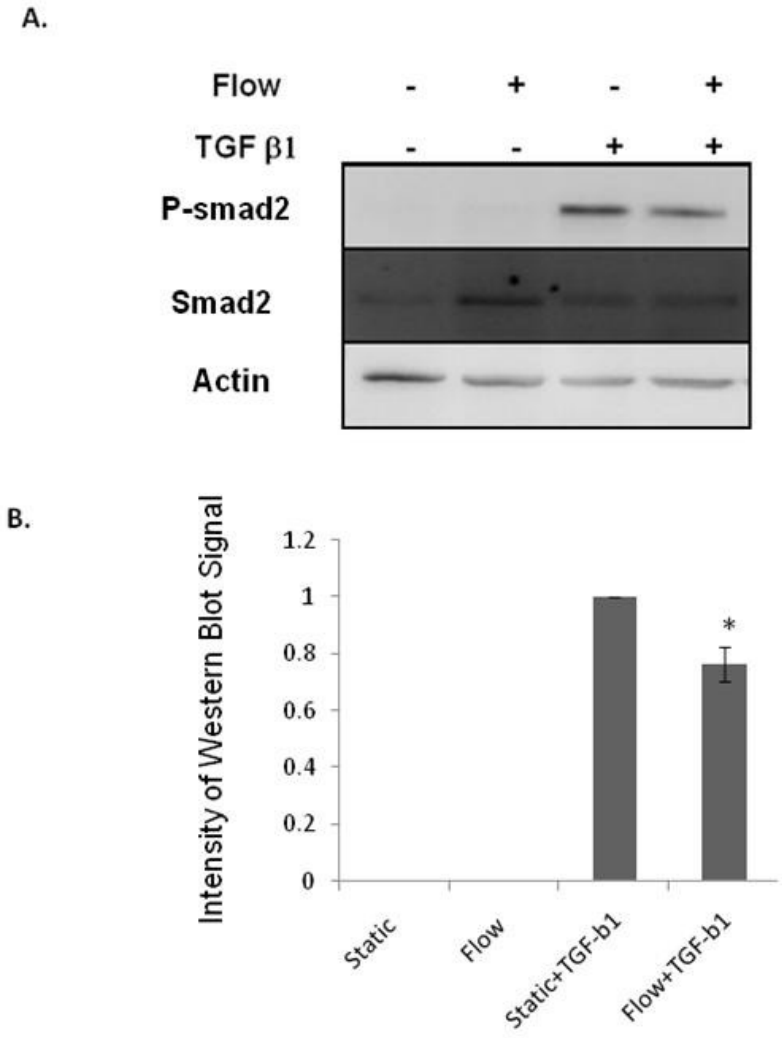

Figure 14. Effects of Applying Fluid Shear Stress before the addition of TGF-β1 on SMAD2 Signaling in human MSCs.

Human MSCs were seeded on 2% gelatin coated glass slides. MSCs were then subjected to a shear stress of 6 dynes/cm^2 or kept as static controls for 30 minutes with no TGF-β1 in the media. TGF-β1 was added after exposure to fluid shear stress. Cells were lysed 30 minutes after exposure to TGF-β1.

The concentration of TGF-β1 was 0.1ng/ml.

Western Blot B) Bar graph summarizing the quantification of immunoblotting results. Bars represent mean ± SD.

Statistical significance compared to the static sample w/ TGF-β1 was determined using analysis of variance followed by student t-test.

* indicates $P \leq 0.05$ (N=3)

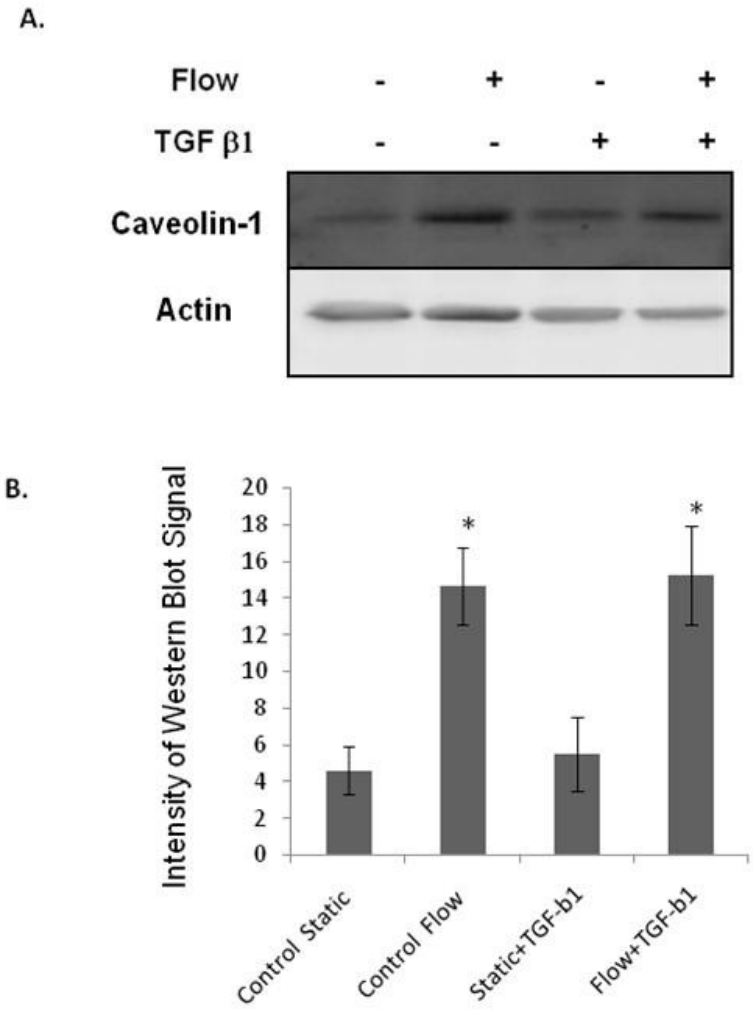

Fig 15. Effects of fluid flow on Caveolin-1 expression in human MSCs.

Human MSCs were subjected a shear stress of 6 dynes/cm^2 or kept as static controls for 30 minutes. Fluid flow causes an increase in Caveolin-1 expression.

The concentration of TGF-β1 was 0.5ng/ml.

A) Western Blot B) Bar graph summarizing the quantification of immunoblotting results. Bars represent mean ± SD. Statistical significance compared to static control was determined using analysis of variance followed by student t-test. * indicates $P \leq 0.05$ (N=6)

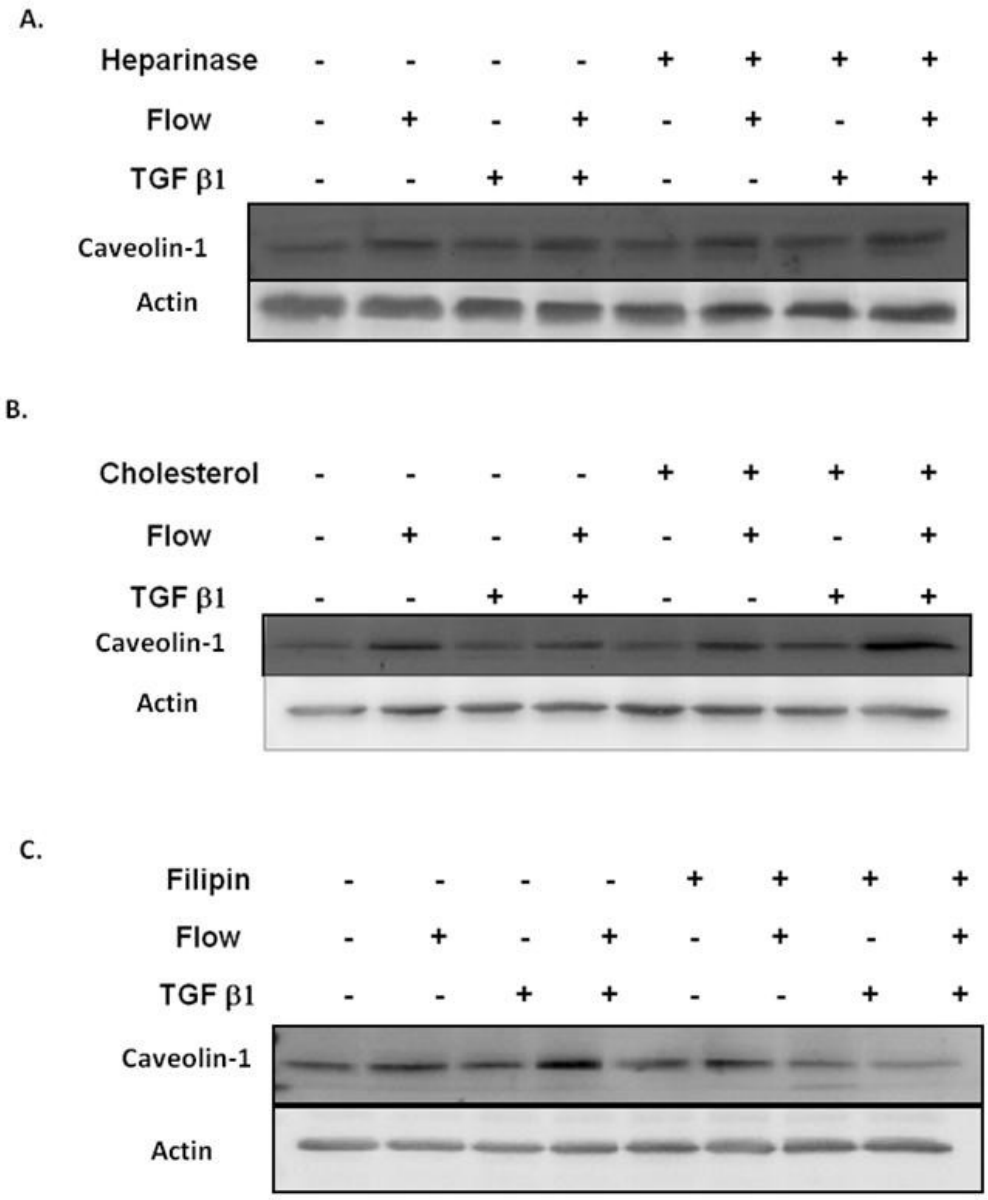

Figure 16. Effects of fluid flow in combination with various chemical treatments on Caveolin-1 in human MSCs.
Human MSCs were seeded on 2% gelatin coated glass slides. MSCs were then subjected to a shear stress of 6 dynes/cm^2 or kept as static controls for 30 minutes.
Prior to experiments, MSCs were pre-treated with
A) Heparinase III (4U/ml) for 3 hours; B) Cholesterol (100 μM) for 3 hours ; and C) Filipin III (1.5U/ml) for 15 min.
The concentration of TGF-β1 was 0.5ng/ml in all experiments.

Chapter 3

Effects of Laminar Fluid Shear Stress on Human Neural Crest Stem Cell Function

Abstract

Abstract—Neural crest stem cells (NCSCs) are multipotent cells that give rise to various tissues during the embryonic development of vertebrates. Presently, little is known about the effects of fluid shear stress on NCSC function. In this study, NCSCs derived from induced pluripotent stem cells were exposed to a laminar fluid shear stress of 10 dynes/cm^2 for various time periods. We found that laminar fluid shear stress increased NCSC proliferation and ERK2 phosphorylation in a time-dependent manner. Fluid shear stress also caused an increase in Calponin1 expression in the first 24 hrs of exposure. In addition, we observed that exposure to fluid shear stress had no effect on myogenic, neurogenic or osteogenic differentiation in NCSCs. We found, however, that exposure to fluid shear stress suppressed adipogenic differentiation. Further investigation into the effects of mechanical stimulation on the function of NCSCs will be necessary to provide a rational basis for the use of these cells in tissue engineering applications.

Keywords—neural crest stem cells, laminar fluid shear stress, differentiation, proliferation.

Introduction

The neural crest refers to a population of cells located between the neural tube and the dorsal ectoderm during the embryonic development of vertebrates [1, 2]. Neural crest cells are multipotent cells that undergo epithelial to mesenchymal transition and migrate extensively to give rise to a variety of tissues: cranial and facial bone, cartilage, nerve tissue, smooth muscle, connective tissue and even melanocytes [3].

NCSCs have been studied extensively in rodent and avian models. They have been isolated from embryonic and adult rodent tissues: bone marrow [4], skin [5], cornea [6] , heart tissue [7], hair follicle [8] and gut [9]. Markers for NCSCs include: p75, human natural killer protein 1 (HNK1), Nestin, Activating Protein 2 (AP2) and Vimentin [10-12].

Recently, NCSCs have been derived from mouse and human ESCs and iPSCs [13, 14]. Since it is not possible to conduct in-vivo studies on human NCSCs, this approach yields new possibilities for research in the study of human development and regenerative medicine.

NCSCs derived from ESCs and iPSCs have been shown to differentiate into peripheral neurons, Schwann cells, chondrocytes, osteoblasts, adipocytes and smooth muscle cells [12, 15]. NCSCs could provide a potential cell source for tissue engineering because they give rise to smooth muscle tissue during development [1]. Human NCSCs have also been shown to differentiate into smooth muscle cells in-vitro [15]. In order to use these stem cells for tissue engineering applications, however, a better understanding of the effects of biomechanical factors on NCSC differentiation and proliferation is still needed.

Hemodynamic forces such as mechanical strain and fluid shear stress are known to play a role during embryonic development and in stem cell development [16-22]. A recent study has reported that cyclic uniaxial strain enhanced the proliferation of NCSCs and promoted the expression of smooth muscle cell markers, calponin-1 and smooth muscle myosin. Cyclic uniaxial strain was also shown to suppress the differentiation of NCSCs into Schwann cells [23]. NCSC differentiation and proliferation may also be affected by fluid flow. The effects of fluid shear stress on these processes in NCSC, however, have not yet been examined.

In this study, we determine how shear stress affects the differentiation and proliferation of human NCSCs. We applied laminar shear stress on human NCSCs derived from iPSCs using a parallel-plate flow chamber. Our results showed that laminar shear stress had a negligible effect on the differentiation of human NCSCs but increased the rate of proliferation of these cells.

Materials and Methods

NCSC derivation and Cell Culture

iPSCs derived from human bone marrow MSCs were used to derive human NCSCs. The following protocol was previously described in Wang et al [12].
To derive NCSCs, hMSC-iPSCs were detached with collagenase IV (1 mg/ml) and dispase (0.5 mg/ml). The resulting cell aggregates were cultured in ESC maintenance medium without basic fibroblast growth factor (bFGF) for 5 days. The cell aggregates were subsequently transferred onto TC dishes pre-coated with CellStart (Invitrogen, Carlsbad, CA). The adherent colonies were cultured for 7 days in StemProH, NSC serum-free neural induction medium (Invitrogen, Carlsbad, CA.) The colonies with rosette structures were handpicked, cultured in suspension in StemProH, NSC serum-free neural induction medium for 7 days before being transferred onto TC dishes pre-coated with CellStart. The colonies were then cultured for 3 additional days.
Colonies were dissociated into single cells with TryplE Select (Invitrogen, Carlsbad, CA.) and cultured as a monolayer in StemProH, NSC serum-free neural induction medium. Cells were then purified by flow-activated cell sorting to obtain homogeneous populations that were positive for neural crest markers. The NCSCs derived from iPSCs were maintained in StemPro NSC serum-free neural induction medium (Invitrogen, Carlsbad,CA)for expansion without differentiation.

Cell Seeding Prior to Shear Stress Experiments

Autoclaved glass slides (Erie Scientific, Portsmouth, NH) were exposed to ultraviolet (UV) light for 1 hour for sterilization. Slides were then coated with 2% gelatin (Sigma Aldrich, St. Louis, MO) and placed under UV light for 1 hour at room temperature to allow for protein adsorption before being washed with phosphate buffered saline (PBS, pH 7.4). Human NCSCs were seeded onto the gelatin-coated slides at approximately 50% confluency. The cells will be allowed to grow to 80% confluency in StemPro NSC serum-free neural induction medium (Invitrogen, Carlsbad,CA) before shear stress experiments.

Fluid Shear Stress Experiments

Laminar fluid shear stress was applied to NCSCs using a parallel-plate flow chamber. Glass slides seeded with NCSCs were mounted on a rectangular flow channel created by sandwiching a silicone gasket between a glass slide and a polycarbonate flow chamber base.

NCSCs were subjected to a laminar shear stresses of 10 dynes/cm^2 for 66 hours (unless otherwise specified). The circulating media contained Dulbecco's modified Eagle's medium (DMEM) with 10% fetal bovine serum (FBS) and supplemented with 1% penicillin-streptomycin (Invitrogen Co., Carlsbad, CA). Culture medium was circulated throughout the system using a peristaltic pump. All shear stress experiments included static controls: NCSCs cultured on glass slides were kept under static condition in the same incubator. The flow system was set up in a humidified cell culture incubator (37 ºC, 5 %CO_2).

Materials and Methods

NCSC Differentiation

This protocol was previously described and slightly modified from Wang et al [12].

For NCSC differentiation into Schwann cells, NCSCs were cultured for 2 weeks in N2 medium supplemented with 10 ng/ml ciliary neurotrophic factor (R&D Systems Inc., Minneapolis, MN.), 10 ng/ml bFGF (Invitrogen Corp. Carlsbad, CA), 1 mM dibutyryl-cAMP (Sigma-Aldrich Corp., St. Louis, MO) and 20 ng/ml neuregulin1b (R&D Systems Inc., Minneapolis, MN).

For NCSC differentiation into peripheral neurons, NCSCs were cultured for 2 weeks in N2 medium supplemented with 20 ng/ml brain-derived neurotrophic factor (R&D Systems Inc., Minneapolis, MN.), 10 ng/ml nerve growth factor (R&D Systems Inc., Minneapolis, MN.), 10 ng/ml glial cell line-derived neurotrophic factor (R&D Systems Inc., Minneapolis, MN.) and 1 mM dibutyryl-cAMP (Sigma-Aldrich Corp., St. Louis, MO.)

For NCSC differentiation into SMC lineage, NCSCs were cultured for 4 weeks in Minimum Essential Medium α Medium (Invitrogen Corp. Carlsbad, CA) containing 10% Fetal Bovine Serum(Invitrogen Corp., Carlsbad, CA) with 10 ng/ml TGF-b1 (Pepro Tech Inc., Rocky Hill, NJ).

For adipogenic differentiation, confluent NCSCs were treated with 10 mg/ml insulin (Sigma-Aldrich Corp., St. Louis, MO), 1 mM dexamethasone (Sigma-Aldrich Corp., St. Louis, MO) and 0.5 mM isobutylxanthine (Sigma-Aldrich Corp., St. Louis, MO) in α MEM medium containing 10% FBS for 4 weeks.

For osteogenic differentiation, NCSCs were seeded at a low density (10^3 cells/cm2) and grown in α MEM medium containing 10% FBS for 2 weeks in the presence of 10 mM b-glycerol phosphate (Sigma-Aldrich Corp. St. Louis, MO), 0.1 mM dexamethasone and 200 mM ascorbic acid (Sigma-Aldrich Corp. St. Louis, MO).

Immunofluorescent Staining and Confocal Microscopy

NCSCs were fixed with 4% paraformaldehyde in PBS for 15 min, permeabilized with 0.5% Triton X-100 in PBS for 10 min, and blocked with 1% BSA for 30 min. The samples were incubated overnight at 4^o C with primary antibodies, followed by incubation with the appropriate secondary antibodies for 1hr. For nuclear staining, samples were incubated in PBS with DAPI for 5 min (Invitrogen Corp., Carlsbad CA).
We used a Zeiss LSM 510 Meta confocal microscope to capture multiple *Z*-sections for each sample (0.2 to 0.4 μm thick sections over a range of 20 μm). These sections were subsequently integrated to create maximum intensity projections of each sample using Zeiss LSM Imaging Software.
To characterize NCSCs, the following primary antibodies were used: p75 (Abcam Inc., Cambridge, MA), HNK1 (Sigma-Aldrich Corp., St. Louis, MO), vimentin (Dako North America Inc., Carpinteria, CA) and nestin (Abcam Inc. Cambridge, MA).

For differentiation into Schwann cells, cells were immunostained for Schwann cell markers S100β (S1542, Sigma-Aldrich Corp.) and glial fibrillary acidic protein (GFAP; AB5804, Millipore Corp., Billerica, MA).
For differentiation into peripheral neurons, cells were immunostained for peripheral neuron markers peripherin (AB1530, Millipore Corp.), Neural filament M (NFM, N4142, Sigma-Aldrich Corp., St. Louis MO.) and class-III b-tubulin (Tuj1; MMS-435P, Covance Inc., Princeton, NJ).
For differentiation into smooth muscle cells, Cells were immunostained with smooth muscle markers CNN1 (1806-1, Epitomics Inc., Burlingame, CA), smooth muscle a-actin (SMA; A5228, Sigma-Aldrich Corp., St. Louis MO.) and Myosin Heavy Chain (MHC, Sc-79079, Santa Cruz Biotechnology, Santa Cruz CA.)
To verify adipogenic differentiation, samples were stained with Oil red.
For osteogenic differentiation, cells were fixed in 4% paraformaldehyde, and stained with Alizarin red.

RNA Isolation and Quantitative Polymerase Chain Reaction (qPCR)

Each cells sample was lysed with 1 ml of Trizol (Invitrogen Corp., Carlsbad, CA.) RNA was extracted by using chloroform and phenol extractions, precipitated by isopropanol, and the resulting RNA pellet was washed with 75% ethanol. RNA pellets were resuspended in 20 ml DEPC-treated water and were quantified with RiboGreen RNA Quantification Kit (Invitrogen Corp. Carlsbad, CA). cDNA was synthesized by using two-step reverse transcription (RT) with the ThermoScript RT-PCR system (Invitrogen Corp. Carlsbad, CA), followed by qPCR using SYBR green reagent and the ABI Prism 7000 Sequence Detection System (Life Tech Corp., Carlsbad, CA). Primers for the genes of interest were designed with the ABI Prism Primer Express™ software v.2.0 (Applied Biosystems, Foster City, CA) and are listed in Table1.
The gene expression of each sample was normalized to the level of 18S ribosomal RNA in the sample. Results were analyzed with ABI Prism 7000 SDS software (Life Tech Corp., Carlsbad, CA.)

TABLE 1. Primers for qPCR.

Gene name	Forward primer (5'–3')	Reverse primer (5'–3')
SMA	CAGCTCCAGCTATGTGTGAAGAA	GCAAAGCCGGCCTTACAGA
CNN1	GCATGTCCTCTGCTCACTTCAA	GGGCCAGCTTGTTCTTAACCT
MHC	CCTGGCGGCGAATGC	GGCTTTGATCATGAGAATGCAG
NES	ACTCCCGGCTGCAAACAC	AGCTTGGGGTCCTGAAAGCT
TUJ1	GGGCCAAGTTCTGGGAAGTC	CGAGTCGCCCACGTAGTTG
PECAM1	TGCACTGCAGGTATTGACAAAGT	GGGCTGGGAGAGCATTTCA
VECAD	AATGACAATTGGCCTGTGTTTTC	CAGAGGTCCCTATAGCTGACATCTC
TGF-β1	CCGTGGAGGGGAAATTGAG	GAACCCGTTGATGTCCACTTG
KLF4	TCCTTCCTGCCCGATCAG	GGCATGAGCTCTTGGTAATGG
18S rRNA	CGCAGCTAGGAATAATGGAATAGG	CATGGCCTCAGTTCCGAAA

Materials and Methods

Protein isolation and Immunoblotting

Cells were lysed with 150 μL of RIPA buffer (25 mM Tris (pH 7.4), 0.5 M NaCl, 1% TritonX-100, 0.1% SDS, 1 mM PMSF, 10 lg/mL leupeptin, and 1 mM Na3VO4). The protein samples were then centrifuged to isolate the supernatant. The protein concentration in all samples was quantified using DC Protein Assay (Biorad, Hercules, CA.) Protein samples were prepared in SDS sample buffer (2% SDS, 10% (v/v) glycerol, 60 mM Tris, and 0.05% (v/v) mercaptoethanol) and boiled for 5 min prior loading onto 10% SDS-PAGE gels. After electrophoresis, the separated proteins were transferred onto a nitrocellulose membrane (Biorad, Hercules, CA.) The membrane was blocked with Tris-buffered saline containing 3% non-fat powdered milk for 1 h and then incubated with the primary antibody in Tris-buffered saline-Tween overnightat 4 °C. The blots were subsequently washed in Tris-buffered saline-Tween and then incubated with an appropriate horseradish peroxidase-conjugated secondary antibody in Tris-buffered saline-Tween. Proteins were visualized using enhanced chemiluminescence (Biorad, Hercules, CA.) Image analysis was performed with the Image J software package (NIH).

Cell Proliferation Assay

After exposure to fluid shear stress, NCSCs were cells were fixed with 4% paraformaldehyde for 15 min, washed twice with 3% BSA in PBS and permeabilized with 0.5% Triton X-100 for 20 min. After washing with 3%BSA in PBS, samples were incubated in a 10μM Edu reaction cocktail prepared following the Click-iT™ EdU Imaging Kit (Invitrogen Corp., Carlsbad, CA). After 30 minutes of incubation in the dark, the stained samples were washed again with 3%BSA in PBS. Samples were subsequently incubated for 30 minutes in 5μg/ml Hoechst solution for nuclear staining. Images were captured on a Zeiss LSM 510 Meta confocal microscope. For each sample, the percentage of proliferating cells was calculated by averaging the percentage of EdU-positive cells over randomly selected viewing fields. Three independent experiments were carried out.

Statistical Analysis

For all data, we first performed an analysis of variance (ANOVA) to determine statistical significance.
For the proliferation data, significant difference compared to static control was determined by a Student's t-test ($p < 0.05$.)
For qPCR data, significant difference compared to static control was determined by using log-transformed one-sample t-test ($p < 0.05$.).

Results

Characterization of NCSCs derived from iPSCs.

Figure 1 shows that NCSCs derived from iPSCs expressed NCSC markers: p75, HNK1, nestin and vimentin. These cells were also able to expand without differentiation (data not shown). In addition, NCSCs were able to differentiate into different cell types: peripheral neurons (figure 11, a-d); Schwann cells (figure 12, a-d) ; smooth muscle cells (figure 13, a-f); adipocytes and osteoblasts (figure 10, a-c). These results demonstrated the multipotency of NCSCs, which is consistent with previously reported findings.

Effects of Laminar Fluid Shear Stress on NCSC Proliferation

To determine the effects of shear stress on NCSC proliferation, we used a novel alternative to BrdU (5-bromo-2-deoxyuridine) labelling. EdU (5-ethynyl-2´-deoxyuridine) is a nucleoside analog of thymidine and is incorporated into DNA during active DNA synthesis (S-phase). Detection was based on a copper catalyzed reaction between the alkyne contained in Edu and the azide contained in the Alexa Fluor® dye. We applied laminar fluid shear stress (10 dyn/cm^2) to NCSCs for 24,48 and 72hrs respectively. Figure 3A. shows that the percentage of Edu-positive cells was greater in sheared samples compared to static control samples for all time points: 46% greater after 24hrs, 43% greater after 48hrs and 55% greater after 72hrs. For both static controls and samples exposed to shear stress, the total fraction of Edu-positive cells was greater at 24hrs compared to later time-points (figures 2 and 3A). To continue, figure 3B demonstrates that fluid shear stress consistently increased ERK2 phosphorylation in the first 48hrs and shows the highest level of phosphorylation at the 24hr time point. The activation of ERK1/2 is known to play an important role in cell proliferation.

Effects of Laminar Fluid Shear Stress on NCSC Gene Expression

The effects of laminar fluid shear stress on a select number of genes were examined by quantitative reverse transcription polymerase chain reaction (qRT-PCR). Laminar fluid shear stress (10 dyn/cm^2) was applied to NCSCs for 24 and 66hrs respectively. Changes in gene expression were reported at 24hrs and 66hrs for the following: smooth muscle a-actin (SMA); calponin1 (CNN1); myosin heavy chain (MHC); nestin ;class-III b-tubulin (Tuj1); platelet endothelial cell adhesion molecule (Pecam 1); vascular endothelial cadherin (Vecad); transforming growth factor β1 (TGF- β1); and Krüppel-like factors 4 (Klf4).
Figure 4 shows that the gene expression of smooth muscle cell marker SMA decreased by 30% on average compared to static controls both at the 24hr and 66hr timepoints. The smooth muscle cell marker CNN1 decreased by 20% compared to static control at the 24hr timepoint or by 90% at the 24hr timepoint . Myosin heavy chain gene expression increases by 2.5 folds after 24hrs and decreases by 40 % compared to

Results

Effects of Laminar Fluid Shear Stress on NCSC Gene Expression (continued)

static after 66hrs.There is also decreased expression of NCSC marker nestin (NES) at both time points. The changes in gene expression for peripheral neuron marker, class-III b-tubulin (Tuj1) were not considered to be significant. To continue, fluid shear stress did not significantly affect the gene expression of transforming growth factor β1 (TGF-β1). Figure 4 also shows changes in gene expression for platelet endothelial cell adhesion molecule (Pecam 1) and vascular endothelial cadherin (Vecad): while Pecam1 decreased by 60% compared to static controls, Vecad increased by almost 2 folds in the first 24 hours and, by 4 folds after 66 hours. Interestingly, there is a significant increase (6 and 7 folds respectively at 24hrs and 66hrs) in the gene expression of Krüppel-like factors 4 (Klf4). This result is consistent with the proliferation data shown on figures 2 and 3.

Effects of Laminar Fluid Shear Stress on NCSC Protein Expression

Laminar fluid shear stress (10 dyn/cm^2) was applied to NCSCs for 66hrs to determine its effects on NCSC protein expression. Samples were then immunostained to examine changes in the expression of a select number of proteins.
Figure 6 shows that NCSC markers (HNK1, p75, Vimentin) are still strongly expressed after 66hrs in both static control samples and samples exposed to shear stress. The expression of nestin, however, appears much weaker than other NCSC markers (fig.6 g,h).
To continue, laminar shear stress does not seem to affect the protein expression of peripheral neuron markers (peripherin, class-III b-tubulin and neural filament M) as seen in figure 7. The same can be noted for Schwann cell markers (glial fibrillary acidic protein and S100-β) shown in figure 8. There are no significant differences to be reported in the protein expression of smooth muscle cell markers after 66hrs of exposure to shear stress: smooth muscle α-actin (fig.9 a,b), Calponin1 (fig.9 c,d), smooth muscle myosin heavy chain(fig.9 e,f), and SM22a (fig.9 g,h).
It is interesting to note that NCSCs appear to express all these markers simultaneously at the 66hr timepoint. Furthermore, immunoblotting analysis of calponin1 expression in the first 24 hrs shows that shear stress increases levels of calponin1 protein expression (figure 5). Figure 5 also shows that after the 12hr timepoint, the expression of calponin 1 starts to decrease in the samples exposed to shear stress. This result is consistent with qPCR data reported in figure 4.

Results

Effects of Laminar Fluid Shear Stress on NCSC Multipotency

To demonstrate the effects of laminar fluid shear stress on the differentiation potential of NCSCs, cells were exposed to fluid flow (10 dyn/cm^2) or kept in static cultures for 66hrs. Subsequently, cells were transferred to the specific differentiation media (osteognic, adipogenic, myogenic and neurogenic) described in the material and methods section. The duration of cell culture varied between 14 and 30 days depending on the lineage.
Applying shear stress to NCSCs for 66hrs did not affect osteogenic differentiation (fig.10 a,b). Adipogenic differentiation, however, was not observed in samples exposed to shear stress (fig.10d). Figures 11 and 12 show that NCSCs were able to differentiate into peripheral neurons and Schwann cells even after exposure to laminar fluid shear stress for 66hrs. Similarly, figure 13 (a-f) shows that NCSCs cultured in the myogenic differentiation medium were positive for smooth muscle cells markers: calponin1 (fig.13 a,b), smooth mucle α-actin (fig.13 c,d) and smooth muscle myosin heavy chain(fig.13 e,f) in spite of their prior exposure to laminar fluid shear stress.

Discussion

Laminar shear stress is known to play an important role in normal vascular function, which includes the inhibition of proliferation and inflammation in the vessel wall and the regulation of vessel caliber [24]. Laminar fluid stress is known to affect the function of various cell types including endothelial cells (EC), smooth muscle cells (SMC), mesenchymal stem cells (MSC), neural stem cells (NSC).

In human endothelial cells, laminar shear stress has been found to activate multiple signaling pathways: focal adhesion kinase (FAK), mitogen-activated protein kinase (MAPK), phosphoinositide-3 kinase (PI3-K), Akt and Rho family GTPases, and increases integrin clustering and integrin-ligand binding [25].

Studies on the effects of fluid shear stress on SMC have produced conflicting results. Some studies have claimed that shear stress inhibits proliferation in vitro [26, 27]; yet other studies support the opposite view [28, 29]. The divergence in these conclusions may be due to differences in cell populations, flow patterns and the intensity of shear stress applied on SMCs.

In human bone marrow derived MSCs, shear stress has been shown to activated protein kinase (MAPK) signaling pathways. These pathways are known to play an important role in cellular mechanotransduction. It was also reported that fluid shear stress induced global changes in gene expression in MSCs [30].

NCSCs are an attractive cell source for the development tissue engineered vascular grafts but the effects of laminar shear stress on neural crest stem cells have not yet been investigated. In this study, we set the level of laminar shear stress at 10 dynes/cm^2 because we found that higher levels of shear stress caused NCSCs to detach from the glass slides.

We find that a laminar shear stress of 10 dynes/cm^2 caused an increase in NCSC proliferation and ERK1/2 phosphorylation. It is known that ERK1/2 activation promotes cell proliferation [31]. In addition, we found a significant increase in the gene expression of Krüppel-like factors 4 (Klf4) after 24 hours of exposure to shear stress (SS). Klf4 has been identified as an anti-proliferative shear stress-responsive gene. The over-expression of Klf4 in vascular SMCs has been shown to induce growth arrest [32]. This finding suggests that Klf4 may be expressed in order to attenuate cell proliferation after the first 24 hours. Previous studies have shown that cyclical uniaxial strain increases NCSC proliferation and affects differentiation in a directionally dependent manner [23, 33].

To continue, we observed that laminar shear stress caused an increase in the expression of Calponin1 within the first 24hrs. Gene expression data showed, however, that the transcription of the gene for Calponin1 decreases after the first 24hrs. The increase in Calponin1 expression is therefore only transient. More work will be necessary to elucidate a mechanism behind the activation of Calponin 1 by laminar fluid shear stress.

After 66 hrs of exposure to SS, we observed that NCSCs still expressed their characteristic markers while simultaneously expressing some neurogenic, myogenic, markers without changes in morphology. Despite their prior exposure to SS for 66hrs, NCSCs were still capable of neurogenic, myogenic and osteogenic differentiating. It was only in the case of adipogenic differentiation that prior exposure to SS appeared to have a suppressive effect. It may be possible that exposure to higher levels of fluid shear stress (>10 dynes/cm^2), to different flow profile patterns, or to longer exposure times may abrogate NCSC differentiation potential but more experimentation will be required to verify this hypothesis.

In conclusion, our results show that while exposure to shear stress for a period of 66hrs can promote NCSC proliferation, it is not sufficient to affect the terminal differentiation of these cells. It is possible that higher levels of shear stress, longer exposure times, non-linear shear or oscillatory flow may illicit different behavioral responses from NCSCs. In this case, however, biochemical factors appear to play a stronger role in driving NCSC differentiation. Further investigation of the effects of shear stress on NCSC function will be necessary to provide a stronger rational for the use of these cells in tissue engineering applications.

ACKNOWLEDGMENTS

Many thanks to Dr. Aijun Wang for providing the cell line used in this study.
Thanks to Julia Chu for her assistance with the quantitative PCR analysis.

REFERENCES

1. Dupin, E., et al., *Neural crest progenitors and stem cells.* C R Biol, 2007. **330**(6-7): p. 521-9.
2. Bronner-Fraser, M., *Origins and developmental potential of the neural crest.* Exp Cell Res, 1995. **218**(2): p. 405-17.
3. Crane, J.F. and P.A. Trainor, *Neural crest stem and progenitor cells.* Annu Rev Cell Dev Biol, 2006. **22**: p. 267-86.
4. Woodbury, D., et al., *Adult rat and human bone marrow stromal cells differentiate into neurons.* J Neurosci Res, 2000. **61**(4): p. 364-70.
5. Wong, C.E., et al., *Neural crest-derived cells with stem cell features can be traced back to multiple lineages in the adult skin.* J Cell Biol, 2006. **175**(6): p. 1005-15.
6. Yoshida, S., et al., *Isolation of multipotent neural crest-derived stem cells from the adult mouse cornea.* Stem Cells, 2006. **24**(12): p. 2714-22.
7. Tomita, Y., et al., *Cardiac neural crest cells contribute to the dormant multipotent stem cell in the mammalian heart.* J Cell Biol, 2005. **170**(7): p. 1135-46.
8. Sieber-Blum, M., et al., *Pluripotent neural crest stem cells in the adult hair follicle.* Dev Dyn, 2004. **231**(2): p. 258-69.
9. Kruger, G.M., et al., *Neural crest stem cells persist in the adult gut but undergo changes in self-renewal, neuronal subtype potential, and factor responsiveness.* Neuron, 2002. **35**(4): p. 657-69.
10. Morrison, S.J., et al., *Prospective identification, isolation by flow cytometry, and in vivo self-renewal of multipotent mammalian neural crest stem cells.* Cell, 1999. **96**(5): p. 737-49.
11. Stemple, D.L. and D.J. Anderson, *Isolation of a stem cell for neurons and glia from the mammalian neural crest.* Cell, 1992. **71**(6): p. 973-85.
12. Wang, A., et al., *Induced pluripotent stem cells for neural tissue engineering.* Biomaterials, 2011. **32**(22): p. 5023-32.
13. Lee, G., et al., *Isolation and directed differentiation of neural crest stem cells derived from human embryonic stem cells.* Nat Biotechnol, 2007. **25**(12): p. 1468-75.
14. Lee, G., et al., *Derivation of neural crest cells from human pluripotent stem cells.* Nat Protoc, 2010. **5**(4): p. 688-701.
15. Wang, A., et al., *Derivation of smooth muscle cells with neural crest origin from human induced pluripotent stem cells.* Cells Tissues Organs, 2012. **195**(1-2): p. 5-14.
16. Adamo, L., et al., *Biomechanical forces promote embryonic haematopoiesis.* Nature, 2009. **459**(7250): p. 1131-5.
17. North, T.E., et al., *Hematopoietic stem cell development is dependent on blood flow.* Cell, 2009. **137**(4): p. 736-48.
18. Bai, H. and Z.Z. Wang, *Directing human embryonic stem cells to generate vascular progenitor cells.* Gene Ther, 2008. **15**(2): p. 89-95.

19. Shimizu, N., et al., *Cyclic strain induces mouse embryonic stem cell differentiation into vascular smooth muscle cells by activating PDGF receptor beta.* J Appl Physiol, 2008. **104**(3): p. 766-72.
20. Metallo, C.M., et al., *The response of human embryonic stem cell-derived endothelial cells to shear stress.* Biotechnol Bioeng, 2008. **100**(4): p. 830-7.
21. Yamamoto, K., et al., *Fluid shear stress induces differentiation of Flk-1-positive embryonic stem cells into vascular endothelial cells in vitro.* Am J Physiol Heart Circ Physiol, 2005. **288**(4): p. H1915-24.
22. Blatnik, J.S., G.W. Schmid-Schonbein, and L.A. Sung, *The influence of fluid shear stress on the remodeling of the embryonic primary capillary plexus.* Biomech Model Mechanobiol, 2005. **4**(4): p. 211-20.
23. Li, X., et al., *Uniaxial mechanical strain modulates the differentiation of neural crest stem cells into smooth muscle lineage on micropatterned surfaces.* PLoS One, 2011. **6**(10): p. e26029.
24. Cunningham, K.S. and A.I. Gotlieb, *The role of shear stress in the pathogenesis of atherosclerosis.* Lab Invest, 2005. **85**(1): p. 9-23.
25. Park, J.S., et al., *Mechanobiology of mesenchymal stem cells and their use in cardiovascular repair.* Front Biosci, 2007. **12**: p. 5098-116.
26. Ueba, H., M. Kawakami, and T. Yaginuma, *Shear stress as an inhibitor of vascular smooth muscle cell proliferation. Role of transforming growth factor-beta 1 and tissue-type plasminogen activator.* Arterioscler Thromb Vasc Biol, 1997. **17**(8): p. 1512-6.
27. Civelek, M., et al., *Smooth muscle cells contract in response to fluid flow via a Ca2+-independent signaling mechanism.* J Appl Physiol, 2002. **93**(6): p. 1907-1917.
28. Haga, M., et al., *Oscillatory shear stress increases smooth muscle cell proliferation and Akt phosphorylation.* J Vasc Surg, 2003. **37**(6): p. 1277-84.
29. Shigematsu, K., et al., *Direct and indirect effects of pulsatile shear stress on the smooth muscle cell.* Int Angiol, 2000. **19**(1): p. 39-46.
30. Glossop, J.R. and S.H. Cartmell, *Effect of fluid flow-induced shear stress on human mesenchymal stem cells: differential gene expression of IL1B and MAP3K8 in MAPK signaling.* Gene Expr Patterns, 2009. **9**(5): p. 381-8.
31. Mebratu, Y. and Y. Tesfaigzi, *How ERK1/2 activation controls cell proliferation and cell death: Is subcellular localization the answer?* Cell Cycle, 2009. **8**(8): p. 1168-75.
32. Autieri, M.V., *Kruppel-like factor 4: transcriptional regulator of proliferation, or inflammation, or differentiation, or all three?* Circ Res, 2008. **102**(12): p. 1455-7.
33. Li, X., et al., *Anisotropic effects of mechanical strain on neural crest stem cells.* Ann Biomed Eng, 2012. **40**(3): p. 598-605.

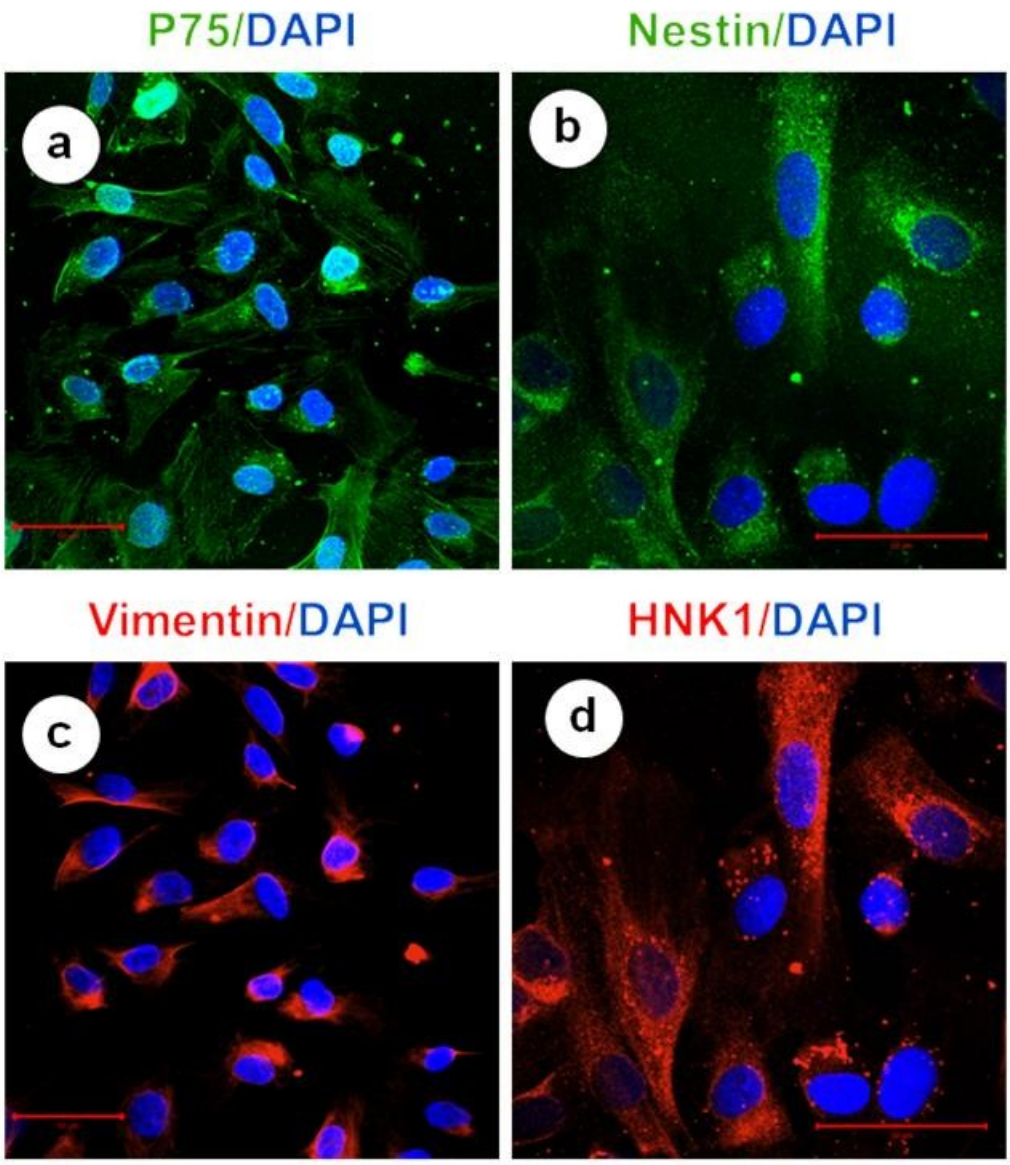

FIGURE 1. Characterization of NCSCs derived from iPSCs. Immunofluorescent staining of NCSC markers (a) P75, (b) Nestin, (c) Vimentin, and (d) HNK1. Nuclei were stained with DAPI in blue. Scale bar = 100 μm.

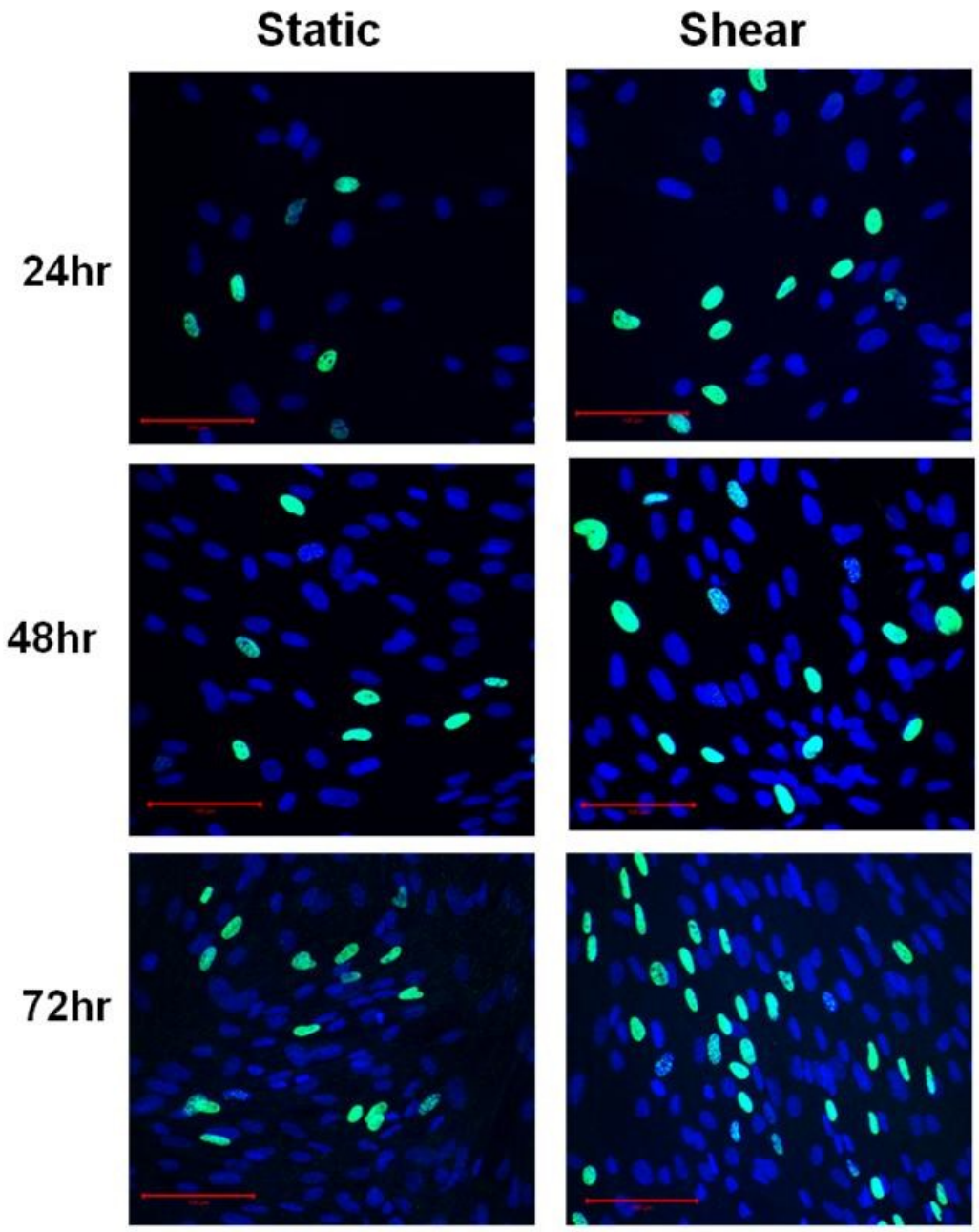

FIGURE 2. Effects of fluid shear stress on the proliferation of NCSCs derived from iPSCs.
NCSCs were subjected to a fluid shear stress of 10 dyn/cm^2 or kept as static controls. Fluorescent double-staining of cells in S-phase (in green) and nuclei (Hoechst staining in blue). Scale bar = 100 μm.

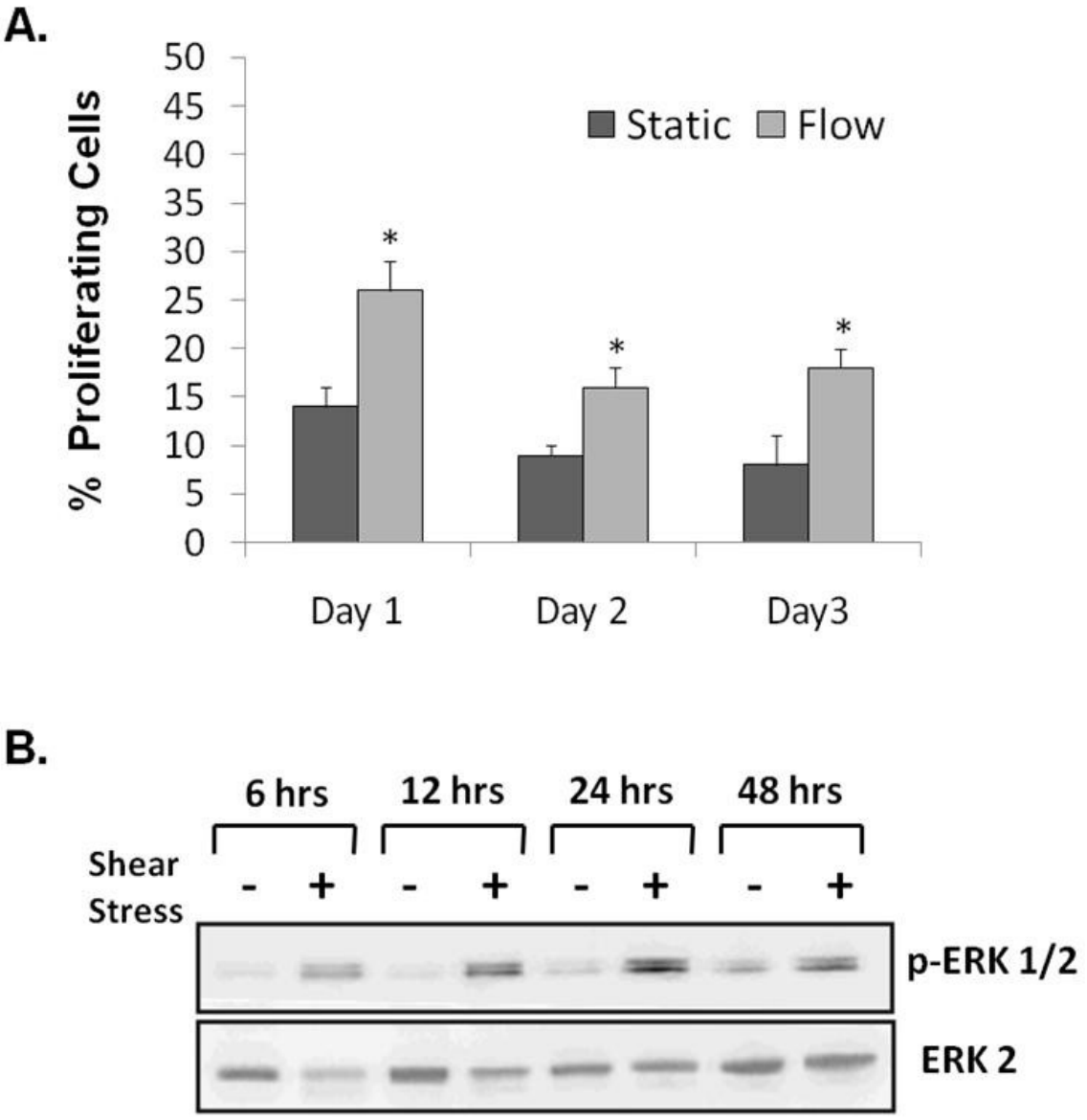

FIGURE 3. Effects of fluid shear stress on NCSC proliferation. NCSCs were subjected to a fluid shear stress of 10 dyn/cm^2 or kept as static controls. (A) Statistical analysis of cell proliferation. Bars represent mean + standard deviation (SD) of the percentage of EdU-positive cells quantified from three independent experiments. Significant difference compared to static control was determined by a Student's t-test. *indicates $p < 0.05$ ($n = 3$). (B) Immunoblotting analysis of p-ERK1/2 and ERK2 expression.

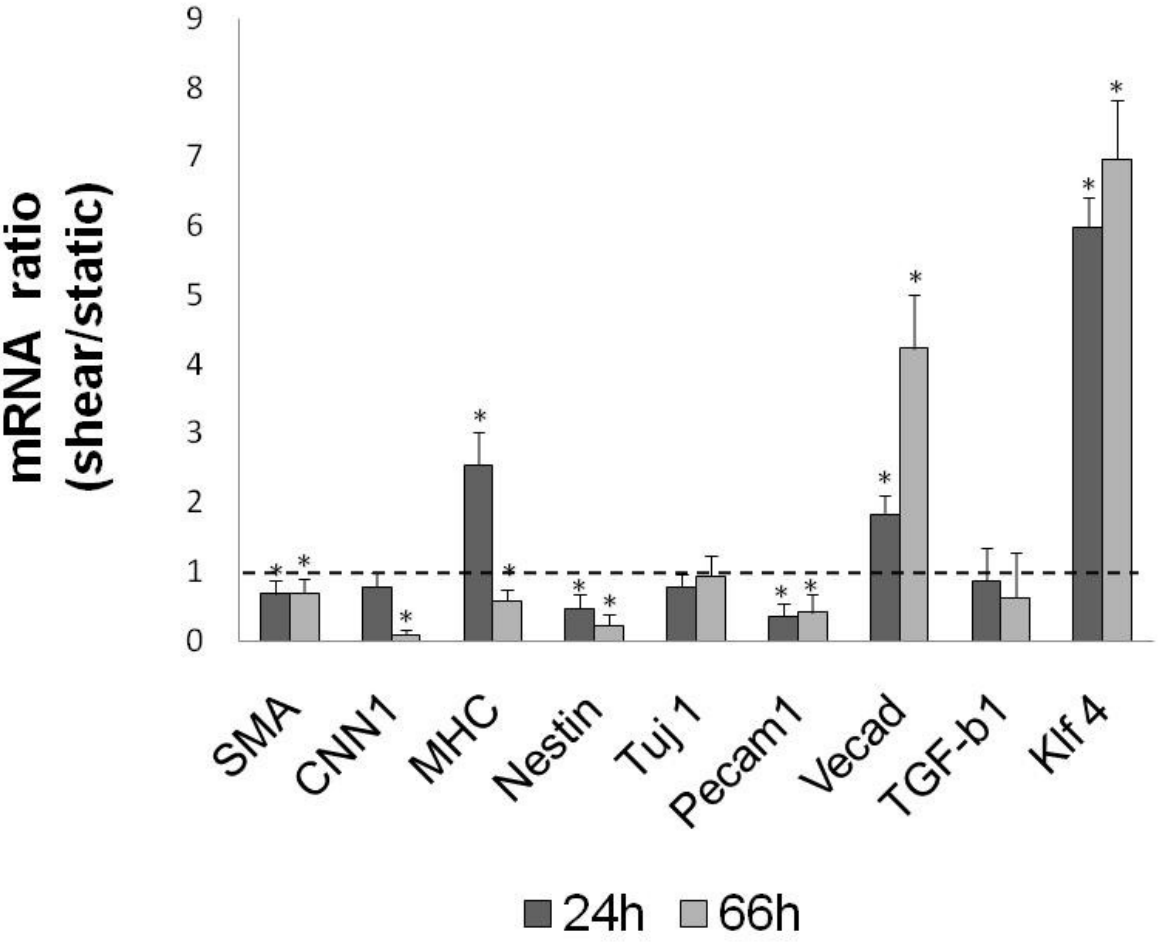

FIGURE 4. Effects of fluid shear stress on the gene expression in NCSCs derived from iPSCs.

NCSCs were subjected to a shear stress of 10 dyn/cm^2 or kept as static controls. qRT-PCR shows the expression of selected genes . SMA: smooth muscle α-actin; CNN1:calponin1; MHC: myosin heavy chain; Nestin ;TUJ1: class-III b-tubulin;
Pecam 1: platelet endothelial cell adhesion molecule (CD31);
Vecad: vascular endothelial cadherin (CD144); TGF- β1: transforming growth factor β1; Klf4: Krüppel-like factors 4.
Bars represent mean + standard deviation (SD). Significant difference compared to static control was determined by using log-transformed one-sample t-test. *indicates $p < 0.05$ ($n = 3$).

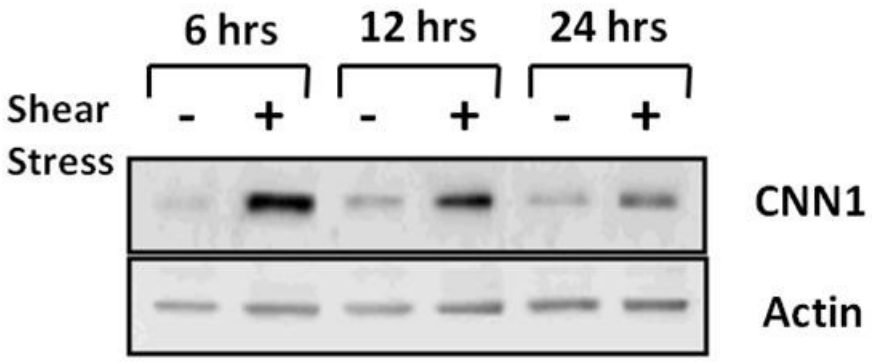

FIGURE 5. Effects of fluid shear stress on Calponin 1 expression of NCSCs derived from iPSCs.
Immunoblotting analysis showing calponin1 (CNN1) protein expression. The level of total actin was used to verify equal loading.

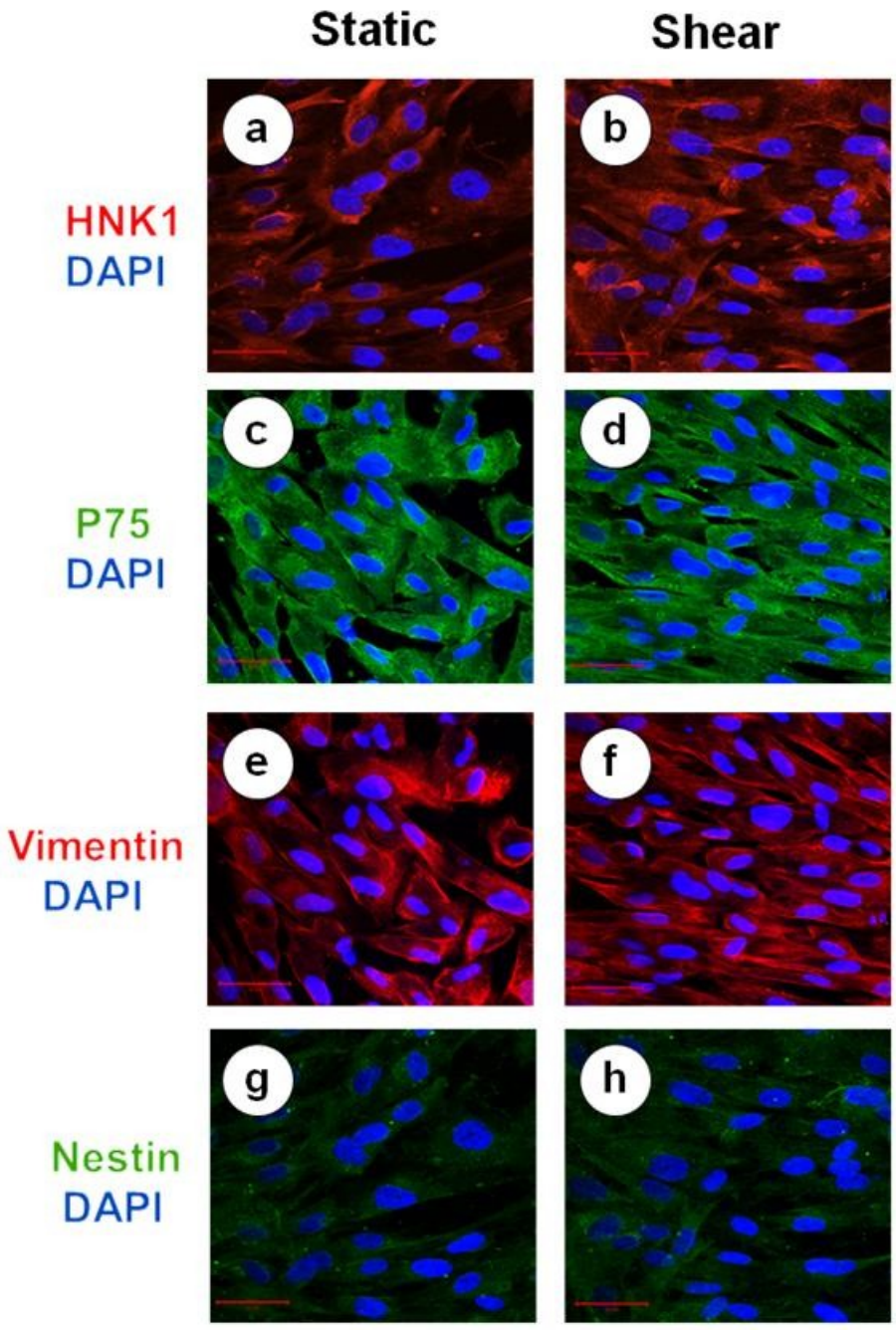

FIGURE 6. Effects of fluid shear stress on the protein expression of NCSCs derived from iPSCs.
NCSCs were subjected to a shear stress of 10 dyn/cm^2 (b,d,f,h) or kept as static controls for 66hrs (a,c,e,g). Immunofluorescent staining of NCSC markers: HNK1(a,b), p75(c,d), Vimentin (e,f), and Nestin (g,h). Nuclei were stained with DAPI in blue. Scale bar = 100 μm

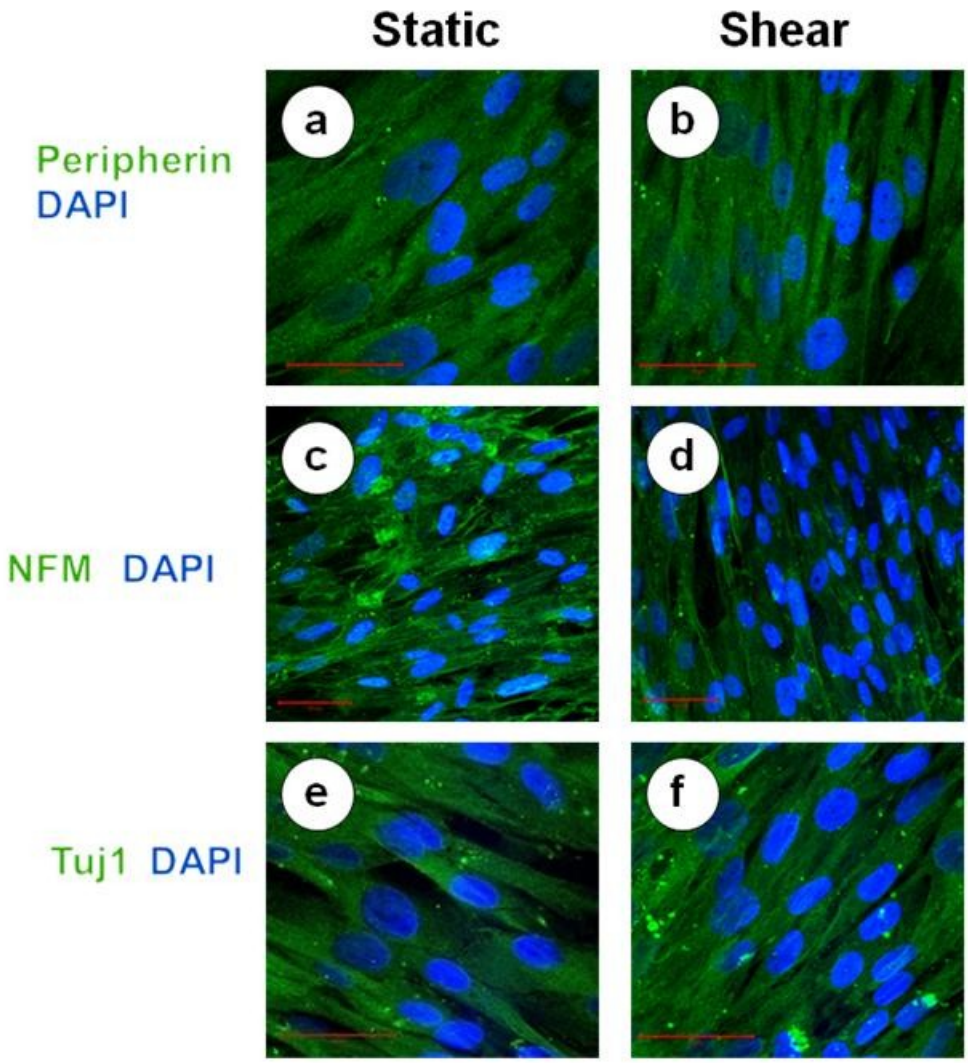

FIGURE 7. Effects of fluid shear stress on the protein expression of NCSCs derived from iPSCs.
NCSCs were subjected to a shear stress of 10 dyn/cm^2 (b,d,f) or kept as static controls for 66hrs (a,c,e). Immunofluorescent staining of peripheral neuron markers: Peripherin (a,b), NFM (c,d) and Tuj1(e,f). Nuclei were stained with DAPI in blue. Scale bar = 100 μm

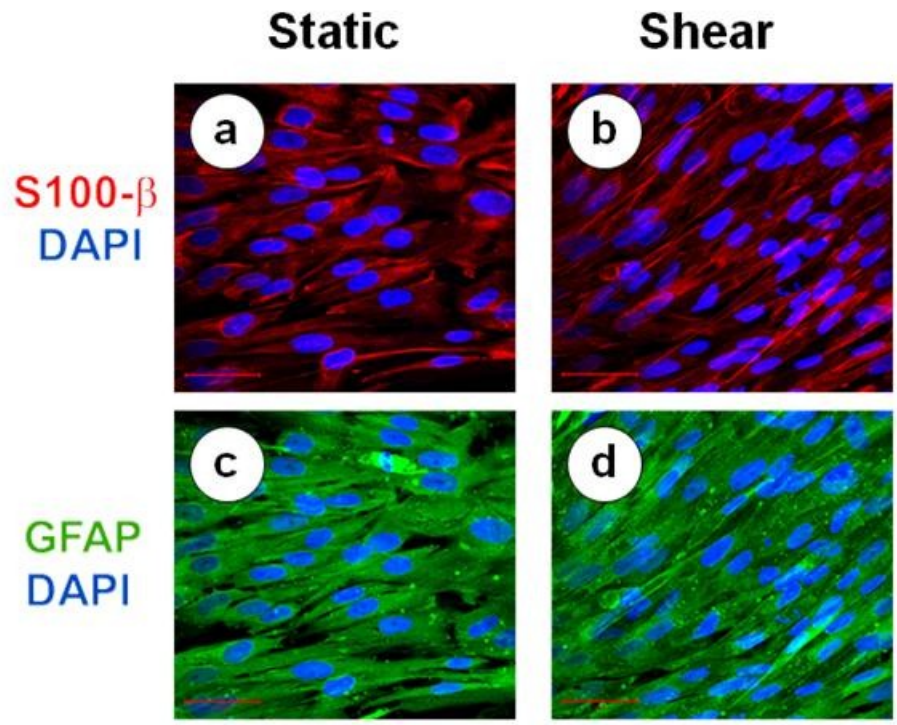

FIGURE 8. Effects of fluid shear stress on the protein expression of NCSCs derived from iPSCs.
NCSCs were subjected to a shear stress of 10 dyn/cm² (b,d,f) or kept as static controls for 66hrs (a,c,e). Immunofluorescent staining of Schwann cell markers:S100-β (a,b) and GFAP (c,d). Nuclei were stained with DAPI in blue. Scale bar = 100 μm

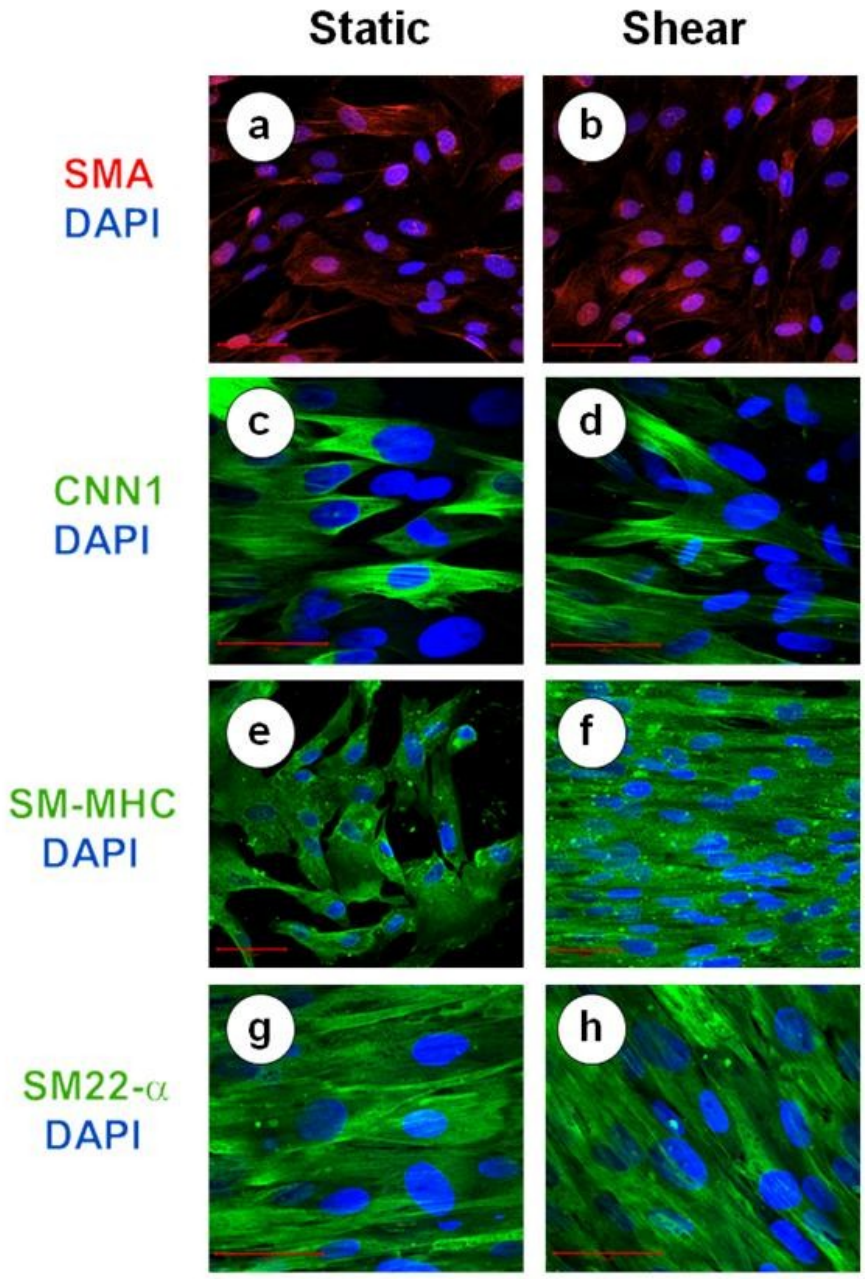

FIGURE 9. Effects of fluid shear stress on the protein expression of NCSCs derived from iPSCs.
NCSCs were subjected to a shear stress of 10 dyn/cm² (b,d,f,h) or kept as static controls for 66hrs (a,c,e,g). Immunofluorescent staining of smooth muscle cell markers: smooth mucle α-actin (a,b), Calponin1 (c,d), Smooth muscle myosin heavy chain(e,f), and SM22α (g,h). Nuclei were stained with DAPI in blue. Scale bar = 100 μm

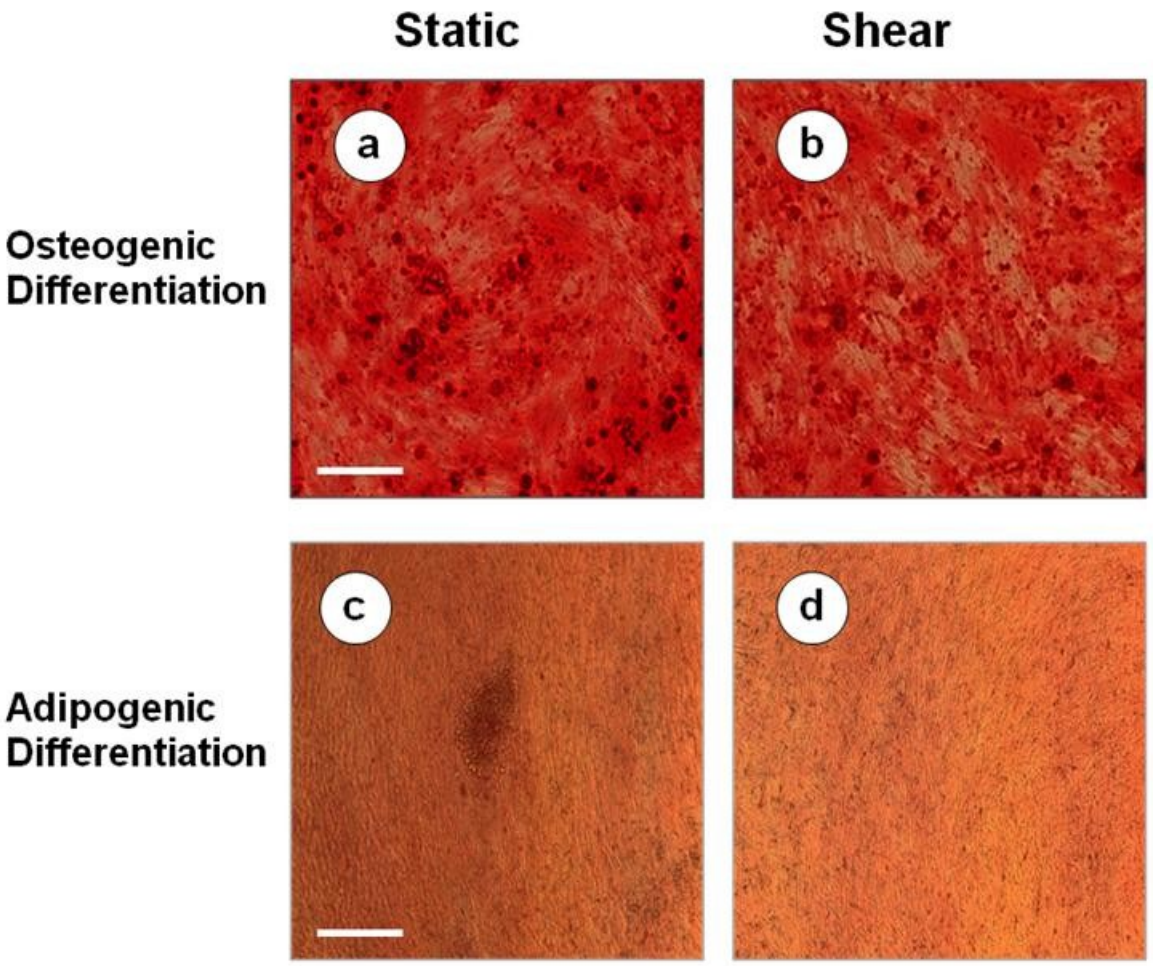

FIGURE 10. Effects of fluid shear stress on the osteogenic and adipogenic differentiation of NCSCs derived from iPSCs. NCSCs were subjected to a fluid shear stress of 10 dyn/cm^2 (b,d) or kept as static controls (a,c) for 66hrs and subsequently cultured in osteogenic differentiation medium for 14 days (a,b) or adipogenic differentiation medium for 30 days . Alizarin red staining (a,b) ; Oil red staining (c,d). Scale bar = 200 μm.

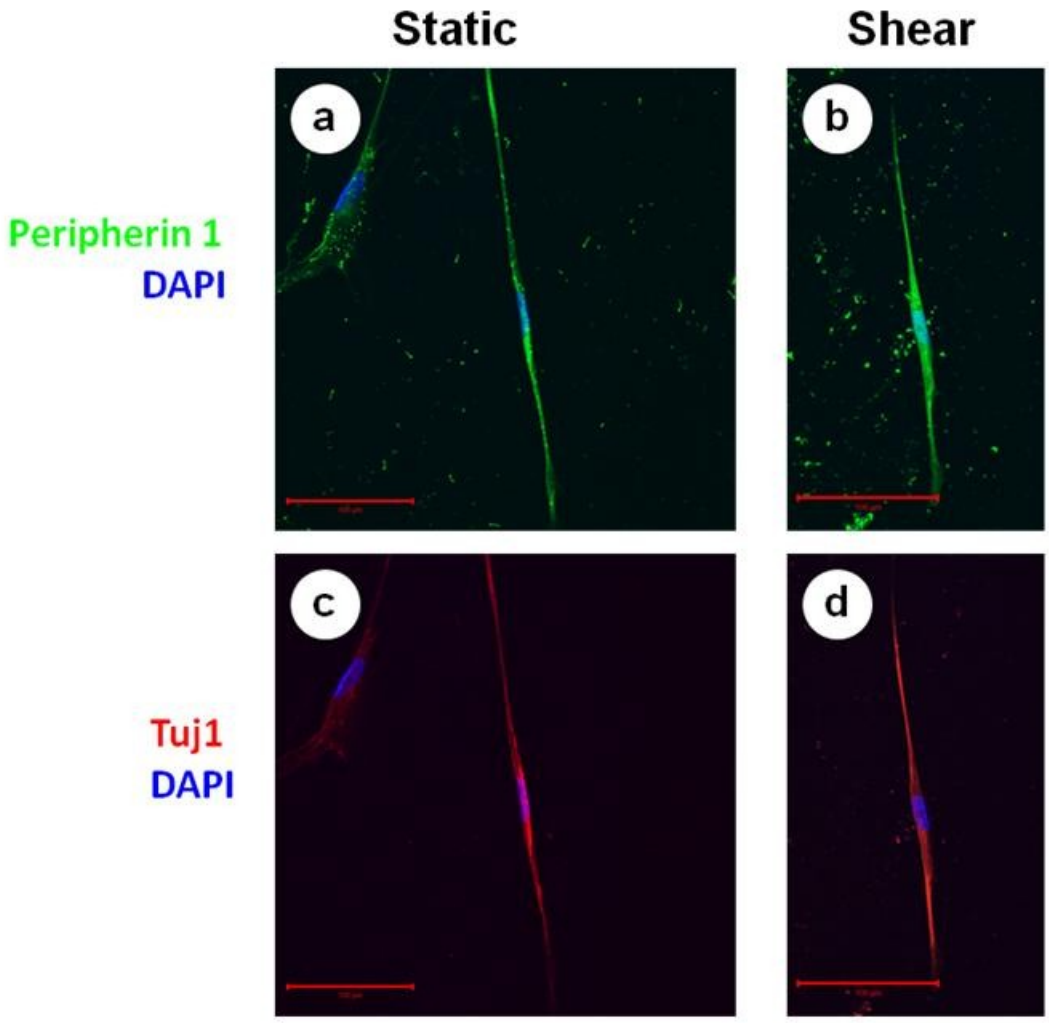

FIGURE 11. Effects of fluid shear stress on the neurogenic differentiation of NCSCs derived from iPSCs.
NCSCs were subjected to a fluid shear stress of 10 dyn/cm² (b,d) or kept as static controls (a,c) for 66hrs and subsequently cultured in peripheral nerve differentiation medium for 14 days.
Immunofluorescent staining of peripheral neuron markers: Peripherin (a,b), Tuj1 (c,d).
Nuclei were stained with DAPI in blue. Scale bar = 100 μm

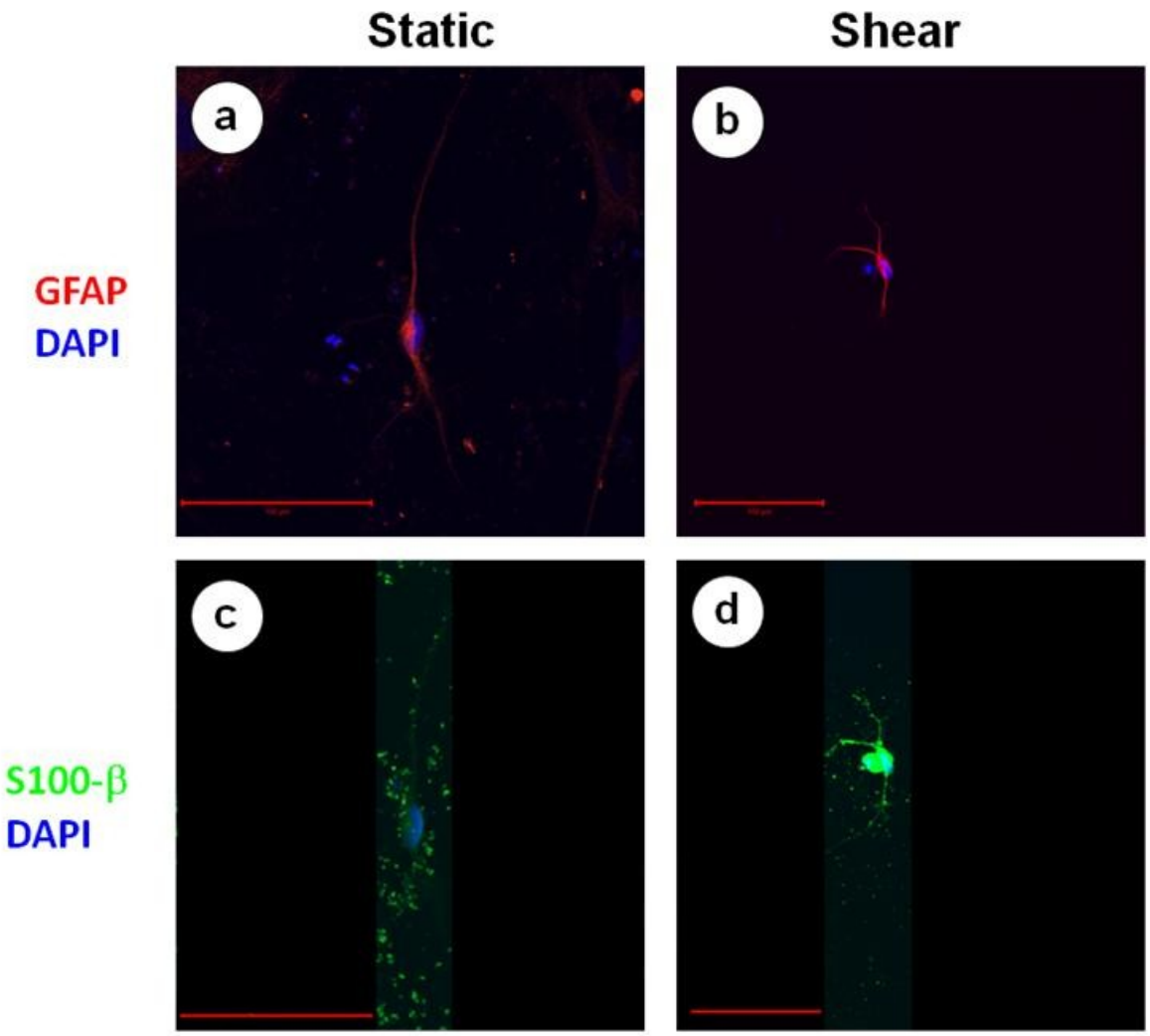

FIGURE 12. Effects of fluid shear stress on Schwann cell differentiation of NCSCs derived from iPSCs.
NCSCs were subjected to a fluid shear stress of 10 dyn/cm^2 (b,d) or kept as static controls (a,c) for 66hrs and subsequently cultured in schwann cell differentiation medium for 14 days. Immunofluorescent staining of schwann cell markers: GFAP (a,b), S100-β (c,d). Nuclei were stained with DAPI in blue. Scale bar = 100 μm

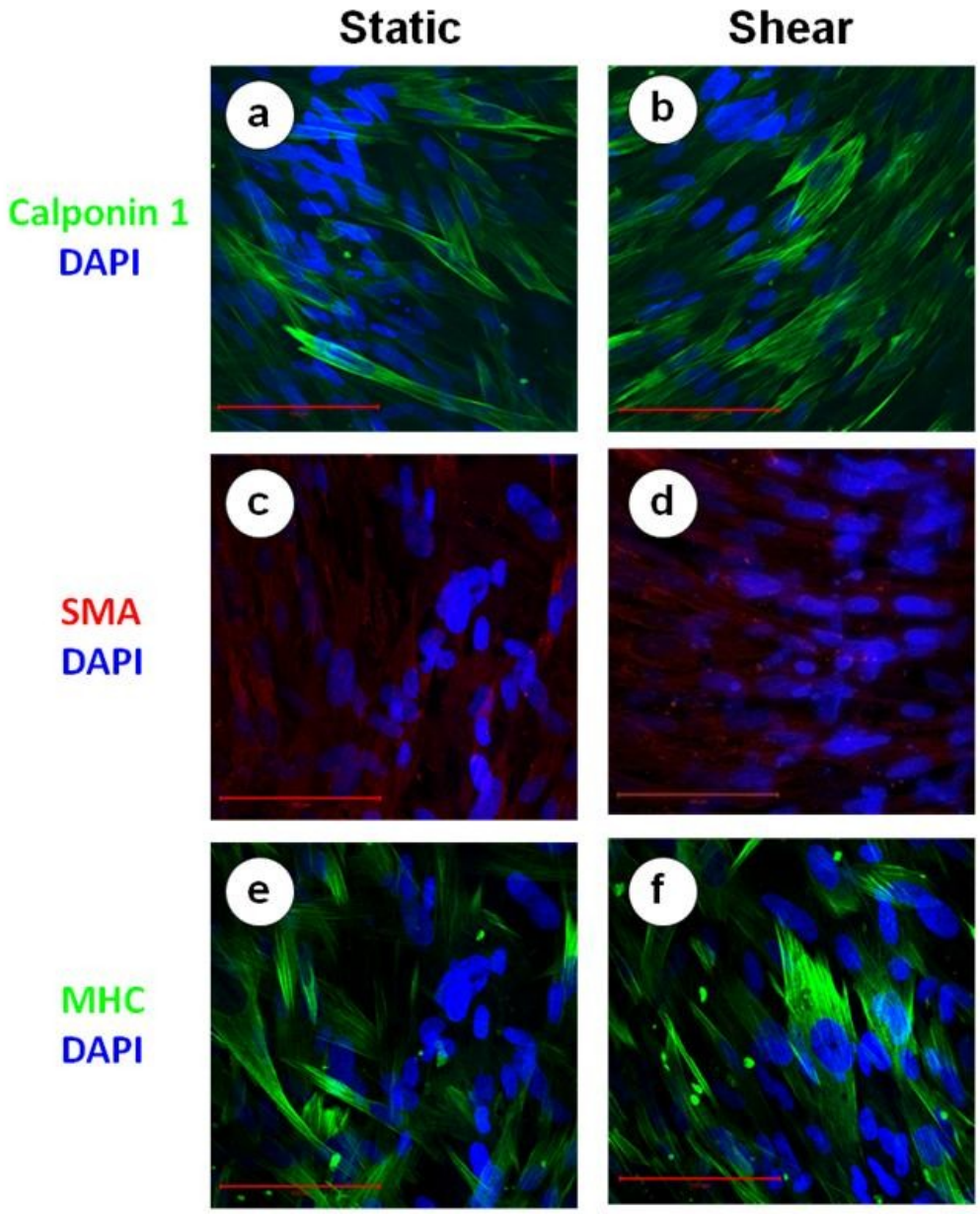

FIGURE 13. Effects of fluid shear stress on the myogenic differentiation of NCSCs derived from iPSCs.
NCSCs were subjected to a fluid shear stress of 10 dyn/cm^2 (b,d) or kept as static controls (a,c) for 66hrs and subsequently cultured in DMEM + 10% FBS for 30 days. Immunofluorescent staining of smooth muscle cell markers: Calponin1 (a,b), smooth mucle α-actin SMA (c,d), myosin heavy chain MHC (e,f). Nuclei were stained with DAPI in blue. Scale bar = 100 μm

Chapter 4

Effects of Laminar Fluid Shear Stress on Multipotent Vascular Stem Cell Function

Abstract

Abstract—Multipotent vascular stem cells (MVSCs) are a population of adult stem cells that have recently been discovered in the medial layer of blood vessels. MVSCs have been shown to give rise to a variety of cell types including: Schwann cells, peripheral neurons, smooth muscle cells, adipocytes, chondrocytes and osteocytes. Presently, little is known about the effects of laminar fluid shear stress on MVSC function. In this study, multipotent vascular stem cells were isolated from rat carotid arteries by passive migration. These cells were then expanded without differentiation and exposed to a laminar fluid shear stress of 6 dynes/cm^2. It was found that laminar fluid shear stress increased rat MVSC proliferation and ERK1/2 phosphorylation in a time-dependent manner. Fluid shear stress also caused a decrease in the gene expression of smooth muscle cell markers and an increase in the gene expression of osteoblastic differentiation markers. In addition, we observed that prior exposure to fluid shear stress for 3 days did not affect myogenic, osteogenic or schwann cell differentiation in MVSCs. Further investigation into the effects of mechanical stimulation on the function of MVSCs will be necessary to provide a rational basis for the use of these cells in tissue engineering applications

Keywords—multipotent vascular stem cells, laminar fluid shear stress, differentiation, proliferation.

Introduction

In disease states such as atherosclerosis, intimal hyperplasia and restenosis, it is thought that smooth muscle cells migrate from the medial layer of the blood vessels to the intimal layer. There, smooth muscle cells proliferate and contribute to intimal thickening. It has long been thought that the de-differentiation of mature and contractile smooth muscle cells into proliferative and synthetic smooth muscle cells was involved in these pathological conditions [1, 2]. Contrarily to this generally accepted theory, some have argued that a distinct population of smooth muscle cells within the vessel wall is involved in this phenomenon [3, 4] . This paradigm has once again been called into question by a recent study by Tang et al [5]. The study identified a novel population of adult stem cells within the medial layer of the blood vessel. These cells named "multipotent vascular stem cells" (MVSCs) are positive for Sox10, Sox17, neural crest cell markers, general MSC makers but negative for EC markers. MVSCs express low levels of SMA but do not express SM-MHC or Calponin1. In addition, MVSCs have the potential to differentiate into Schwann cells, peripheral neurons, adipocytes, chondrocytes, osteocytes and mature smooth muscle cells. Furthermore, it was reported that MVSCs are not derived from SMCs. The study also showed that, in vivo, MVSCs become proliferative and contribute significantly to vascular remodeling in response to injury [5]. The effects of fluid shear stress on MVSC function, however, have not yet been examined. In this study, we observed how laminar fluid shear stress affects the differentiation and proliferation of rat MVSCs. Our results showed that laminar fluid shear stress increased the proliferation of vascular stem cells but had negligible effects on their terminal differentiation.

Materials and Methods

Multipotent Vascular Stem Cells Isolation and Cell Culture.

The following protocol was previously described in Tang et al.[5] Segments of tissue were obtained from the carotid arteries of SD rats and were washed three times in phosphate buffered saline (PBS) with 1% penicillin/streptomycin (Invitrogen Co., Carlsbad, CA.) The connective tissue and adventitia were removed by dissection. The endothelial layer was scraped off with a scalpel. The tunica media was then washed three times in PBS with 1% penicillin/streptomycin and cut into mm size squares, which were placed in 6-well plates coated with 1% CellStart (Invitrogen). This tissue culture method relied on the migration and subsequent proliferation of cells out of the tissue. Migratory cells were cultured in a maintenance medium composed of DMEM with 2% chick embryo extract (MP Biomedical), 1% FBS, 1% N2 (Invitrogen), 2% B27 (Invitrogen), 100 nM retinoic acid (Sigma-Aldrich), 50 nM 2-mercaptoethanol (Sigma-Aldrich), 1% P/S and 20 ng/ml bFGF (R&D Systems.)

Cell Seeding Prior to Shear Stress Experiments

Autoclaved glass slides (Erie Scientific, Portsmouth, NH) were exposed to ultraviolet (UV) light for 1 hour for sterilization. Slides were then coated with 2% gelatin (Sigma Aldrich, St. Louis, MO) and placed under UV light for 1 hour at room temperature to allow for protein adsorption before being washed with sterile phosphate buffered saline (PBS, pH 7.4). Rat MVSC were seeded onto the gelatin-coated slides at approximately 50% confluency. The cells were allowed to grow to 80% confluency in the maintenance medium described previously.

Fluid Shear Stress Experiments

Laminar fluid shear stress was applied to MVSCs using a parallel-plate flow chamber. Glass slides seeded with MVSCs were mounted on a rectangular flow channel created by sandwiching a silicone gasket between the glass slide and a polycarbonate flow chamber base. MVSCs were subjected to a laminar shear stresses of 6 dynes/cm^2 for 66 hours (unless otherwise specified). The circulating media contained Dulbecco's modified Eagle's medium (DMEM) with 10% fetal bovine serum (FBS) and supplemented with 1% penicillin-streptomycin (Invitrogen Co., Carlsbad, CA). Culture medium was circulated throughout the system using a peristaltic pump. All shear stress experiments included static controls: MVSCs cultured on glass slides were kept under static condition in the same incubator.
The flow system was set up in a humidified cell culture incubator (37 ºC, 5 %CO_2).

Materials and Methods

Multipotent Vascular Stem Cells Differentiation

This protocol was previously described and slightly modified from Wang et al [6].

For MVSC differentiation into Schwann cells, MVSCs were cultured for 1 week in N2 medium supplemented with 10 ng/ml ciliary neurotrophic factor (R&D Systems Inc., Minneapolis, MN.), 10 ng/ml bFGF (Invitrogen Corp. Carlsbad, CA), 1 mM dibutyryl-cAMP (Sigma-Aldrich Corp., St. Louis, MO) and 20 ng/ml neuregulin1b (R&D Systems Inc., Minneapolis, MN).

For MVSC differentiation into peripheral neurons, MVSCs were cultured for 1 week in N2 medium supplemented with 20 ng/ml brain-derived neurotrophic factor (R&D Systems Inc., Minneapolis, MN.), 10 ng/ml nerve growth factor (R&D Systems Inc., Minneapolis, MN.), 10 ng/ml glial cell line-derived neurotrophic factor (R&D Systems Inc., Minneapolis, MN.) and 1 mM dibutyryl-cAMP (Sigma-Aldrich Corp., St. Louis, MO.)

For MVSC differentiation into SMC lineage, MVSCs were cultured for 10 days in Minimum Essential Medium α Medium (Invitrogen Corp. Carlsbad, CA) containing 10% Fetal Bovine Serum(Invitrogen Corp., Carlsbad, CA) with 10 ng/ml TGF-b1 (Pepro Tech Inc., Rocky Hill, NJ).

For adipogenic differentiation, confluent MVSCs were treated with 10 mg/ml insulin (Sigma-Aldrich Corp., St. Louis, MO), 1 mM dexamethasone (Sigma-Aldrich Corp., St. Louis, MO) and 0.5 mM isobutylxanthine (Sigma-Aldrich Corp., St. Louis, MO) in α MEM medium containing 10% FBS for 3 weeks.

For osteogenic differentiation, MVSCs were seeded at a low density (10^3 cells/cm2) and grown in α MEM medium containing 10% FBS for 2 weeks in the presence of 10 mM b-glycerol phosphate (Sigma-Aldrich Corp. St. Louis, MO), 0.1 mM dexamethasone and 200 mM ascorbic acid (Sigma-Aldrich Corp. St. Louis, MO).

Immunofluorescent Staining and Confocal Microscopy

MVSCs were fixed with 4% paraformaldehyde in PBS for 15 min, permeabilized with 0.5% Triton X-100 in PBS for 10 min, and blocked with 1% BSA for 30 min. The samples were incubated overnight at 4^{o} C with primary antibodies, followed by incubation with the appropriate secondary antibodies for 1hr. For nuclear staining, samples were incubated in PBS with DAPI for 5 min (Invitrogen Corp., Carlsbad CA).
We used a Zeiss LSM 510 confocal microscope to capture multiple *Z*-sections for each sample (0.2 to 0.4 μm thick sections over a range of 20 μm). These sections were subsequently integrated to create maximum intensity projections of each sample using the LSM browser imaging software.
To characterize MVSCs, the following primary antibodies were used: Sox10 (MAB2864, R&D Systems Inc., Minneapolis, MN.) , Sox 17 (MAB1924, R&D Systems Inc., Minneapolis, MN.), S100β (S2532, Sigma-Aldrich Corp.), p75 (AB10494, Abcam Inc.,

Materials and Methods

Cambridge, MA), HNK1 (C6680, Sigma-Aldrich Corp., St. Louis, MO), vimentin (M0725, Dako North America Inc., Carpinteria, CA) nestin (AB5988,Abcam Inc. Cambridge, MA), Neural filament M (NFM, N4142, Sigma-Aldrich Corp., St. Louis MO.) calponin 1 (CNN1;1806-1, Epitomics Inc., Burlingame, CA), smooth muscle α-actin (SMA; A2547, Sigma-Aldrich Corp., St. Louis MO.), Myosin Heavy Chain (MHC, Sc-6956, Santa Cruz Biotechnology, Santa Cruz CA.), SM22-α (AB14106, Abcam Inc., Cambridge, MA), VE-cadherin (Sc-6458, Santa Cruz Biotechnology, Santa Cruz CA.) and CD31 (MAB1393, Millipore Corp.,Billerica, MA.)
For differentiation into Schwann cells, cells were immunostained for Schwann cell markers S100β (S2532, Sigma-Aldrich Corp.) and glial fibrillary acidic protein (GFAP; AB5804, Millipore Corp., Billerica, MA.)
For differentiation into peripheral neurons, cells were immunostained for peripheral neuron markers peripherin (AB1530, Millipore Corp., Billerica, MA), vimentin (M0725, Dako North America Inc., Carpinteria, CA), class-III β -tubulin (Tuj1, MAB1637, Millipore Corp., Billerica, MA) and neural filament M (NFM, N4142, Sigma-Aldrich Corp., St. Louis MO.)
For differentiation into smooth muscle cells, cells were immunostained with smooth muscle markers calponin 1 (CNN1;1806-1, Epitomics Inc., Burlingame, CA), smooth muscle α-actin (SMA; A2547, Sigma-Aldrich Corp., St. Louis MO.) and Myosin Heavy Chain (MHC, Sc-79079 Santa Cruz Biotechnology, Santa Cruz CA.)
To verify adipogenic differentiation, samples were stained with Oil red.
For osteogenic differentiation, cells were fixed in 4% paraformaldehyde, and stained with Alizarin red.

Protein isolation and Immunoblotting

Cells were lysed with 150 μL of RIPA buffer (25 mM Tris (pH 7.4), 0.5 M NaCl, 1% TritonX-100, 0.1% SDS, 1 mM PMSF, 10 lg/mL leupeptin, and 1 mM Na3VO4). The protein samples were then centrifuged to isolate the supernatant. The protein concentration in all samples was quantified using DC Protein Assay (Biorad, Hercules, CA).
Protein samples were prepared in SDS sample buffer (2% SDS, 10% (v/v) glycerol, 60 mM Tris, and 0.05% (v/v) mercaptoethanol) and boiled for 5 min prior loading onto 10% SDS-PAGE gels. After electrophoresis, the separated proteins were transferred onto a nitrocellulose membrane (Biorad, Hercules, CA.) The membrane was blocked with Tris-buffered saline containing 3% non-fat powdered milk for 1 h and then incubated with the primary antibody in Tris-buffered saline-Tween overnightat 4 °C. The blots were subsequently washed in Tris-buffered saline-Tween and then incubated with an appropriate horseradish peroxidase-conjugated secondary antibody in Tris-buffered saline-Tween. Proteins were visualized using enhanced chemiluminescence (Biorad, Hercules, CA.) Image analysis was performed with the Image J software package (NIH).

Materials and Methods

RNA Isolation and Quantitative Polymerase Chain Reaction (qPCR)

Each cell sample was lysed with 1 ml of Trizol (Invitrogen Corp., Carlsbad, CA) RNA was extracted by using chloroform and phenol extractions, precipitated by isopropanol, and the resulting RNA pellet was washed with 75% ethanol. RNA pellets were resuspended in 20 ml DEPC-treated water and were quantified with RiboGreen RNA Quantification Kit (Invitrogen Corp. Carlsbad, CA). cDNA was synthesized by using two-step reverse transcription (RT) with the ThermoScript RT-PCR system (Invitrogen Corp. Carlsbad, CA), followed by qPCR using SYBR green reagent and the ABI Prism 7000 Sequence Detection System (Life Tech Corp., Carlsbad, CA). Primers for the genes of interest were designed with the ABI Prism Primer Express™ software v.2.0 (Applied Biosystems, Foster City, CA) and are listed in table1.
The gene expression of each sample was normalized to the level of 18S ribosomal RNA in the sample. Results were analyzed with ABI Prism 7000 SDS software (Life Tech Corp., Carlsbad, CA.)

TABLE 1. Primers for qPCR.

Gene name	Forward primer (5'–3')	Reverse primer (5'–3')
Sox10	CTGGAGGTTGCTGAACGAGAGT	GTCCGGATGGTCTTTTTTGTG
SMA	TCCTGACCCTGAAGTATCCGATA	GGTGCCAGATCTTTTCCATGTC
CNN1	AGAACAAGCTGGCCCAGAAA	CACCCCTTCGATCCACTCTCT
MHC	TTCCGGCAACGCTACGA	TCCATCCATGAAGCCTTTGG
SM22-α	CACAAACGACCAAGCCTTTTC	CACGGCTCATGCCATAGGAT
MYCD	TCTTACAGTTACGGCTTCAACAGAGA	CCTCGGGTCATGGAACTCA
S100-β	CTGTCTACCCTCCTAGTCCTTGGA	GAGGCTCCTGGTCACCTTTTG
TUJ1	GGGAGATCGTGCACATCCA	CTATGCCATGCTCGTCACTGA
NFM	TCGAGTCGGTGCGAGGCACT	AGCTGCTGGATGGTGTCCTGGTAG
KLF4	GGCCCAGCTACCCTCCTTT	GCATGAGCTCTTGATAATGGAGAGA
BGLAP	GCAGACCTAGCAGACACCATGA	AGGTCAGAGAGGCAGAATGCA
Cbfa1	TCAATGGTTGGGAGAGAAGCA	CCTTCTGCACCTCCTTTAGCA
18S rRNA	GCCGCTAGAGGTGAAATTCTTG	CATTCTTGGCAAATGCTTTCG

Materials and Methods

Cell Proliferation Assay

After exposure to laminar fluid shear stress, MVSCs were fixed with 4% para-formaldehyde for 15 min, washed twice with 3% BSA in PBS and permeabilized with 0.5% Triton X-100 for 20 min. After washing with 3%BSA in PBS, samples were incubated in a 10μM Edu reaction cocktail prepared following the Click-iT™ EdU Imaging Kit (Invitrogen Corp., Carlsbad, CA). After 30 minutes of incubation in the dark, the stained samples were washed again with 3%BSA in PBS. Samples were subsequently incubated for 30 minutes in 5μg/ml Hoechst solution for nuclear staining. Images were captured on a Zeiss LSM 510 confocal microscope. For each sample, the percentage of proliferating cells was calculated by averaging the percentage of EdU-positive cells over randomly selected viewing fields. Three independent experiments were carried out.

Statistical Analysis

For all data, we first performed an analysis of variance (ANOVA) to determine statistical significance.
For the proliferation data, significant difference compared to static control was determined by a Student's t-test ($p < 0.05$.)
For qPCR data, significant difference compared to static control was determined by using log-transformed one-sample t-test ($p < 0.05$.).

Results

Characterization of MVSCs.

Figures 1 through 4 illustrate that MVSCs were positive for the following markers: sox10, sox17, vimentin, nestin, p75, S100-β, peripherin, neural filament M (NFM) and SM22α. Figures 1 through 4 also show that MVSC did not express calponin1 (CNN1), myosin heavy chain (MHC), glial fibrillary acidic protein (GFAP), HNK1, class-III β-tubulin (Tuj1) or platelet endothelial cell adhesion molecule (CD31). In addition, figure 4 indicates that MVSCs express low levels of smooth muscle α–actin (SMA). It should be noted that α–actin was not organized in stress fibers in MVSCs. To continue, MVSCs were able to differentiate into various cell types: Schwann cells (figure 5, a-d); peripheral neurons (figure 6, a-d); smooth muscle cells (figure 7, a-d) and osteocytes (figure 8 b.) These results demonstrate the multipotency of MVSCs, which is consistent with previously reported findings. Although multipotent vascular stem cells have been shown to differentiate into adipocytes in previous studies, no adipogenic differentiation was noted in this study.

Effects of Laminar Fluid Shear Stress on MVSC Proliferation

To determine the effects of shear stress on MVSC proliferation, we used the Click-iT™ EdU Imaging Kit (made by Invitrogen) as an alternative to BrdU (5-bromo-2-deoxyuridine) labeling. We applied laminar fluid shear stress (6 dyn/cm^2) to MVSCs for 24, 48 and 72hrs respectively. Figure 10A shows that, when comparing sheared samples to static controls, the percentage of Edu-positive cells was 16% higher after 24hrs but only 2% higher after 48hrs and 13% lower after 72hrs. For both static controls and samples exposed to shear stress, the percentage of proliferating cells was higher in the first 24hrs compared to later time-points (figures 9 and 10A). Figure 10B demonstrates that fluid shear stress increased ERK2 phosphorylation in a time-dependent manner. The highest level of phosphorylation is observed in the first 24hours.

Effects of Laminar Fluid Shear Stress on MVSC Gene Expression

The effects of laminar fluid shear stress on a select number of genes were examined by quantitative reverse transcription polymerase chain reaction (qRT-PCR). A laminar fluid shear stress of 6 dyn/cm^2 was applied to MVSCs for 66 hours. Figure 11 summarizes the results. The graph shows that shear stress increased the gene expression of sox 10 over 2 folds while decreasing the expression of smooth muscle markers such as smooth muscle α-actin (SMA); calponin1 (CNN1); myosin heavy chain (MHC) and transgelin (SM22-α). Even the expression of myocardin, which has been identified as a master regulator of smooth muscle gene expression was 20% lower than in static control samples.

Results (continued)

While the expression of nestin decreased to less than half (compared to static controls), there were notable increases in the expression of peripheral neuron markers: class-III β-tubulin (1.5 folds) and neural filament M (over 3 folds.) To continue, fluid shear stress did not significantly affect the expression of glial fibrillary acidic protein (GFAP). The expression of Schwann cell marker S100-β, however, was 10 times lower when compared to static controls.
Interestingly, the gene expression of cbaf1 (a transcriptional regulator of osteoblast differentiation and osteocalcin (BGLA) were respectively 1.5 and 2 folds higher in samples exposed to fluid shear stress. Furthermore, there was a significant increase (over 2.5 folds) in the gene expression of Krüppel-like factors 4 (Klf4). This result is consistent with the proliferation data shown on figures 9 and 10.

Effects of Laminar Fluid Shear Stress on MVSC Protein Expression

Laminar fluid shear stress (6 dyn/cm^2) was applied to MVSCs for 66hrs to determine its effects on MVSC protein expression. Samples were then immunostained to examine changes in the protein expression.
Figure 12 shows that multipotent MVSC marker sox 10 was more strongly expressed in samples exposed to shear stress. MVSCs were, however, negative for sox 17 in both the static control and sheared samples (fig. 12 c,d). The expression of GFAP appeared much weaker than that of S100-β, another Schwann cell marker (fig 13) but fluid shear stress did not affect protein expression when compared to static controls.
To continue, laminar shear stress did not significantly affect the protein expression of peripheral neuron markers (nestin, class-III b-tubulin and neural filament M) as seen in figure 14. There was a lower expression of smooth muscle protein markers after exposure to shear stress: smooth muscle α-actin (fig.15 a,b), calponin1 (fig.15 c,d), and smooth muscle myosin heavy chain(fig.15 e,f). Transgelin (SM22-α) was, however, equally strongly expressed in both static control and sheared samples.

Effects of Laminar Fluid Shear Stress on MVSC Multipotency

To demonstrate the effects of laminar fluid shear stress on the differentiation potential of MVSCs, cells were exposed to fluid flow (6 dyn/cm^2) or kept in static cultures for 3 days. Subsequently, cells were transferred to specific differentiation media (osteognic, adipogenic, myogenic and neurogenic) described in the material and methods section. The duration of cell culture varied between 7 and 18 days depending on the lineage.
Figure 16 shows that some MVSCs were able to differentiate into Schwann cells even after exposure to laminar fluid shear stress for 3 days. Figure 17 does not show the

Results (continued)

terminal differentiation of MVSC into peripheral neurons because we could not allow enough time for the cell to differentiate completely. Figure 17 shows, however, that the cells are positive for vimentin and Tuj1 in both static and sheared samples. Similarly, applying laminar fluid shear stress to MVSCs for 3 days did not affect myogenic differentiation (fig.18). MVSCs cultured in myogenic differentiation medium were similarly positive for smooth muscle cells markers: smooth mucle α-actin (fig.18 a,b), calponin1 (fig.18 c,d), smooth muscle myosin heavy chain(fig.18 e,f) and transgelin, SM22- α (fig.18 g,h) in spite of their prior exposure to laminar fluid shear stress. Finally, osteogenic differentiation was not affected as no difference was observed between samples exposed to shear stress and static controls (fig.19).

Discussion

SMCs are known to exist in different morphologic phenotypes within the layers of healthy blood vessel walls [7]. It is unclear, however, if mature SMCs can undergo phenotypic modulation because there is no direct evidence for SMC de-differentiation or plasticity. Smooth muscle cells (SMCs) are also known to play a key role in vascular pathology [8]. Until recently, the accepted theory was that vascular intimal injury promotes the migration and proliferation of mature smooth muscle cells in the intimal layer. This ultimately leads to the formation of an atheromatous plaque below the endothelium [9]. New research, however, suggests the possibility that stem cells, rather than mature SMCs, are responsible for vascular remodeling in disease states. Stem cells may also be responsible for SMC heterogeneity in blood vessel walls. In a recent publication, Tang et al., index a novel population of stem cells in the medial layer of the blood vessel called multipotent vascular stem cells (MVSCs), which they argue are responsible for vascular remodeling [5].

In this study, we confirm previously reported observations that rat MVSCs express Sox10, Sox17, and neural markers (s100-β, peripherin, nestin, vimentin and neural filament M.) MVSCs are negative for SM-MHC, Calponin1, HNK1, glial fibrillar protein (GFAP) and, EC marker, CD31. MVSCs express low levels of SMA, which are not organized in stress fibers. Rat MVSCs are also capable of differentiation into multiple lineages: myogenic, neurogenic and osteogenic. Adipogenic differentiation was not observed in this study although this type of differentiation has been reported in Tang et al.

In the current study, we show that exposure to laminar fluid shear stress increases the percentage of MVSCs in the proliferating S phase (figures 9 and 10B.) in a time-dependent manner. MVSCs proliferate rapidly in the first 24hours and begin to reduce their rate of proliferation thereafter. We also report that ERK1/2 is activated in a time-dependent manner. ERK 1/2 is most strongly activated in the first 24 hours of exposure to laminar fluid shear stress. It is known that ERK1/2 activation plays an important role in cell proliferation [10]. In addition, we observe a 2 fold increase in the gene expression of Krüppel-like factors 4 (Klf4) after 66 hours of exposure to shear stress. Klf4 is known to be an anti-proliferative shear stress-responsive gene. The over-expression of Klf4 in vascular SMCs has been shown to induce growth arrest [11]. This finding suggests that Klf4 may be expressed in MVSCs in order to attenuate cell proliferation.

Furthermore, we report that exposure to laminar fluid shear stress for 66 hours decreases the gene expression of smooth muscle cell markers (smooth muscle α-actin, calponin1, myosin heavy chain and transgelin**),** and increases the gene expression of osteoblastic differentiation markers (osteocalcin and cbaf1.) If MVSCs do indeed contribute to vascular remodeling, this data gives credence to the hypothesis that MVSCs may contribute to intimal calcification in disease states by differentiating into osteblasts.

Finally, we demonstrate that exposing MVSCs to laminar fluid shear stress for 66 hours before inducing in-vitro differentiation, does not affect their multipotency. Biochemical factors can still drive the differentiation of MVSCs toward multiple lineages (myogenic, osteogenic and neurogenic) despite the cells' prior exposure to laminar fluid shear stress. One could infer from this data that, even if MVSCs become exposed to blood

flow in-vivo, they may still retain the ability to differentiate into multiple cell types. It may be possible that exposure to higher levels of fluid shear stress (>6 dynes/cm^2), to different flow profile patterns, or to longer exposure time may affect MVSC differentiation potential but additional experiments will be required to verify this hypothesis.

In conclusion, the discovery of MVSCs in the blood vessel wall could provide a new explanation for the heterogeneity of SMC phenotype in healthy vessel walls and for vascular remodeling after injury. More research will be necessary, however, to challenge the accepted theory that SMCs can modulate their phenotype and contribute extensively to vascular remodeling. In addition, further investigation into the effects of shear stress on the differentiation of MVSCs will be necessary to have a better understanding of their function.

ACKNOWLEDGMENTS

I thank Dr. Aijun Wang and Dr. Zhenyu Tang for providing the cell line used in this study. I also thank Julia Chu for her assistance with the quantitative PCR analysis.

REFERENCES

1. Ross, R., *Atherosclerosis--an inflammatory disease.* N Engl J Med, 1999. **340**(2): p. 115-26.
2. Thyberg, J., *Phenotypic modulation of smooth muscle cells during formation of neointimal thickenings following vascular injury.* Histol Histopathol, 1998. **13**(3): p. 871-91.
3. Murry, C.E., et al., *Monoclonality of smooth muscle cells in human atherosclerosis.* Am J Pathol, 1997. **151**(3): p. 697-705.
4. Pearson, T.A., et al., *Clonal markers in the study of the origin and growth of human atherosclerotic lesions.* Circ Res, 1978. **43**(1): p. 10-8.
5. Tang, Z., et al., *Differentiation of multipotent vascular stem cells contributes to vascular diseases.* Nat Commun, 2012. **3**: p. 875.
6. Wang, A., et al., *Induced pluripotent stem cells for neural tissue engineering.* Biomaterials, 2011. **32**(22): p. 5023-32.
7. Gittenberger-de Groot, A.C., et al., *Smooth muscle cell origin and its relation to heterogeneity in development and disease.* Arterioscler Thromb Vasc Biol, 1999. **19**(7): p. 1589-94.
8. Manabe, I. and R. Nagai, *Regulation of smooth muscle phenotype.* Curr Atheroscler Rep, 2003. **5**(3): p. 214-22.
9. Libby, P., *Inflammation in atherosclerosis.* Arterioscler Thromb Vasc Biol, 2012. **32**(9): p. 2045-51.
10. Mebratu, Y. and Y. Tesfaigzi, *How ERK1/2 activation controls cell proliferation and cell death: Is subcellular localization the answer?* Cell Cycle, 2009. **8**(8): p. 1168-75.
11. Autieri, M.V., *Kruppel-like factor 4: transcriptional regulator of proliferation, or inflammation, or differentiation, or all three?* Circ Res, 2008. **102**(12): p. 1455-7.

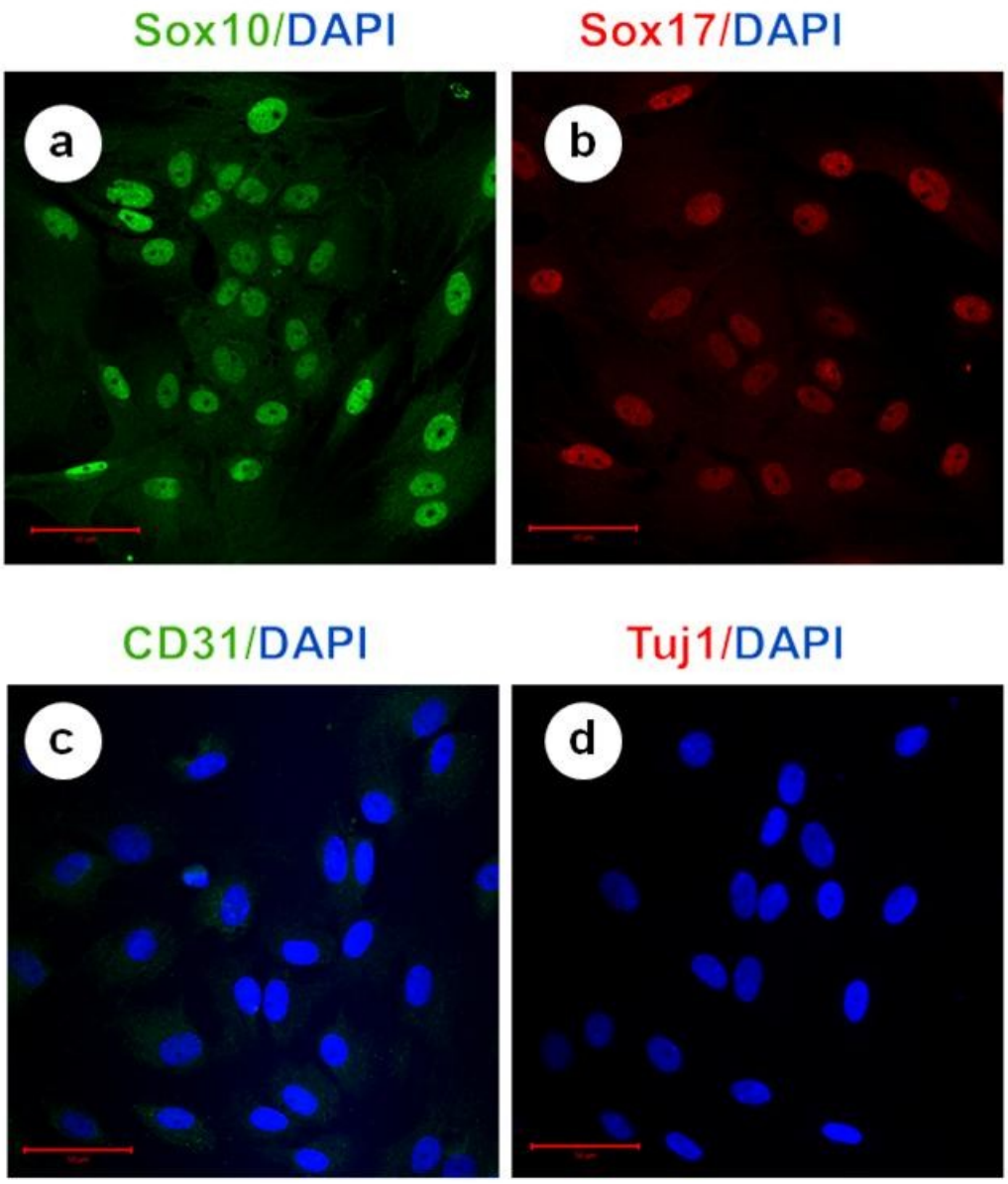

FIGURE 1. Characterization of MVSCs.
Immunofluorescent staining of MVSC markers (a) Sox10, (b) Sox17 as well as (c) CD31, and (d) Tuj1. Nuclei were stained with DAPI in blue. Scale bar = 50 μm.

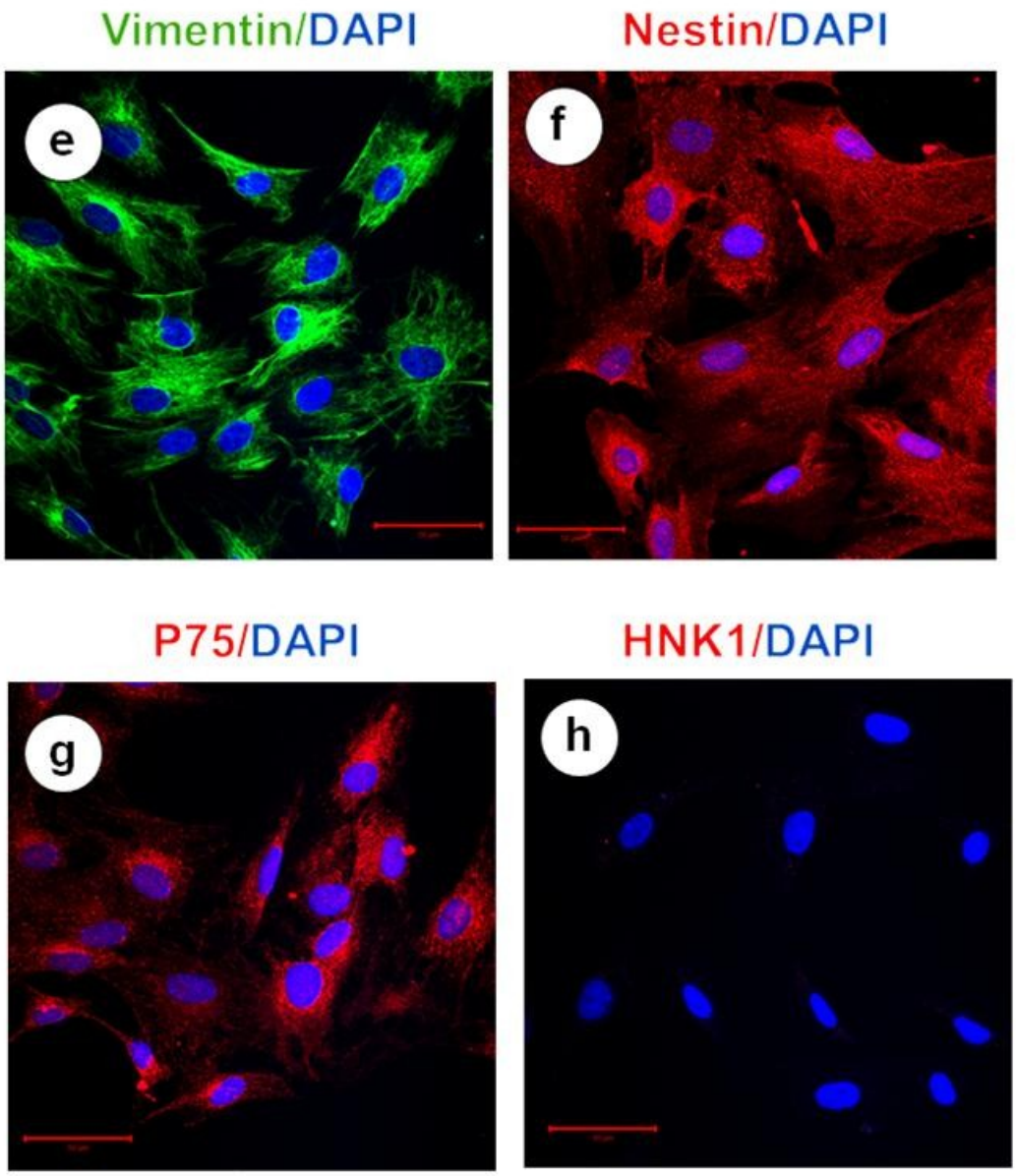

FIGURE 2. Characterization of MVSCs.
Immunofluorescent staining of markers (e) vimentin, (f) nestin, (g) P75, and (h) HNK1. Nuclei were stained with DAPI in blue. Scale bar = 50 μm.

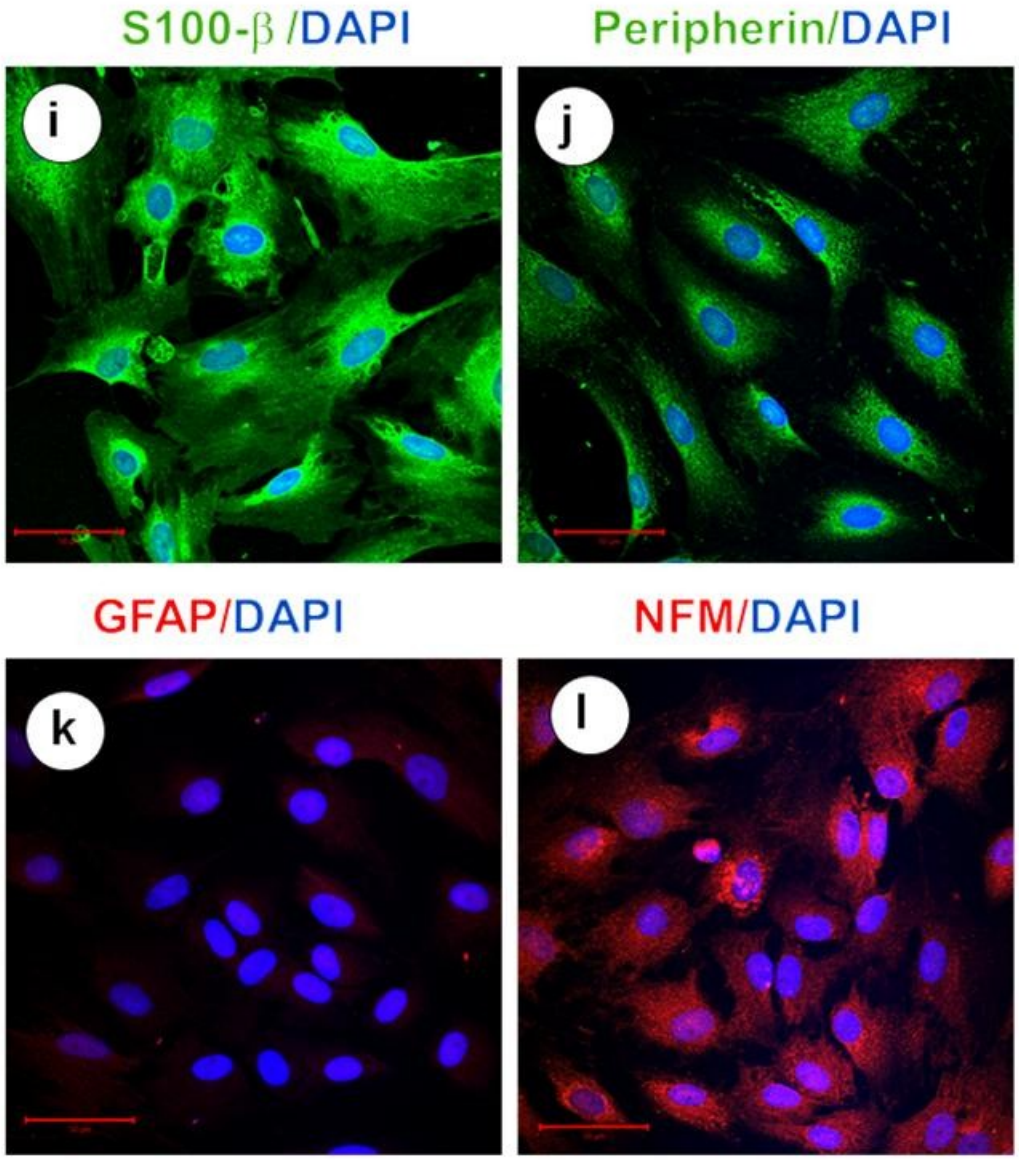

FIGURE 3. Characterization of MVSCs.
Immunofluorescent staining of markers (i) S100-β, (j) peripherin, (k) glial fibrillary acidic protein (GFAP) and, (l) neural filament M (NFM.)
Nuclei were stained with DAPI in blue. Scale bar = 50 μm.

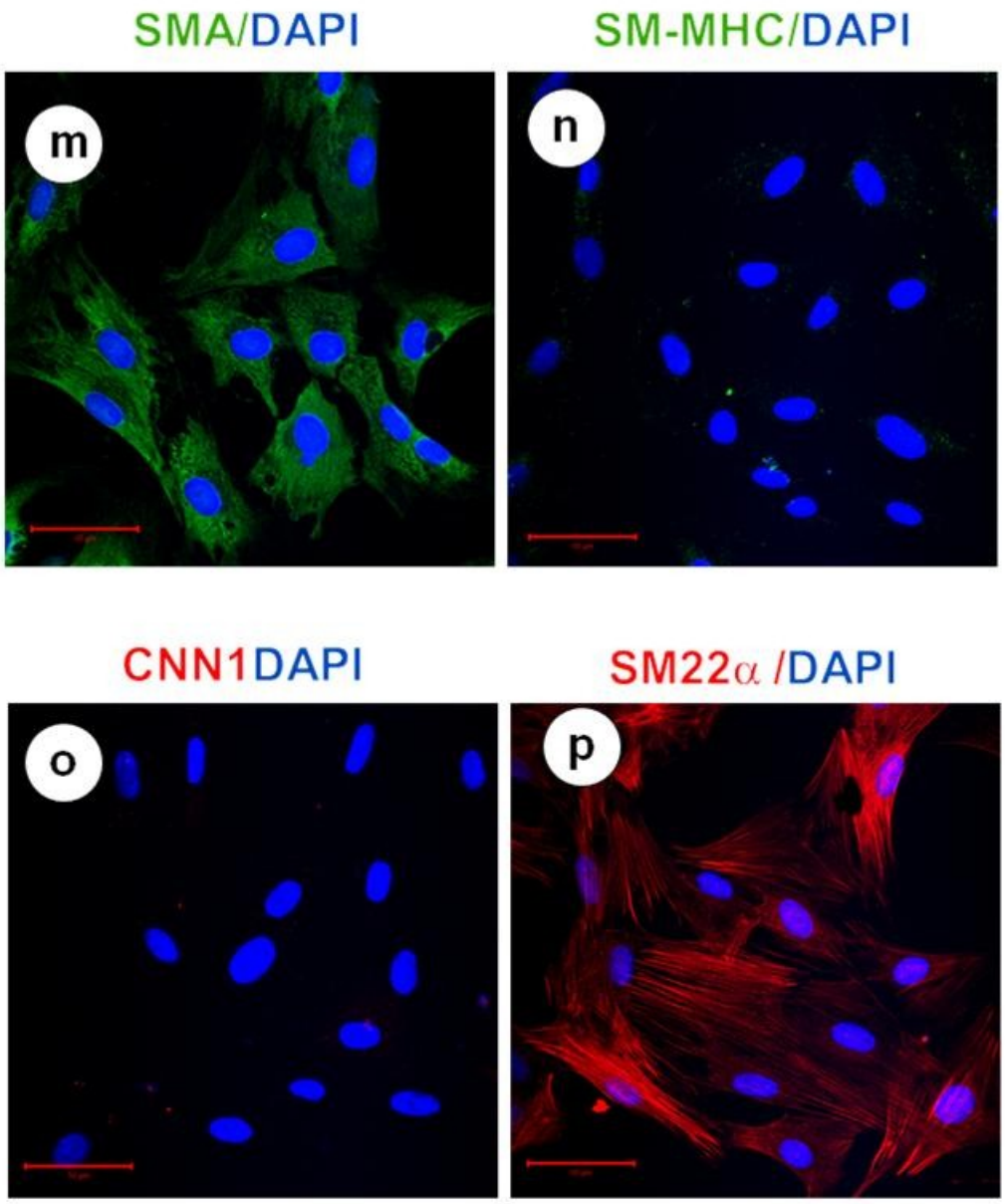

FIGURE 4. Characterization of MVSCs.
Immunofluorescent staining of markers (m) smooth muscle α-actin (SMA), (n) smooth muscle myosin heavy chain (SM-MHC), (o) calponin 1 (CCN1) and, (p) transgelin (SM22-α). Nuclei were stained with DAPI in blue. Scale bar = 50 μm.

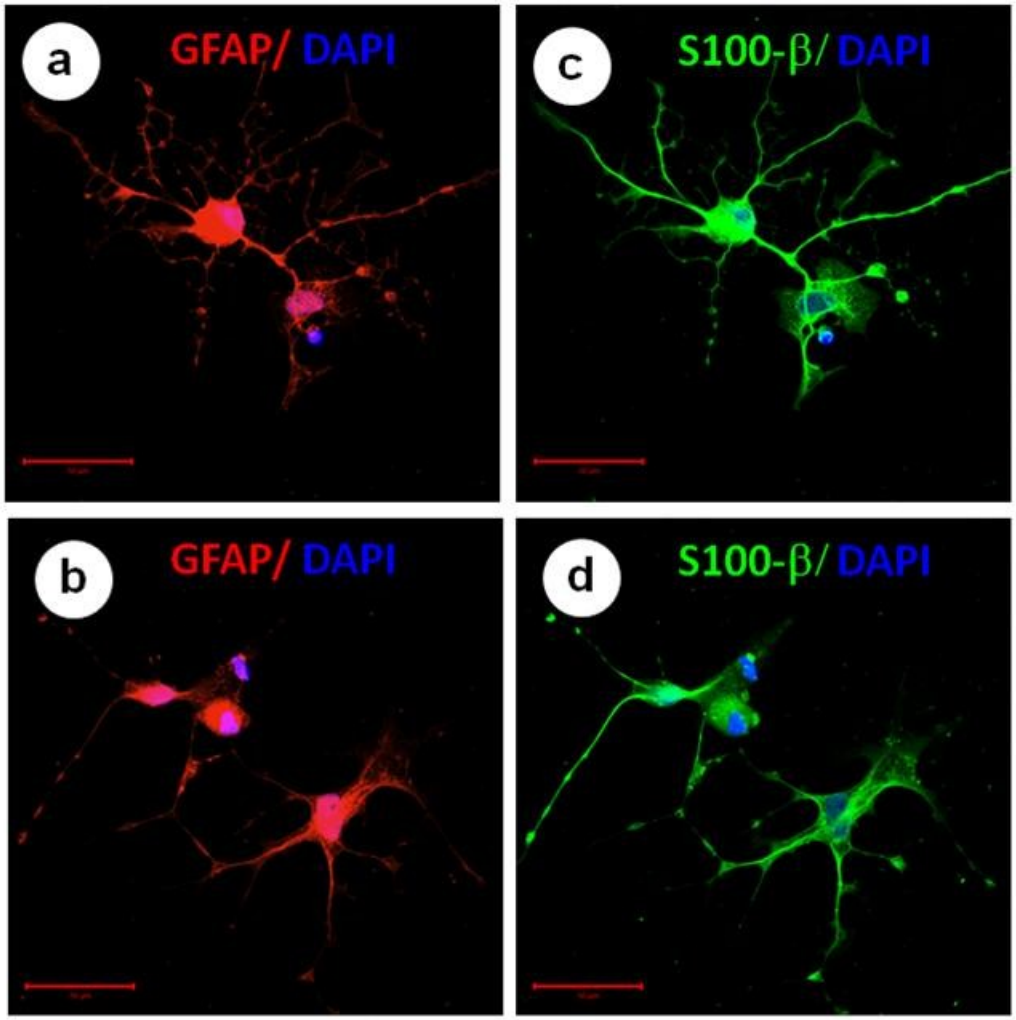

FIGURE 5. Schwann cell differentiation of MVSCs. MVSCs were cultured in schwann cell differentiation medium for 7 days. Immunofluorescent staining of schwann cell markers: GFAP (a,b), S100-β (c,d). Nuclei were stained with DAPI in blue. Scale bar = 50 μm

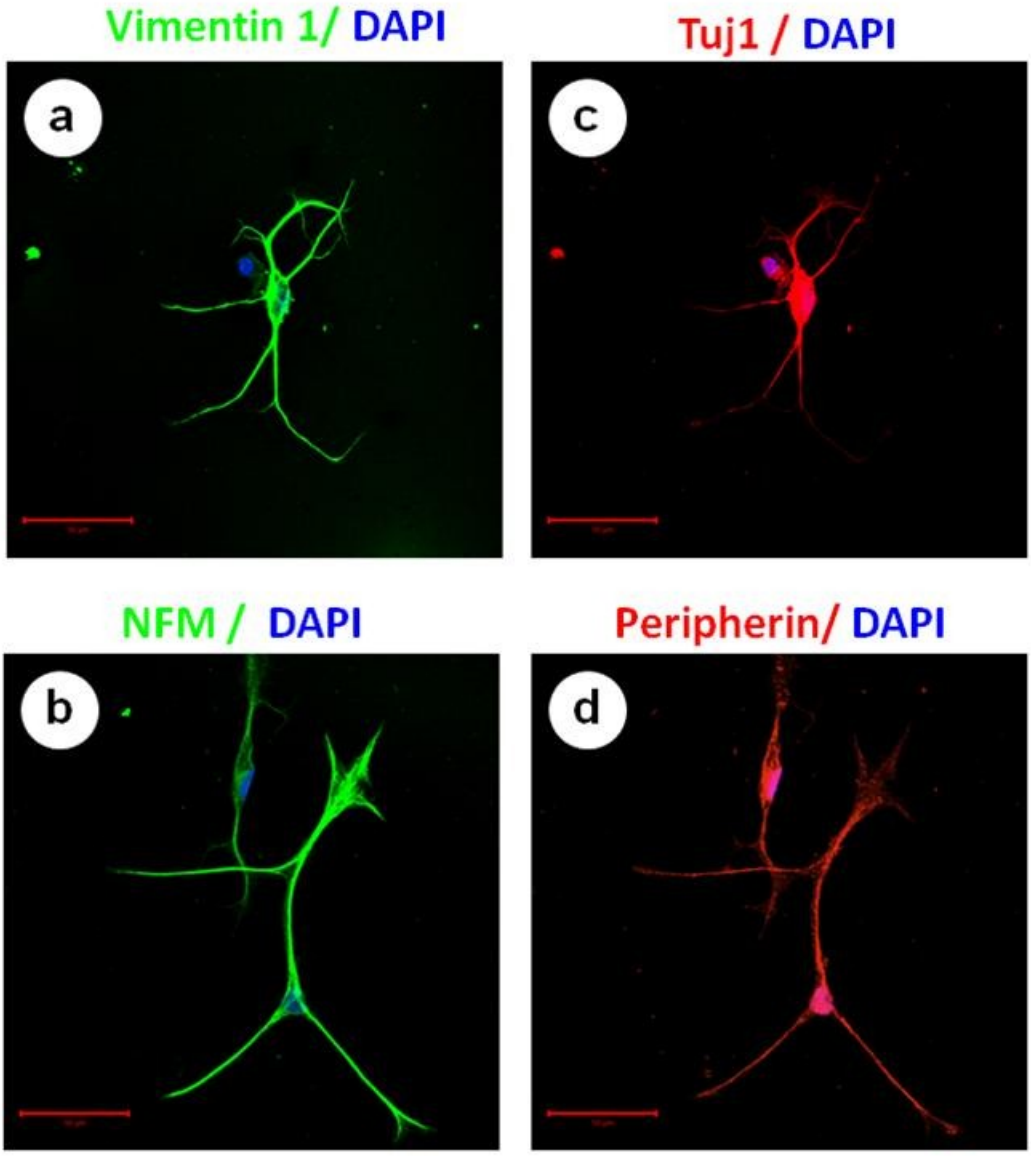

FIGURE 6. Neurogenic differentiation of MVSCs.
MVSCs cultured in peripheral nerve differentiation medium for 7 days. Immunofluorescent staining of peripheral neuron markers:
(a) Vimentin, (b) NFM, (c) Tuj1 , (d) Peripherin.
Nuclei were stained with DAPI in blue. Scale bar = 50 μm

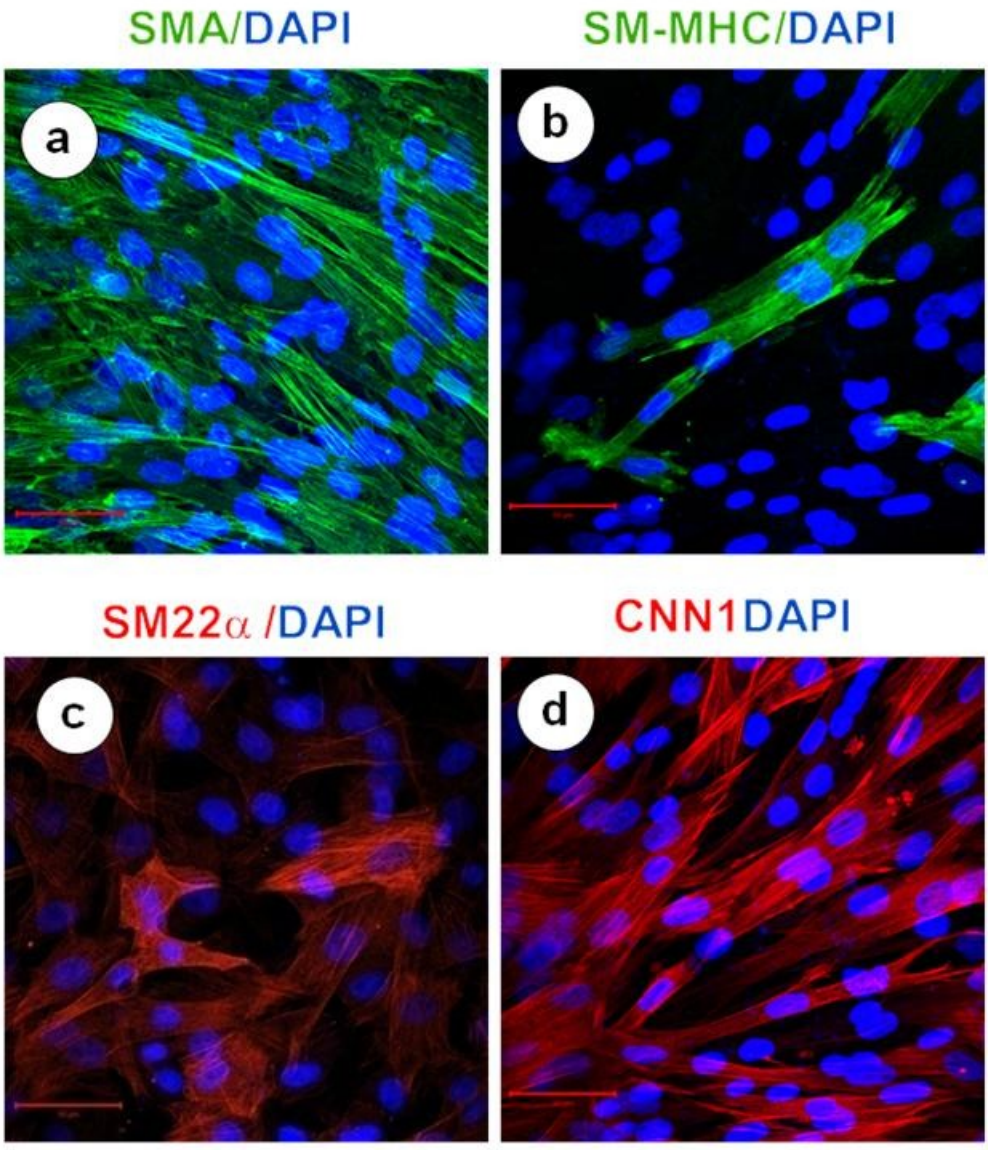

FIGURE 7. Myogeninc differentiation of MVSCs.
MVSCs were cultured in myogenic differentiation medium for 10 days . Immunofluorescent staining of smooth muscle cell markers: (a) Smooth muscle α-actin, (b) Smooth muscle myosin heavy chain, (c) Transgelin (SM22α), and (d) Calponin1 (CNN1). Nuclei were stained with DAPI in blue. Scale bar = 50 μm.

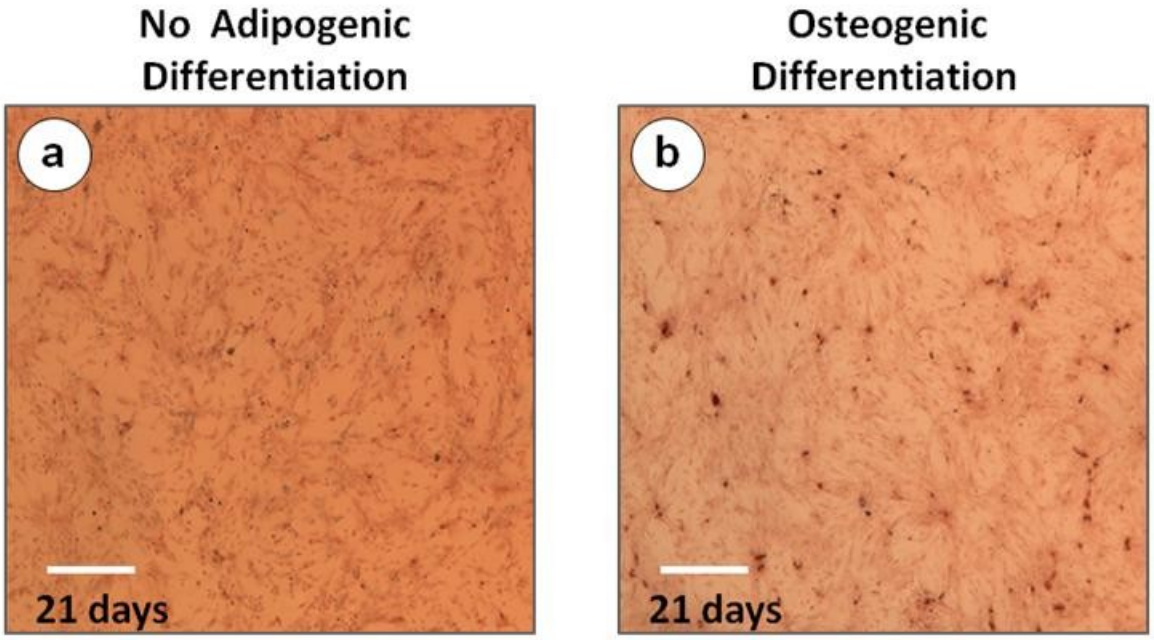

FIGURE 8. Osteogenic and adipogenic differentiation of MVSCs.
MVSCs were cultured in (a) adipogenic differentiation medium for 21 days, Oil red staining or, (b) osteogenic differentiation medium for 21 days, Alizarin red staining.
Scale bar = 200 μm.

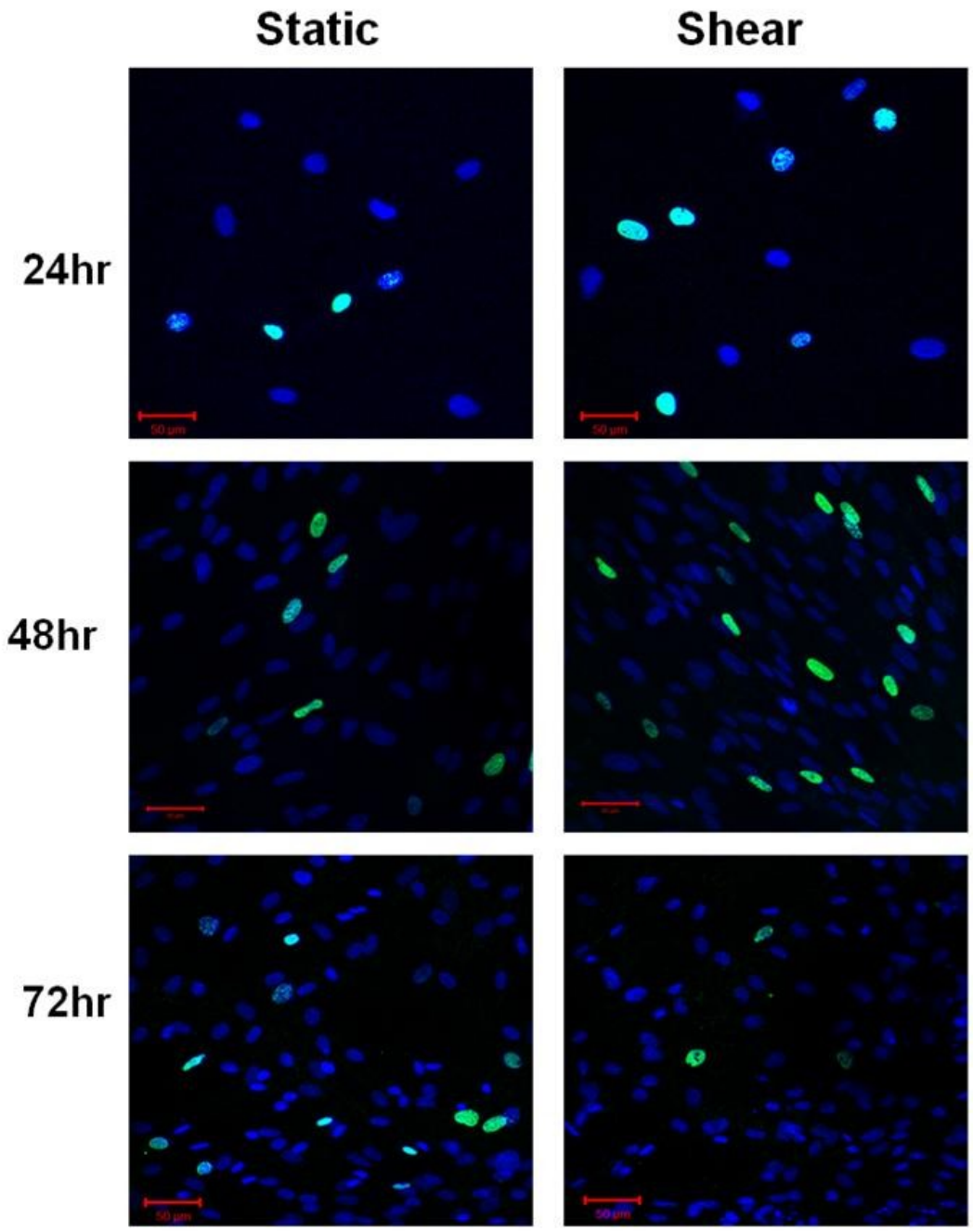

FIGURE 9. Effects of fluid shear stress on the proliferation of MVSCs.
MVSCs were subjected to a fluid shear stress of 6 dyn/cm^2 or kept as static controls. Fluorescent double-staining of cells in S-phase (in green) and nuclei (Hoechst staining in blue). Scale bar = 50 μm.

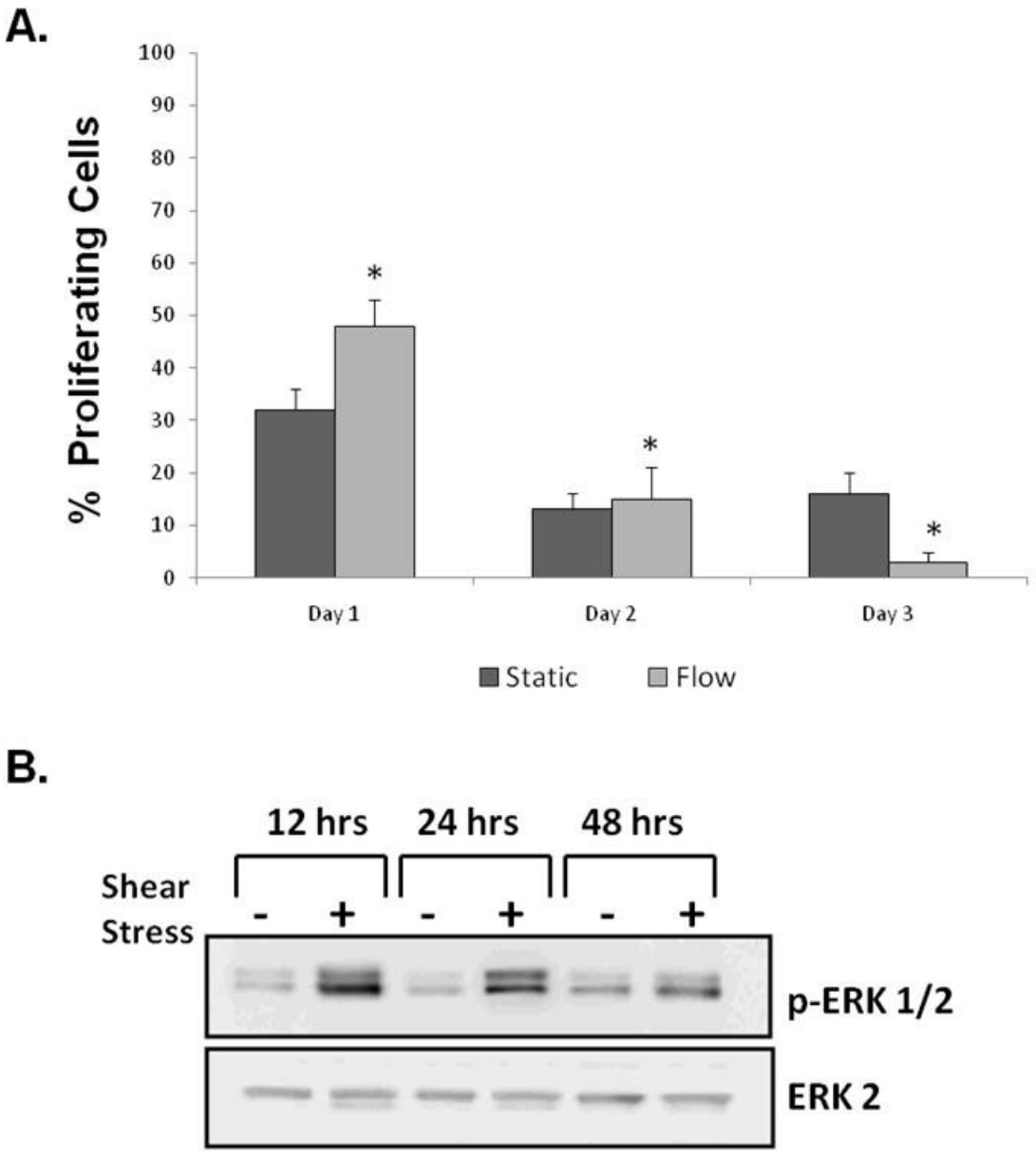

FIGURE 10. Effects of fluid shear stress on MVSC proliferation. MVSCs were subjected to a fluid shear stress of 6 dyn/cm^2 or kept as static controls. (A) Statistical analysis of cell proliferation. Bars represent mean + standard deviation (SD) of the percentage of EdU-positive cells quantified from three independent experiments. Significant difference compared to static control was determined by a Student's t-test. *indicates $p < 0.05$ ($n = 3$).
(B) Immunoblotting analysis of p-ERK1/2 and ERK2 expression.

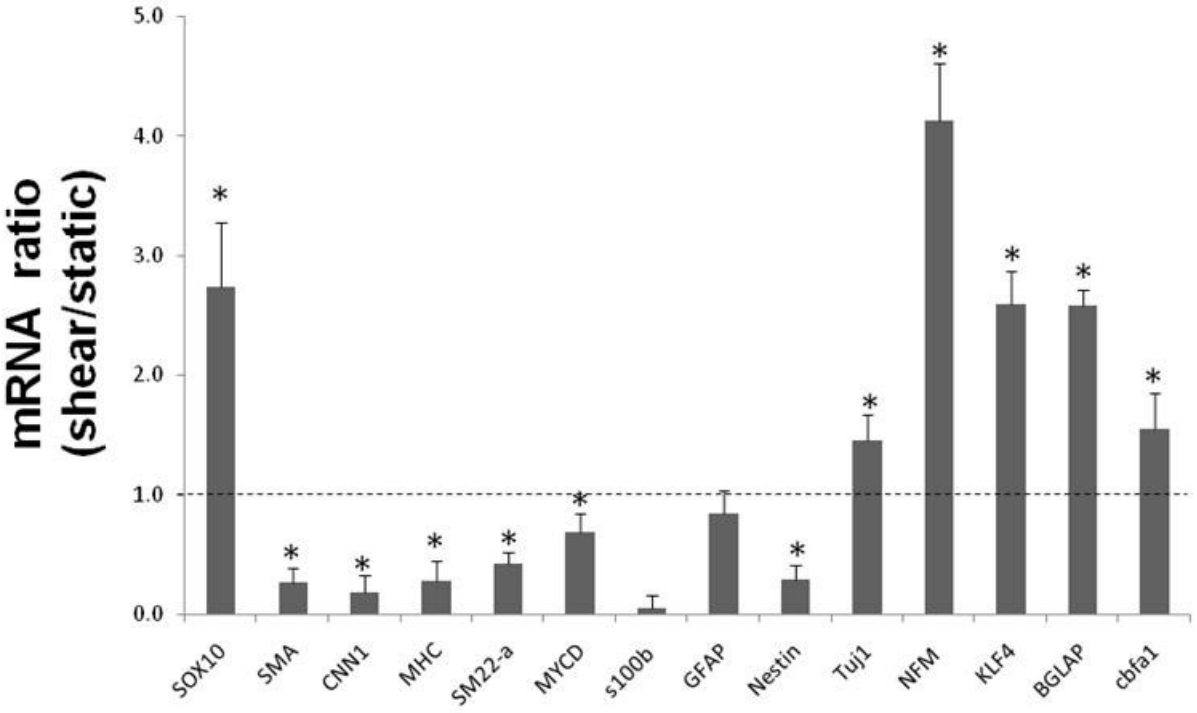

FIGURE 11. Effects of fluid shear stress on the gene expression in MVSCs.

MVSCs were subjected to a shear stress of 6 dyn/cm^2 or kept as static controls for 66hrs. qRT-PCR shows the expression of selected genes. Sox10; SMA:smooth muscle α-actin; CNN1:calponin1; MHC:myosin heavy chain; SM22-α: transgelin; MYCD:myocardin; s100-β ; GFAP:glial fibrillary acidic protein; Nestin; TUJ1:class-III β tubulin; TGF- β1: transforming growth factor β1; Klf4:Krüppel-like factor 4; BGLAP:osteocalcin; and cbfa1.

Bars represent mean + standard deviation (SD). Statistical significance compared to static control was determined by using log-transformed one-sample t-test.

*indicates $p < 0.05$ ($n = 3$).

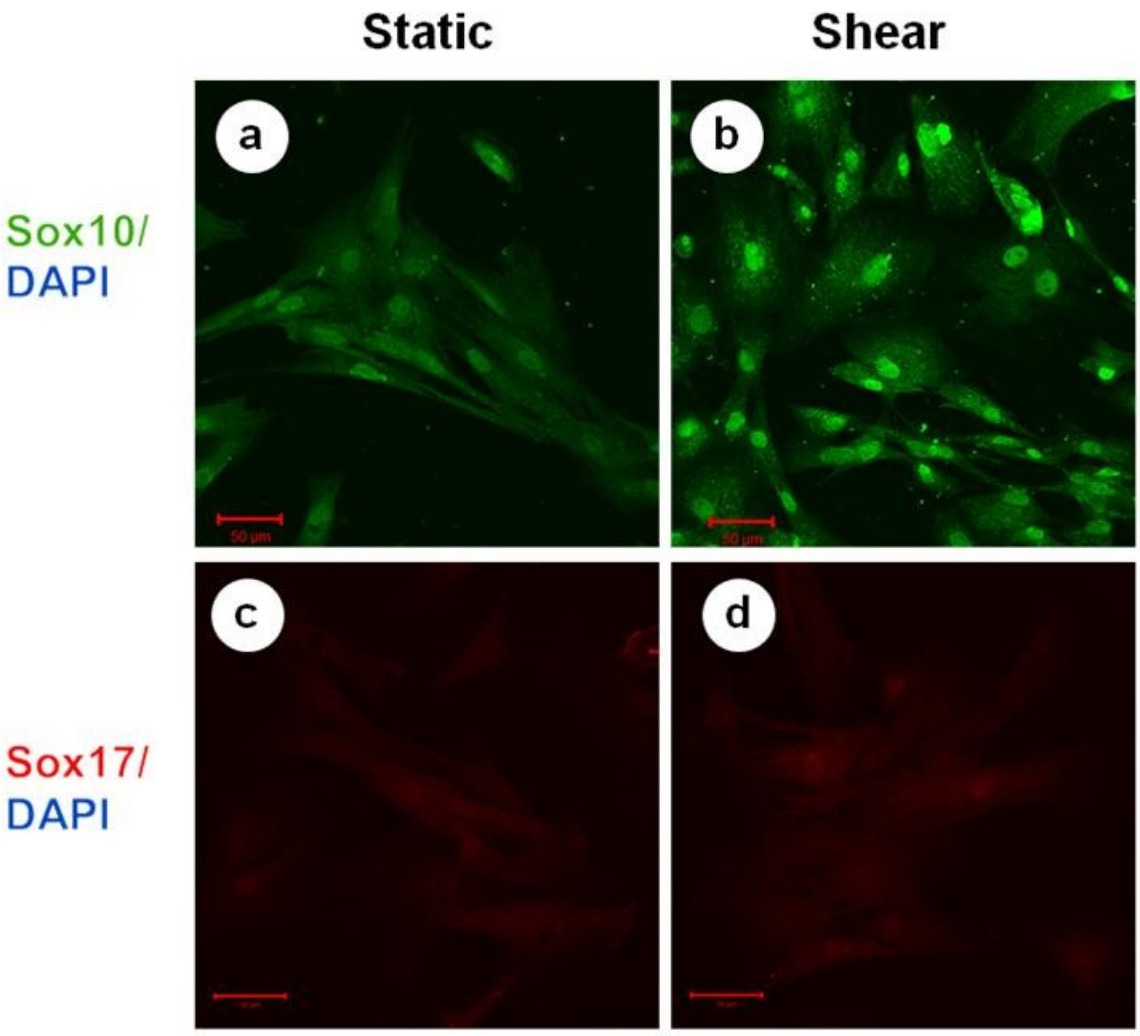

FIGURE 12. Effects of fluid shear stress on the protein expression of MVSCs.
MVSCs were subjected to a shear stress of 6 dyn/cm² (b,d) or kept as static controls for 66hrs (a,c). Immunofluorescent staining of vascular stem cell markers: Sox10 (a,b) and Sox17 (c,d). Nuclei were stained with DAPI in blue. Scale bar = 50 μm

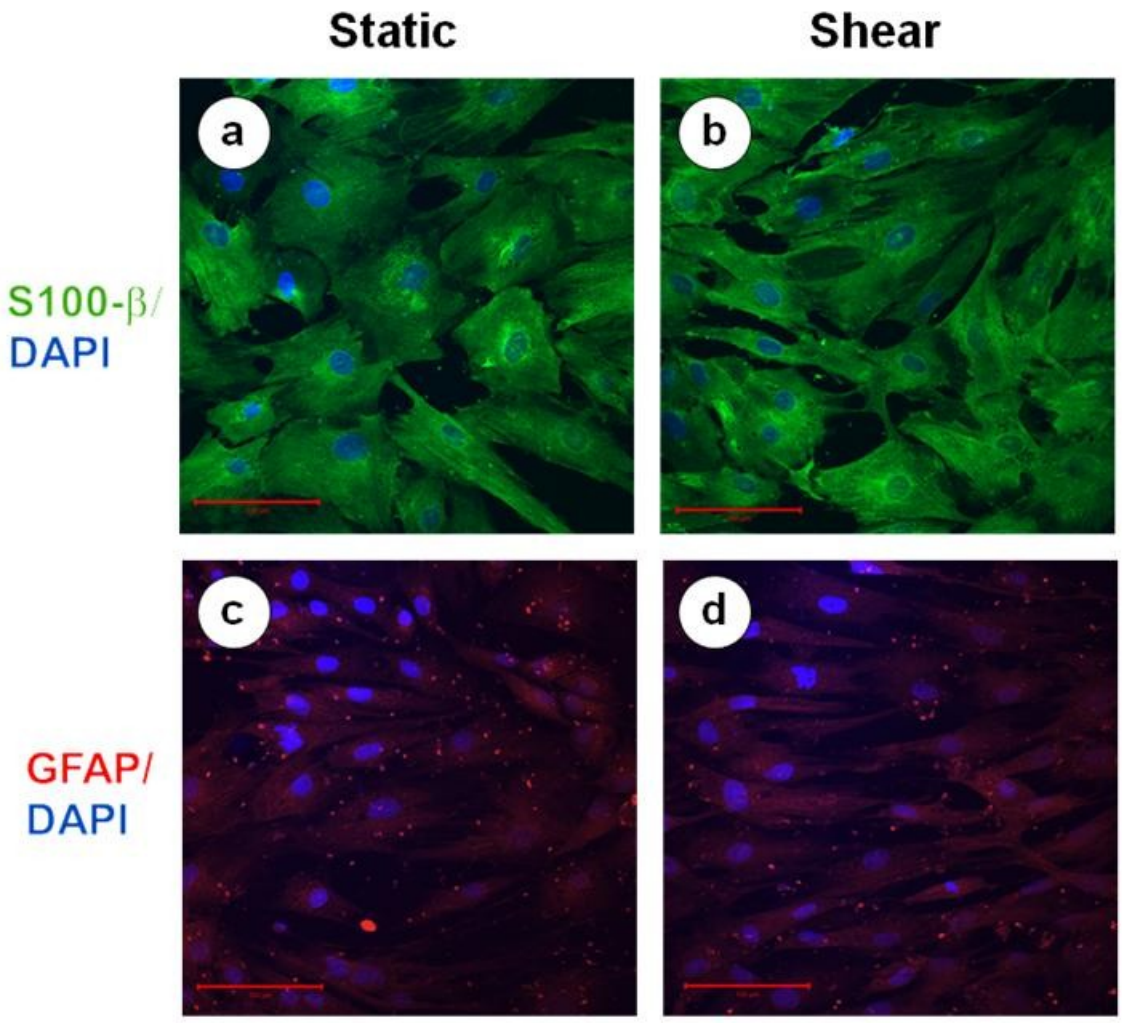

FIGURE 13. Effects of fluid shear stress on the protein expression of MVSCs derived from iPSCs.
MVSCs were subjected to a shear stress of 6 dyn/cm² (b,d) or kept as static controls for 66hrs (a,c). Immunofluorescent staining of Schwann cell markers: S100-β (a,b) and GFAP (c,d). Nuclei were stained with DAPI in blue. Scale bar = 100 μm

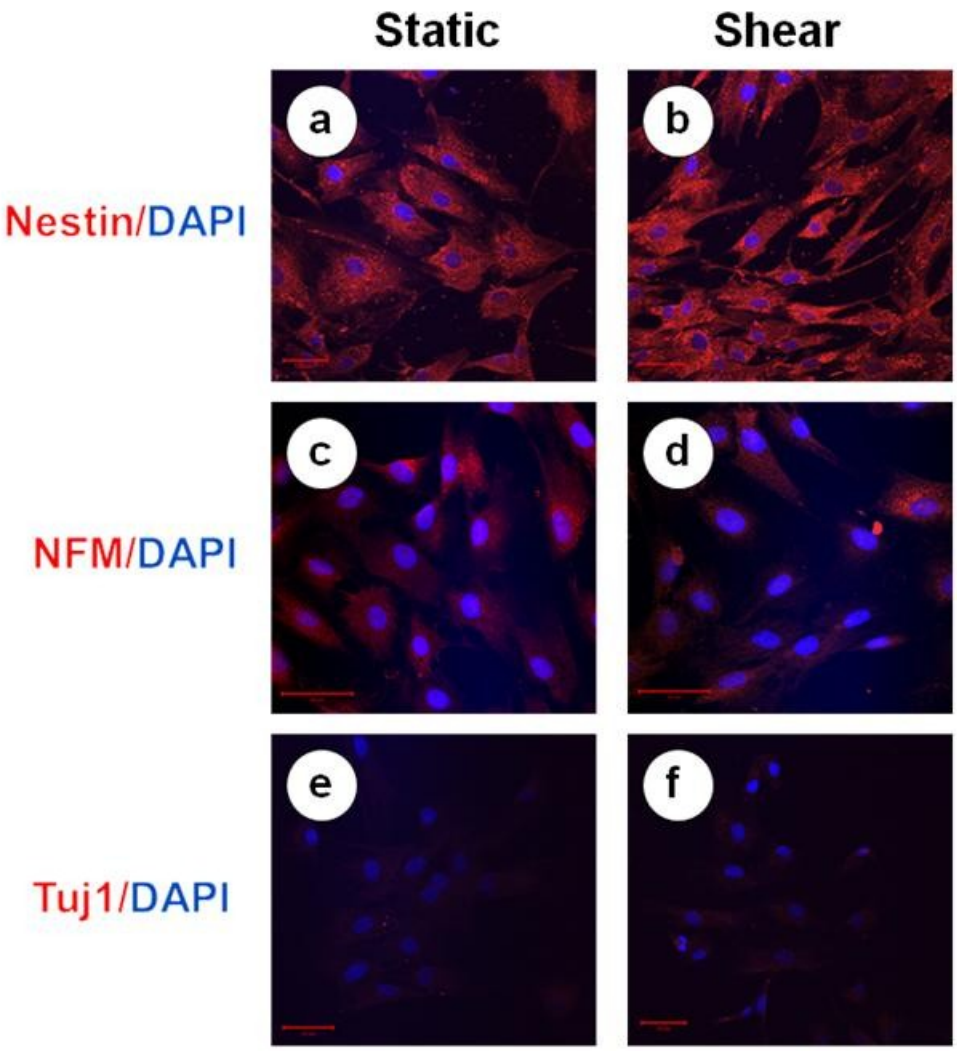

FIGURE 14. Effects of fluid shear stress on the protein expression of MVSCs derived from iPSCs.
MVSCs were subjected to a shear stress of 6 dyn/cm^2 (b,d,f) or kept as static controls for 66hrs (a,c,e). Immunofluorescent staining of peripheral neuron markers: Nestin (a,b), NFM (c,d) and Tuj1(e,f). Nuclei were stained with DAPI in blue.
Scale bar = 50 μm

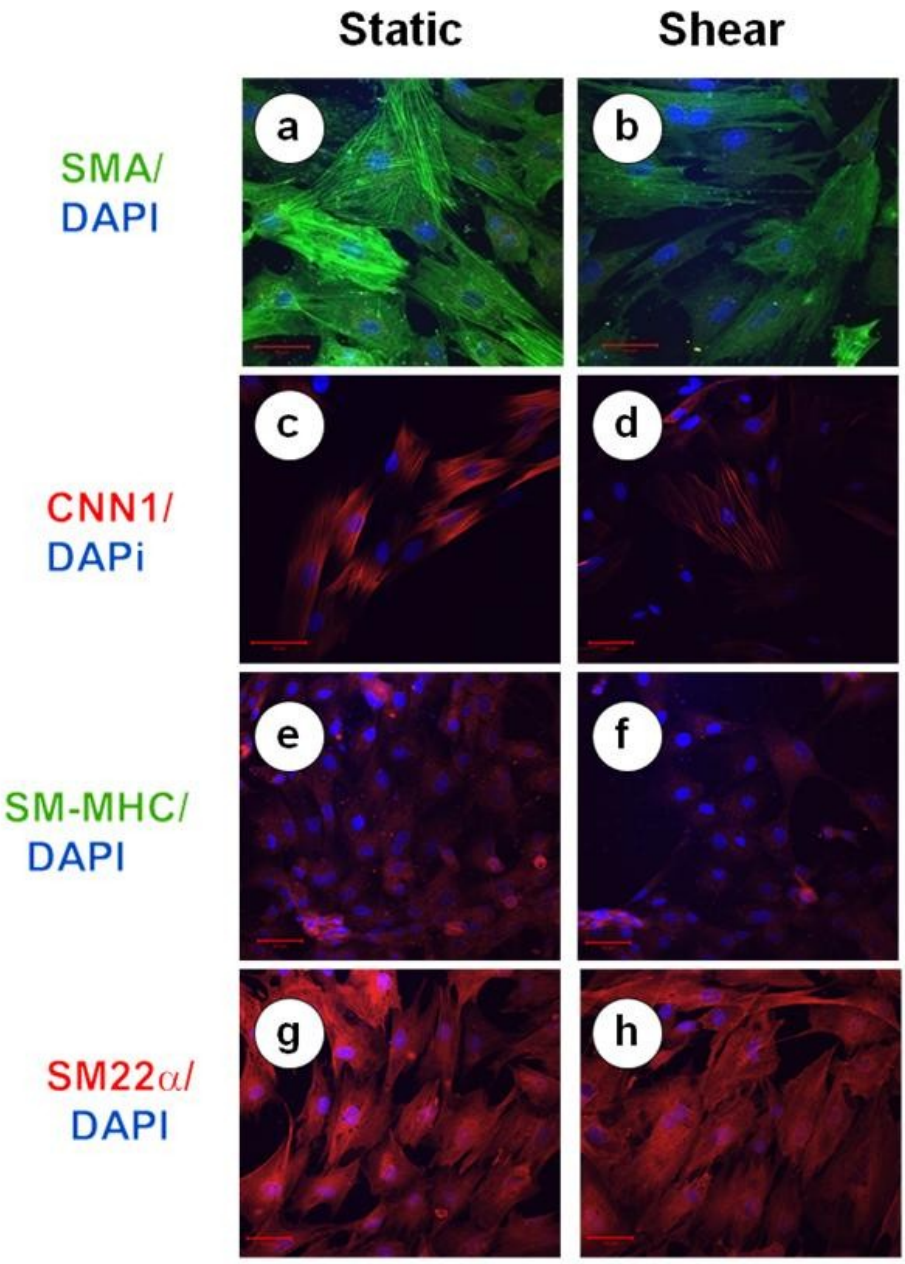

FIGURE 15. Effects of fluid shear stress on the protein expression of MVSCs derived from iPSCs.
MVSCs were subjected to a shear stress of 10 dyn/cm² (b,d,f,h) or kept as static controls for 66hrs (a,c,e,g). Immunofluorescent staining of smooth muscle cell markers: Smooth mucle α-actin (a,b), Calponin1 (c,d), Smooth muscle myosin heavy chain (e,f), and SM22α (g,h). Nuclei were stained with DAPI in blue. Scale bar = 50 μm

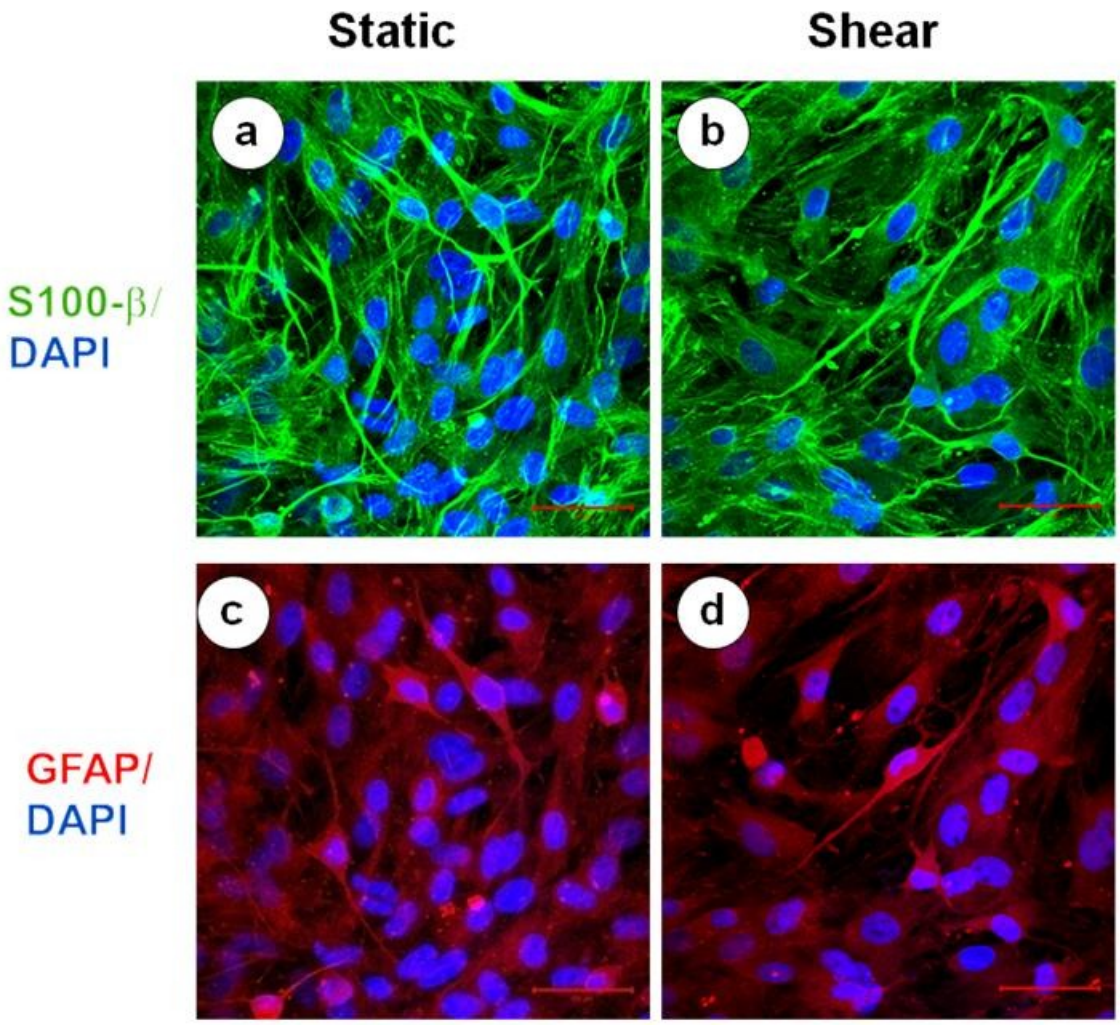

FIGURE 16 . Effects of fluid shear stress on the schawnn cell differentiation of MVSCs.

MVSCs were subjected to a shear stress of 6 dyn/cm² (b,d) or kept as static controls for 3 days (a,c) and subsequently cultured in schwann cell differentiation medium 3 days. Immunofluorescent staining of Schwann cell markers: S100-β (a,b) and GFAP (c,d). Nuclei were stained with DAPI in blue. Scale bar = 100 μm

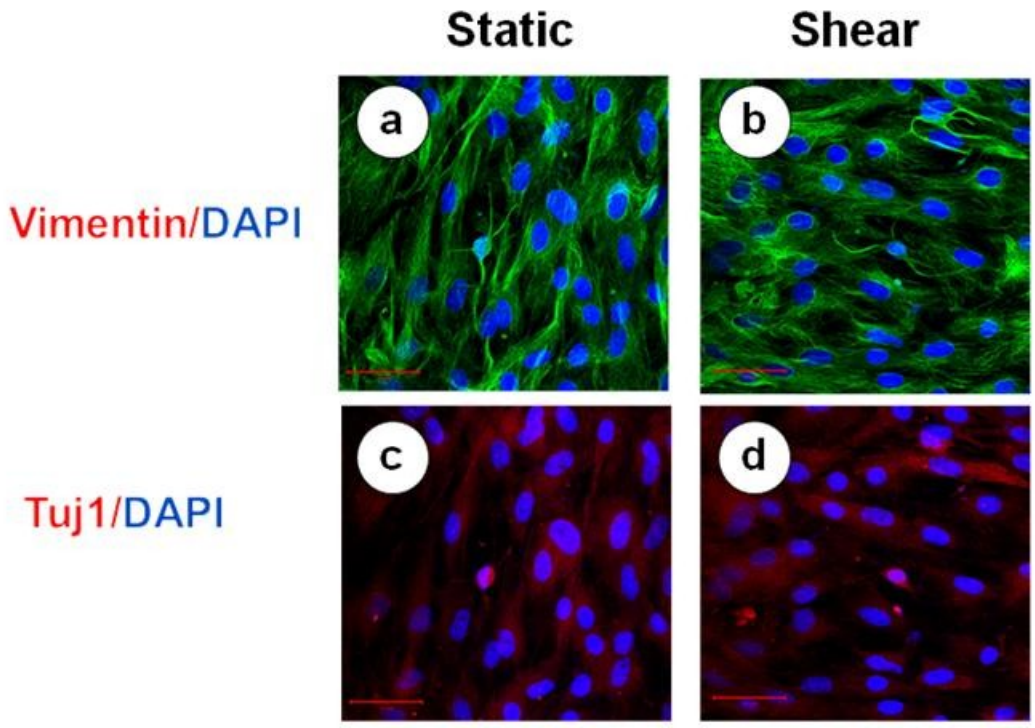

FIGURE 17. Effects of fluid shear stress on the neurogenic differentiation of MVSCs.
MVSCs were subjected to a shear stress of 6 dyn/cm² (b,d,f) or kept as static controls for 3 days (a,c,e) and subsequently cultured in neural differentiation medium 3 days. Immunofluorescent staining of peripheral neuron markers: Vimentin (a,b), and Tuj1 (c,d). Nuclei were stained with DAPI in blue. Scale bar = 50 μm

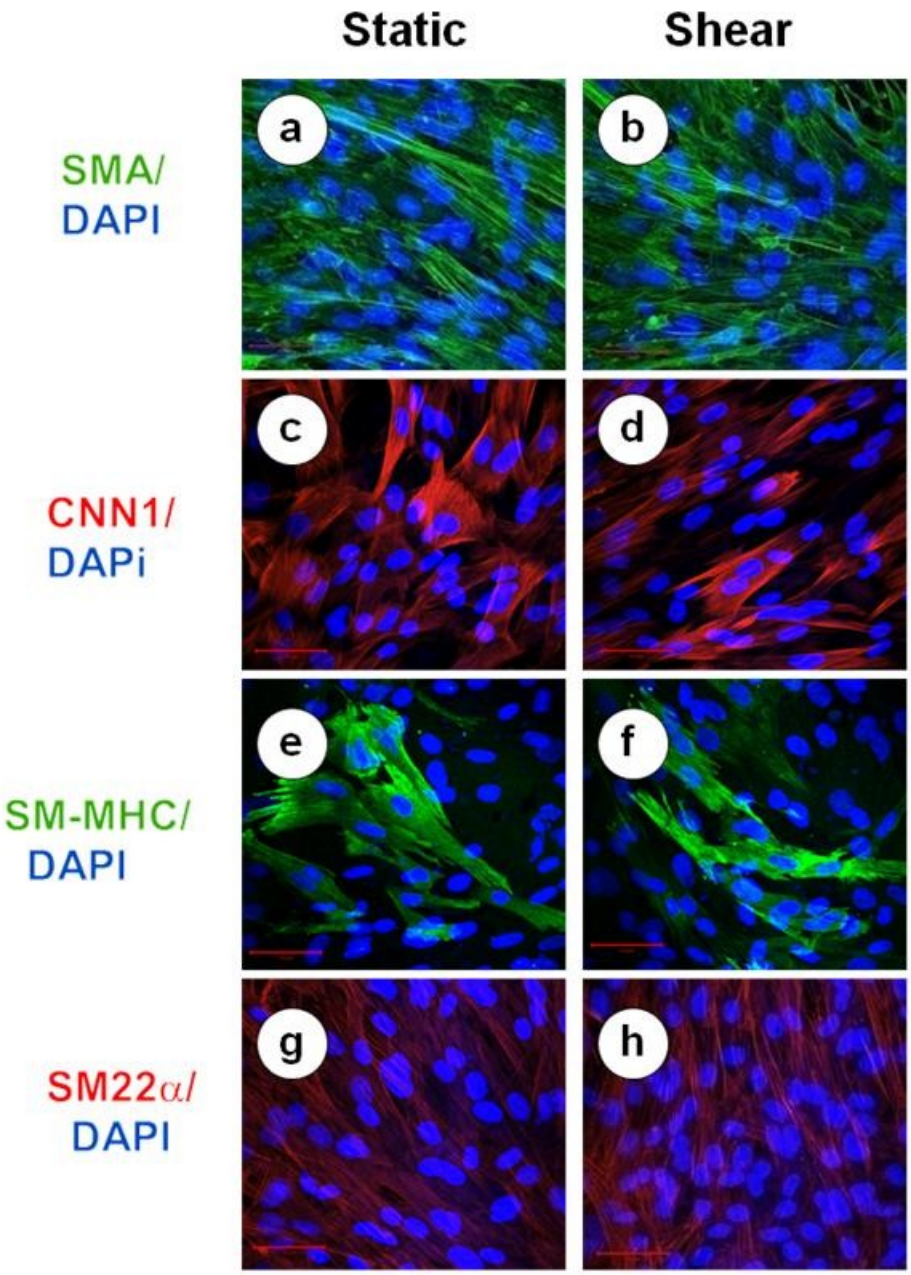

FIGURE 18. Effects of fluid shear stress on the myogenic differentiation of MVSCs.

MVSCs were subjected to a shear stress of 6 dyn/cm^2 (b,d,f,h) or kept as static controls for 3 days (a,c,e,g) and subsequently cultured in myogenic differentiation medium for 10 days . Immunofluorescent staining of smooth muscle cell markers: Smooth mucle α-actin (a,b), Calponin1 (c,d), Smooth muscle myosin heavy chain(e,f), and SM22α (g,h). Nuclei were stained with DAPI in blue. Scale bar = 50 μm

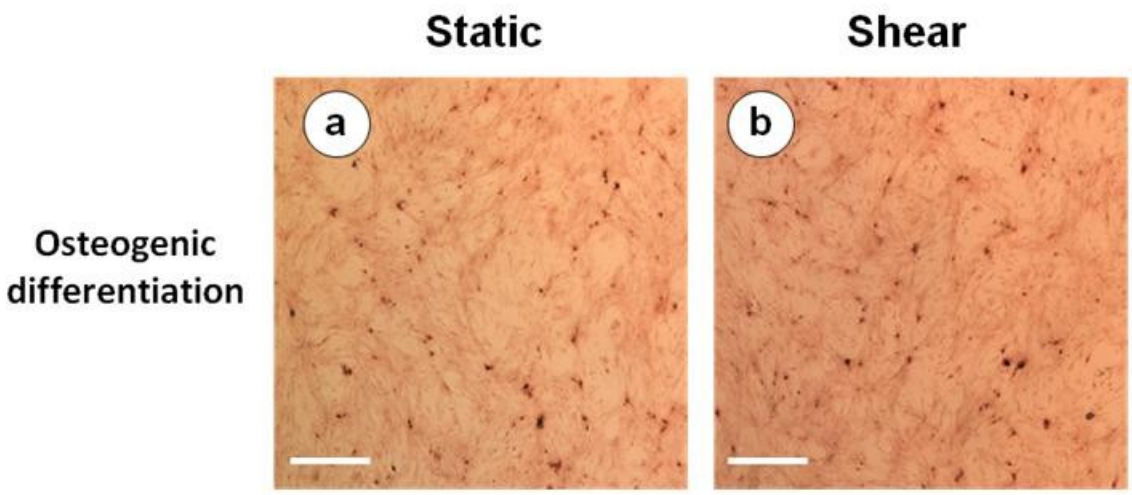

FIGURE 19. Effects of fluid shear stress on the osteogenic differentiation of MVSCs.
MVSCs were subjected to a shear stress of 6 dyn/cm^2 (d) or kept as static controls for 3 days (a) and subsequently cultured in osteogenic differentiation medium for 14 days, Alizarin red staining.
Scale bar = 200 μm.

Chapter 5

Conclusions

and

Future Directions

Conclusions

This dissertation focused on the effects of laminar fluid shear stress on the function of three types of adult stem cells: human mesenchymal stem cells (MSCs), human neural crest stem cells (NCSCs) and multipotent vascular stem cells (MVSCs). The interest in these adult stem cells lies in their potential as autologous cell sources for tissue engineering applications. More research on the mechanobiology of these adult stem cells is needed before they can be used to engineer tissues. The conclusions of this dissertation provide new clues to better understand the effects of mechanical stimulation on the function and differentiation of the aforementioned adult stem cells.

In chapter 2, we examined the effects of fluid flow on TGF-β1/SMAD2 signaling in human mesenchymal stem cells. We found that fluid flow promotes TGF-β1/SMAD2 signaling in a receptor dependent manner. We eliminated several hypotheses, which could explain this phenomenon: 1) shear force transmission through the glycocalyx; 2) changes in cell membrane fluidity; and 3) changes in the internalization of TGF-β receptors. After discarding these hypotheses, we decided to uncouple the effects of fluid shear stress on TGF-β1/SMAD2 signaling from the effects of the flow rate. We found that the increase in TGF-β1/Smad2 signaling when hMSCs were exposed to fluid flow was caused by an increase in the flow rate. We showed that laminar fluid shear stress inhibits TGF-β1/Smad2 signaling. Because fluid shear stress and the flow rate act in concert, we concluded that the positive effects of higher flow rates mask the negative effects of laminar fluid shear stress on TGF-β1/Smad2 signaling. These results put into question the conclusions of previous studies about the effects of laminar fluid shear stress on hMSC function.

Previous studies have shown that human mesenchymal stem cells (hMSCs) are responsive to fluid shear stress, but none has looked at the effects of fluid shear stress separately from those of the flow rate. For example, Glossop et al. investigated the effects of different profiles of fluid shear stress on mitogen-activated protein kinase (MAPK) signaling pathways in human MSCs. They found that fluid shear stress induced global changes in gene expression. In addition, they reported that fluid shear stress caused a consistent upregulation of MAP3K8 and IL1B independent of the magnitude and the duration of exposure. The study concluded that fluid shear stress activates different MAPK signaling pathways by the induction of MAP3K8 in hMSCs [1]. A different study by Bassaneze et al. concluded that fluid shear stress stimulated VEGF and nitric oxide (NO) production in human MSCs [2]. Given the results of the hMSC study in this dissertation, it is possible that the findings, which have been attributed to fluid shear stress, may in fact be caused by changes in the flow rate and fluid motion. Further investigation will be necessary to clarify these conclusions.

In chapter 3, we investigated the effects of laminar shear stress on the function of human neural crest stem cells. We found that laminar fluid shear stress increased NCSC proliferation in a time-dependent manner. We also reported that fluid shear stress increased the activation of ERK1/2 in a time dependent manner. In addition, we observed that exposure to laminar fluid shear stress did not affect the ability NCSCs have to differentiate into multiple lineages.

We found, however, that exposure to fluid shear stress may suppress adipogenic differentiation. The results of this study provide some understanding of the effects of fluid shear stress on the function and the differentiation potential of NCSCs, however, more work will be needed to determine how NCSCs function and differentiate when they are exposed to different profiles and different magnitudes of fluid shear stress.

In chapter 4, we studied the effects of laminar shear stress on the function of multipotent vascular stem cells isolated from rats. We found that laminar fluid shear stress increased MVSC proliferation. Similarly to NCSCs, we showed that fluid shear stress increased ERK1/2 activation in a time dependent manner. Furthermore, fluid shear stress caused a decrease in the gene expression of smooth muscle cell markers and an increase in the expression of osteoblastic differentiation genes. In addition, we observed that exposure to fluid shear stress did not affect the ability that MVSCs have to differentiate into multiple lineages. The conclusions of this study provide new clues to better understand the mechanobiology of MVSCs but more research into effects of hemodynamic forces on MVSC function will be necessary before this type of adult stem cell can be utilized in tissue-engineering applications.

Future Directions

The study of hemodynamic forces on NCSCs and MVSCs could be improved by using three-dimensional (3D) systems. Several studies have already examined the effects of hemodynamic forces on hMSCs using three-dimensional (3D) systems. In these studies, cells are seeded in biocompatible tubular constructs which can be subject to fluid shear stress, cyclical stretch and normal pressure (either in combination or in isolation.) These experimental protocols mimic more closely the geometry and the mechanical environment of the blood vessel wall. For example, Dong et al. fabricated tubular constructs using a copolymer of ε-caprolactone and lactic acid (PCLA) seeded with canine MSCs. These constructs were loaded into a pulsatile bioreactor where fluid shear stress (15 dynes/cm^2) could directly be applied to MSCs. They reported that in-vitro fluid shear stress increased the expression of endothelial cell markers while decreasing smooth muscle [3]. In earlier experiments, Liao et al. seeded human mesenchymal stem cells (hMSCs) in tubular constructs made of collagen and fibrin gel. They subjected cyclic strain to these constructs for three days by applying pressure to silicone tubing inserted through the constructs. Their results indicated that cyclic strain increased the gene expression of two smooth muscle markers α-actin and SM22α [4]. Later, Gong and Niklason claimed that hMSCs could differentiate into “smooth muscle like” cells by seeding cells in a PGA mesh, using an optimized culture medium and by applying cycling mechanical strain to the constructs in a method similar to Liao et al [5]. It is feasible to use similar 3D bioreactors and experimental protocols to study the effects of hemodynamic forces on the differentiation of NCSCs and MVSCs.

Furthermore, the studies in this dissertation focused entirely on laminar fluid shear stress at specific magnitudes and durations but we know that blood vessels must constantly adapt to changing hemodynamic conditions [6]. Fluid flow in blood vessels is normally laminar but secondary flows can be generated at curves and bifurcations [7].

Secondary flows move blood from the inner wall to the interior of the vessel thereby creating unsteady conditions. To continue, it is known that atherosclerotic plaques tend to be localized in sites where wall shear stress oscillates [8]. The narrowing of blood vessels (stenosis) can also cause turbulent flows and high levels of shear stress which can activate platelets and ultimately lead to thrombosis [9]. Because blood flow is dominated by unsteady flow phenomena, future studies should examine the effects of different flow profiles (unsteady or pulsatile, oscillatory and turbulent flows) on the function and the differentiation of MSCs, NCSCs and MVSCs.

Last, the recent discovery of multipotent vascular stem cells (MVSCs) in the medial layer of the blood vessel wall has sparked a controversy in vascular disease research. Up to now, the generally accepted theory had been that, in response to vascular injury, mature smooth muscle cells (SMCs) could de-differentiate, proliferate and migrate to the site of injury [10]. Tang et al., however, claim that MVSCs, rather than SMCs, could be responsible for vascular remodeling after injury or in disease states such as atherosclerosis [11]. One critique of their work is that the team failed to use a conditionally regulated lineage tracing system in their experiments. This system would rigorously identify whether MVSCs differentiate into SMCs to repopulate the site vascular injury. In addition, direct in-vivo lineage tracing is needed to determine if mature SMCs can undergo phenotypic modulation and, are responsible for intimal hyperplasia during vascular injury or in disease states [12]. The resolution of this debate rests in the execution of these challenging experiments.

References

1. Glossop, J.R. and S.H. Cartmell, *Effect of fluid flow-induced shear stress on human mesenchymal stem cells: differential gene expression of IL1B and MAP3K8 in MAPK signaling.* Gene Expr Patterns, 2009. **9**(5): p. 381-8.
2. Bassaneze, V., et al., *Shear Stress Induces Nitric Oxide-mediated VEGF Production in Human Adipose Tissue Mesenchymal Stem Cells.* Stem Cells Dev, 2009.
3. Dong, J.D., et al., *Response of mesenchymal stem cells to shear stress in tissue-engineered vascular grafts.* Acta Pharmacol Sin, 2009. **30**(5): p. 530-6.
4. Liao, S.W., et al., *Mechanical regulation of matrix reorganization and phenotype of smooth muscle cells and mesenchymal stem cells in 3D matrix.* Conf Proc IEEE Eng Med Biol Soc, 2004. **7**: p. 5024-7.
5. Gong, Z. and L.E. Niklason, *Small-diameter human vessel wall engineered from bone marrow-derived mesenchymal stem cells (hMSCs).* FASEB J, 2008. **22**(6): p. 1635-48.
6. Pries, A.R., B. Reglin, and T.W. Secomb, *Remodeling of blood vessels: responses of diameter and wall thickness to hemodynamic and metabolic stimuli.* Hypertension, 2005. **46**(4): p. 725-31.
7. Wootton, D.M. and D.N. Ku, *Fluid mechanics of vascular systems, diseases, and thrombosis.* Annual Review of Biomedical Engineering, 1999. **1**: p. 299-329.
8. Ku, D.N., *Blood flow in arteries.* Annual Review of Fluid Mechanics, 1997. **29**: p. 399-434.
9. Tang, D.L., et al., *Wall stress and strain analysis using a three-dimensional thick-wall model with fluid-structure interactions for blood flow in carotid arteries with stenoses.* Computers & Structures, 1999. **72**(1-3): p. 341-356.
10. Bai, H., et al., *Neointima formation after vascular stent implantation. Spatial and chronological distribution of smooth muscle cell proliferation and phenotypic modulation.* Arterioscler Thromb, 1994. **14**(11): p. 1846-53.
11. Tang, Z., et al., *Differentiation of multipotent vascular stem cells contributes to vascular diseases.* Nat Commun, 2012. **3**: p. 875.
12. Nguyen, A.T., et al., *Smooth muscle cell plasticity: fact or fiction?* Circ Res, 2013. **112**(1): p. 17-22.

Appendix

Derivation of the equation relating fluid shear stress inside the flow chamber to the volumetric flow rate.

1.1 Governing Equations

The flow is governed by the continuity and momentum equations. For incompressible Newtonian flow, using the cartesian coordinate system, these equations are given as

$$\begin{gathered}
\frac{\partial u}{\partial x}+\frac{\partial v}{\partial y}+\frac{\partial w}{\partial z}=0 \\
\rho\left(\frac{\partial u}{\partial t}+u\frac{\partial u}{\partial x}+v\frac{\partial u}{\partial y}+w\frac{\partial u}{\partial z}\right)+\frac{\partial P}{\partial x}=\mu\left(\frac{\partial^2 u}{\partial x^2}+\frac{\partial^2 u}{\partial y^2}+\frac{\partial^2 u}{\partial z^2}\right) \\
\rho\left(\frac{\partial v}{\partial t}+u\frac{\partial v}{\partial x}+v\frac{\partial v}{\partial y}+w\frac{\partial v}{\partial z}\right)+\frac{\partial P}{\partial y}=\mu\left(\frac{\partial^2 v}{\partial x^2}+\frac{\partial^2 v}{\partial y^2}+\frac{\partial^2 v}{\partial z^2}\right) \\
\rho\left(\frac{\partial w}{\partial t}+u\frac{\partial w}{\partial x}+v\frac{\partial w}{\partial y}+w\frac{\partial w}{\partial z}\right)+\frac{\partial P}{\partial z}=\mu\left(\frac{\partial^2 w}{\partial x^2}+\frac{\partial^2 w}{\partial y^2}+\frac{\partial^2 w}{\partial z^2}\right)
\end{gathered} \tag{1.1}$$

1.2 Boundary Conditions

Along the walls of the channel, the no-slip and no penetration boundary conditions apply. That is

$$\begin{aligned}
&on \quad y=\pm h/2: \quad u=0, \quad v=0, \quad w=0 \\
&on \quad z=\pm w/2: \quad u=0, \quad v=0, \quad w=0
\end{aligned} \tag{1.2}$$

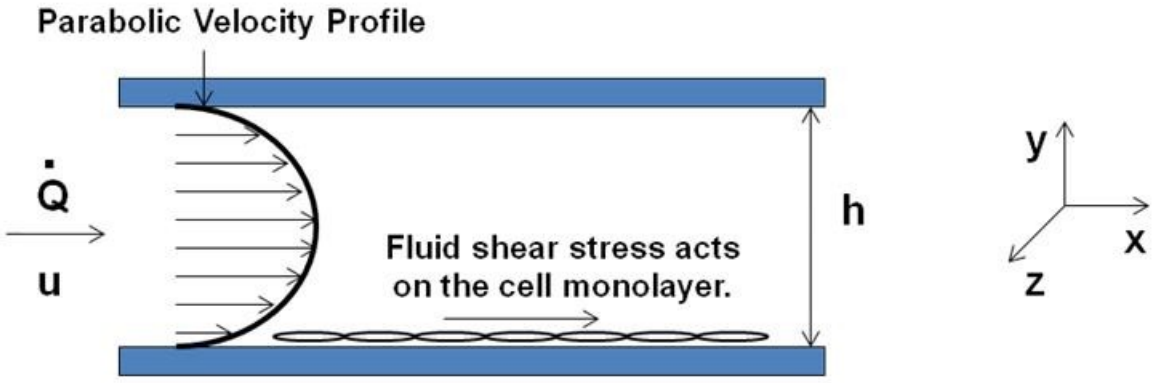

Figure 1. Velocity profile inside the flow chamber

1.3 Solution

1.3.1 Assumptions

$$\vec{u}(\vec{x}) = u(x, y, z)e_x \tag{1.3}$$

We are therefore assuming steady state uni-directional flow. With these assumptions, the continuity equation reduces to

$$\frac{\partial u}{\partial x} = 0 \tag{1.4}$$

Equation 1.4 implies that, the velocity profile does not change along the direction of flow. That is, the flow is fully developed. The condition for the flow to be fully developed is given as

$$\frac{L_h}{L} << 1, \qquad \frac{L_h}{L} = 0.06\epsilon Re, \qquad Re = \frac{\rho U_o h}{\mu}, \qquad \epsilon = \frac{h}{L} \tag{1.5}$$

Where L_h is the entrance length, ϵ the aspect ratio of the channel, and Re the Reynolds number. Because $\partial u/\partial x = 0$, the velocity profile can be at most a function of y and z only. That is

$$u = u(y, z) \tag{1.6}$$

With the above assumptions, the governing equations are simplified to

$$\frac{\partial P}{\partial x} = \mu\left(\frac{\partial^2 u}{\partial y^2} + \frac{\partial^2 u}{\partial z^2}\right), \qquad \frac{\partial P}{\partial y} = 0, \qquad \frac{\partial P}{\partial z} = 0 \tag{1.7}$$

The differential equation to be solved is now

$$\frac{dP}{dx} = \mu\left(\frac{\partial^2 u}{\partial y^2} + \frac{\partial^2 u}{\partial z^2}\right) \tag{1.8}$$

Subject to the no-slip boundary conditions at the wall.

1.3.2 Non-Dimensionalisation

$$\hat{x} = \frac{x}{L}, \quad \hat{y} = \frac{y}{h}, \quad \hat{z} = \frac{z}{w}, \quad \hat{u} = \frac{u}{U_o}, \quad \hat{P} = \frac{h^2 P}{\mu U_o L}, \quad \beta = \frac{h}{w} \tag{1.9}$$

$$\frac{d\hat{P}}{d\hat{x}} = \frac{\partial^2 \hat{u}}{\partial \hat{y}^2} + \beta^2 \frac{\partial^2 \hat{u}}{\partial \hat{z}^2}, \qquad \hat{u}(\pm 1/2, \hat{z}) = 0, \qquad \hat{u}(\hat{y}, \pm 1/2) = 0 \tag{1.10}$$

Analysis for $\beta \to 0$

For $\beta \to 0$, we have a simple, closed form solution for the velocity profile and other variables. That is

$$u = \frac{1}{2\mu} \frac{dP}{dx} \left[y^2 - \left(\frac{h}{2} \right)^2 \right] \tag{1.11}$$

$$\dot{Q} = -\frac{wh^3}{12\mu} \frac{dP}{dx} \tag{1.12}$$

By solving for the pressure gradient, the velocity profile in terms of the volume flow rate now becomes

$$u = -\frac{6\dot{Q}}{wh^3} \left[y^2 - \left(\frac{h}{2} \right)^2 \right], \qquad U_o = \frac{3\dot{Q}}{2wh} \tag{1.13}$$

Where U_o is the maximum velocity occurring at the centerline, $y = 0$. The viscous shear stress distribution is

$$\tau_{xy} = \mu \frac{\partial u}{\partial y} = 12 \frac{\mu \dot{Q}}{wh^3} y \tag{1.14}$$

The absolute value of the shear stress is zero at the centerline and maximum at the walls.